High-Throughput Maturation of Engineered Human Skeletal Muscle Tissue

A Major Qualifying Project
Submitted to the Faculty of
Worcester Polytechnic Institute
in partial fulfillment of the requirements for the
Degree in Bachelor of Science
in
Biomedical Engineering
By

Benjamin Cossette

Annabella Goncalves

Alexander Marry

Mina William

Date: 4/24/17

Project Advisors:

Professor Raymond Page, Advisor

Table of Contents

Table of Figures

Table of Tables

Acknowledgements

The authors would like to sincerely thank the volunteers that made this project possible: Professor Raymond Page (MQP Advisor), Jason Forte (WPI Graduate Student), Lisa Wall and Elyse Favreau (Lab Managers), and Tom Partington (WPI Machinist). The team would also like to acknowledge

Abstract

With 95% of pharmaceutical drug candidates failing to make the transition from the preclinical to clinical phase, the need for predictive disease models is ever rising. Musculoskeletal diseases like Duchenne Muscular Dystrophy especially lack effective treatment options, primarily due to the lack of predictive in-vivo animal models. Tissue-engineered human skeletal muscle constructs could provide advantages over these traditional animal models. These engineered models would ideally offer small functional units of biomimetic skeletal muscle tissue for high-throughput drug screening and may circumnavigate the non-predictive nature of most traditional preclinical model systems. However, current methods of skeletal muscle tissue engineering yield immature tissues that lack biomimicry to native tissue. Tissue maturation strategies such as mechanical and electrical stimulation have been employed in an effort to improve biomimicry, and have been demonstrated to improve myofiber alignment, protein expression, and contractile ability. In this MQP, a device was designed to both mechanically and electrically stimulate hydrogel-assisted self-assembled skeletal muscle constructs in a high-throughput manner.

Chapter 1: Introduction

Over the years, the medical field has struggled with the treatment of muscular diseases, largely due to the fact that there are no appropriately predictive disease models. Researchers have long utilized pharmaceutical drugs as means to treat diseases. Before a drug is issued, rigorous testing must take place. The pharmaceutical drug development process begins with initial drug discovery from large-scale drug screening. Once promising compounds are identified, pre-clinical research begins with *in-vitro* and *in-vivo* testing. Typically, compounds are used to treat in-vitro cell models of the disease in a hope to elucidate treatment efficacy, mechanism of action, and cytotoxicity. If a drug shows promise during in-vitro testing, the compound is next tested in an animal disease model. Only after success in an *in-vivo* animal disease model can the drug advance to clinical trials in humans. It is at this transition from preclinical studies to clinical studies that 95% of drug candidates fail. The prevalence of drug rejection can largely be attributed to the trend for drug candidates to show promise in the preclinical in-vitro cell models and in-vivo animal models, but subsequently fail in human clinical trials. Simply put, animal disease models are poorly predictive of human outcomes [1]. Pharmaceutical spending has skyrocketed to over 5 billion dollars per viable drug due to this inadequacy of animal disease models.

Take for example Duchenne and Becker's muscular dystrophy (DBMD), similar diseases that affect 1 in 3,500 newborns [2]. Both diseases are characterized by a deficiency in dystrophin, a protein that assists in muscle function. This deficiency manifests in progressive muscle weakness, loss of regenerative capability, and ultimately death due to cardiac or respiratory malfunction typically after 20-30 years of life. DBMD is one of the most prevalent orphan diseases and thus is an area of substantial drug development spending [2]. For thirty years, preclinical testing for DBMD drug candidates has been primarily conducted in the mdx

mouse model. The mdx model has a mutation in the dystrophin gene that manifests in a premature stop codon on exon 23; halting translation of the protein and ultimately leading to a disease phenotype similar to human DBMD. However, the mdx mouse model does not perfectly recapitulate the severity and progression of the human diseases [3]. In January of 2016, a promising drug from Biomarin Pharmaceutical was rejected by the FDA due to poor efficacy in human trials. This type of situation is all too familiar within the field of muscle-disease drug development and of drug development as a whole, and a vital need for more reliable model systems is emerging [3].

Tissue-engineered in-vitro (outside of the body) human skeletal muscle models could provide a variety of advantages over standard mouse models for muscle-associated diseases such as DBMD. These models would ideally offer small functional units of human skeletal muscle for high-throughput drug screening and may circumnavigate the issues associated with the non-predictive nature of animal models for human diseases, such as needless spending due to the high failure rate of drugs during the pre-clinical to clinical transition. The models would ideally be completely biomimetic, meaning they would precisely recapitulate all aspects of the native tissue.

A small bench-top model of skeletal muscle would likely take the form of a single fascicle and would be composed of densely packed, aligned myocytes surrounded by the proper ECM, as seen in Figure 2. These high-order features must be recapitulated in a biomimetic model of human skeletal muscle, a feat that has not yet been achieved.

Much work has been invested into the development of bench top in-vitro skeletal muscle models and a variety of approaches have emerged [4,5,6]. These approaches can be categorized into three broad methods: hydrogel/mold systems, hydrogel-assisted self-assembly systems, and

monolayer delamination systems. The first type of system, hydrogel/mold systems, relies on the suspension of precursor cells in a non-native mix of gelatinous protein, such as collagen, that forms a rigid hydrogel. The cell/gel mixture is cast into a small mold in which the precursor cells differentiate to form myotubes. The second type of system, hydrogel-assisted self-assembly, relies on the seeding of precursor cells into a hydrogel, such as fibrin or collagen. This cell/gel mixture is cast into a circular tissue culture well with anchors, and as the tissue matures, it digests and remodels the hydrogel, forming a tissue construct composed of myotubes. The third system, monolayer-delamination, relies on the formation of a confluent single-cell layer of myotubes on the bottom of a culture plate. When two "tissue-anchors" are placed on top of the monolayer, the cell sheet rolls up to form a dense construct of myotubes. Despite significant research and development, none of these systems have been successful in producing biomimetic human skeletal muscle tissues because the in-vitro tissues differ significantly from native tissue in a variety of ways. Some major areas of poor native recapitulation are highlighted in Table 1 below.

Table 1: State of the Art Tissue Metrics Compared to Native Values

	Hydrogel/Mold	Self-assembly in Hydrogel	Monolayer-Delamination	Native Muscle
Alignment	± 15° off axis	Approximately ± 20° off axis	"Fully aligned"	± 0-10° off axis
Myotube Diameter	5-15 μm	<10 μm	< 10 μm	100 μm
Cell Density	~10% myotube	10-20% myotube	30-80% myotube	80-90% myotube
ECM Composition	Ample non-native ECM	Ample non-native ECM	Collagen IV deposition within non-native ECM	Collagen Type IV surrounding myocyte
Sarcomere assembly	Organized striation achievable	Striation present	Noticeable striations, well-defined sarcomeres	Organized grid-like striations

From data presented in Table 1, it is clear that the current state-of-the-art tissue contracts lack the maturity observed in native tissues. Mature myofibers have diameters approaching 100 μm, and all state of the art tissue constructs are composed of immature myotubes of about 10 μm in diameter. Additionally, most state of the art models severely lack the proper cell density that is characteristic of native skeletal muscle (90% myofiber) and are only comprised of around 10-20% myotube. Not only do these in-vitro tissues lack density, but the ECM that they do have is typically non-native protein left over from hydrogels. Ideally, each myocyte would be anchored to the surrounding tissue by type IV collagen [7]. These limitations in tissue maturity prevent the use of human skeletal muscle constructs as models for drug screening. Indeed, a company founded by Herman Vandenburgh, Myomics Inc., attempted to use fibrin-assisted self – assembled tissue, termed mBAMs, as drug screening models. The tissues themselves were

created in 96-well plates and were anchored to two flexible PDMS posts, allowing for contractile assessment via post-deflection upon tetanic contraction. Unfortunately, the lack of tissue maturity caused potential pharmaceutical clients to become hesitant to adopt the drug-screening technology resulting in company failure. Simply put, the Myomics drug-screening platform had all the makings of a successful technology, save for the tissue themselves. The fate of Myomics Inc. highlights the need for skeletal muscle constructs that exhibit increased tissue maturity, and that are ultimately more biomimetic than existing models.

To meet the needs described above, the team planned to design an in-vitro tissue-engineering system capable of producing human skeletal muscle tissue. As current tissue-engineered skeletal muscle tissue does not resemble native tissue closely enough to serve as an accurate model, the primary goal of the project is to produce tissues that are more biomimetic than those produced by current approaches. These tissues are to ultimately serve as disease models for pharmaceutical testing, and thus a secondary goal of the project is to design the tissue-engineering system in a way that allows for high-throughput production and testing.

Chapter 2: Background Research

This chapter details the background research the team conducted to better understand the project. It contains information pertaining to muscle anatomy and physiology, clinical significance of the current project, current approaches to the tissue-engineering of in-vitro skeletal muscle tissue, as well as current strategies for tissue maturity enhancement.

2.1 Skeletal Muscle Anatomy

Skeletal muscles are the basis of structure and function of the human body. Most skeletal muscles attach to two bones: origin and insertion. Skeletal muscles are attached to bones by tendons; strong connective tissue bands. Structurally, they aid with posture, organ protection, shape, strength, and overall mechanical stability. Their most important function is the voluntary action; allowing translocation and movement. This is derived from their ability to produce contractions and relaxations that forces muscle fibers to shorten and lengthen.

2.1.1 Skeletal Muscle Structure

In 3D space, skeletal muscles are surrounded and wrapped in collagen, an extracellular structural protein for connective tissue. Tendons are composed of collagen, which attaches muscle fibers to bone. Skeletal muscle cells are long and slender. Their thickness varies from 10-60μm in diameter. Their length ranges from 1mm-30cm. A skeletal muscle cell can be comprised of multiple fibers, termed bundles. The bundles are sheathed in connective tissue layers for protection and support. The muscle fibers are multinucleated and are surrounded by the sarcolemma; an electrically polarized membrane. The nuclei is located under the sarcolemma. A fasciculus is a bundle of muscle fibers which is surrounded by the perimysium; a strong connective tissue sheath. Each muscle fiber within the fasciculus is then surrounded by the endomysium sheath. The epimysium is the connective tissue sheath that covers each entire muscle; it is tough, protective, and emerges from tendons that are attached to bone. The fascia is

the connective tissue that is outside the epimysium sheath, separating each muscle. Skeletal muscles are striated due to the alternating dark and light bands on the myofibrils, oriented in a parallel scheme. Myofibrils are a threadlike structure in the sarcoplasm, which is the muscle cytoplasm. The contractile units of the muscle fiber are the myofibrils, which can range from 10-100um [4].

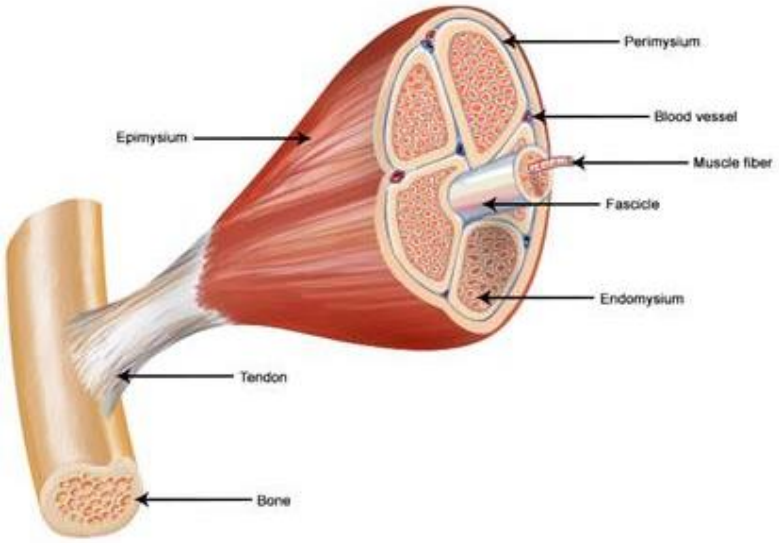

Figure 1. Diagram of a skeletal muscle, highlighting its anatomical components, derived from tendons anchored to bone. Shows the three connective tissue layers [8].

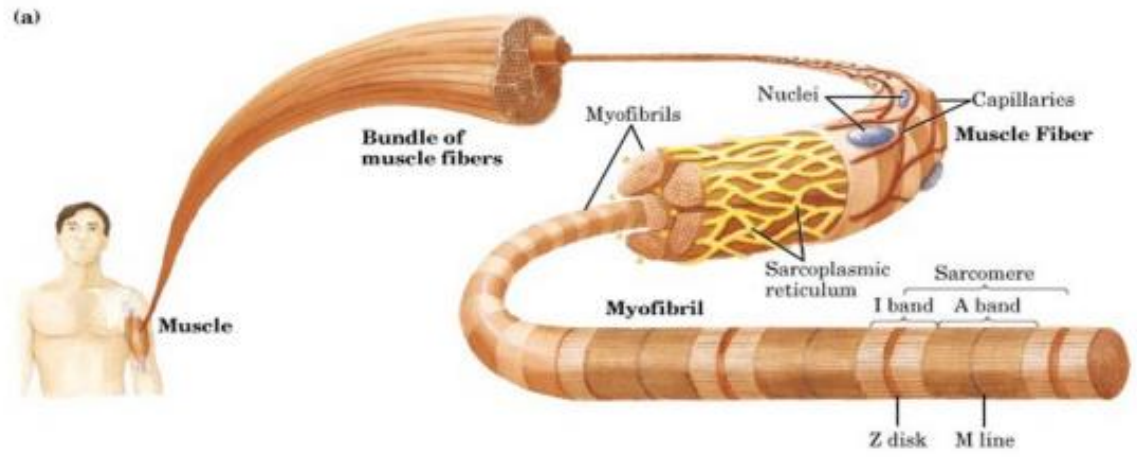

Figure 2. A depiction of the walk-through starting from a muscle group, reaching to the sarcomeres in the myofibrils [8].

The contractile backbone of the myofiber, the sarcomeres, is a cylindrical bundle composed of two types of filaments: a thin filament (actin ~7nm), and thick filament (myosin ~15nm). They are also composed of tropomyosin and troponin. Each sarcomere's end is defined by the Z disc. Dark and light bands, A and I respectively, are the physical representation of myosin filaments under electron microscopy. I bands contain the thin actin filaments, whereas A bands contain the thick myosin filaments. The H zone, diagramed above, is the region where only myosin is observed; actin and myosin overlap each other everywhere else within each interval. The M line is the anchorage of the myosin filament in the middle of the sarcomere.

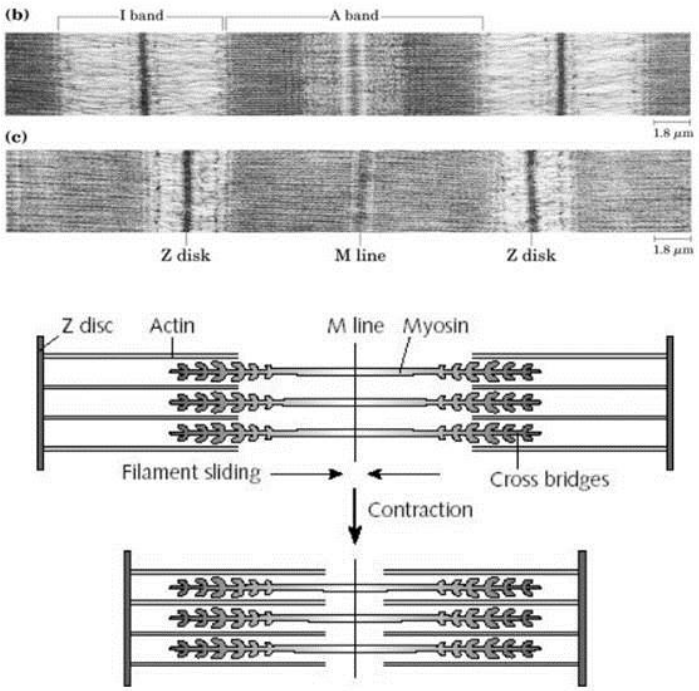

Figure 3. Mechanical components of a sarcomeres unit; highlighting the cross -bridging that induces contractions [8].

2.1.3 Skeletal Muscle Extracellular Matrix

The ECM in an important component of muscle fiber force transmitting, maintenance and repair. Skeletal muscle ECM is composed primarily of collagen, and it accounts for 1-10% of muscle dry weight. In skeletal muscle tissue, collagen is the most abundant and supportive type of ECM. Type I collagen compose tendons, bone and skin. Type II composes hyaline, type III composes blood vessels and fetal skin, and basement membrane is composed of type IV [9].

		Antibodies to collagen		
		Type I	Type III	Type IV
Muscle –	epimysium	+++	+	+
	perimysium	–	+++	–
	endomysium	–	++	++
Tendon –	bundles	++	–	–
	endo-tendineum	–	++	++

Figure 4. Collagen concentrations, in muscle and tendon layers, based on types.

2.2 Mechanism of Action—Contraction

The sliding filament model is the most generally accepted model of skeletal muscle contraction. A contraction occurs when the sliding thin filaments, at each end of the sarcomere, approach each other between the stationary thick filaments. The Z lines become closer and shorten the sarcomere. It is evident that when shortening of the sarcomere takes place, the I band of each myofibril narrows as the thin filaments move to the center of the sarcomere. The lighter region of the A band, the H zone, disappears as the thin filament completely overlap the thick filament while contraction is occurring. This is seen as the A band center becomes a dense dark zone; a resultant from the overlap of thin filaments from opposite ends of a sarcomere.

Thin filament movement is facilitated by the cross-bridging of thick filament myosin heads to thin filament binding sites, followed by the movement of the myosin arm; acting as mechanical pulling devices. Briefly, tropomyosin disassociates from the binding site of myosin, enabling myosin head binding with actin. The myosin head, upon hydrolysis of ATP, undergoes conformational change and provides a propulsive force that pulls the thin filaments towards the center of the sarcomere. When a new ATP molecule then binds to the myosin head, the myosin head and actin detach; enabling a reattachment in a new position on actin [10]

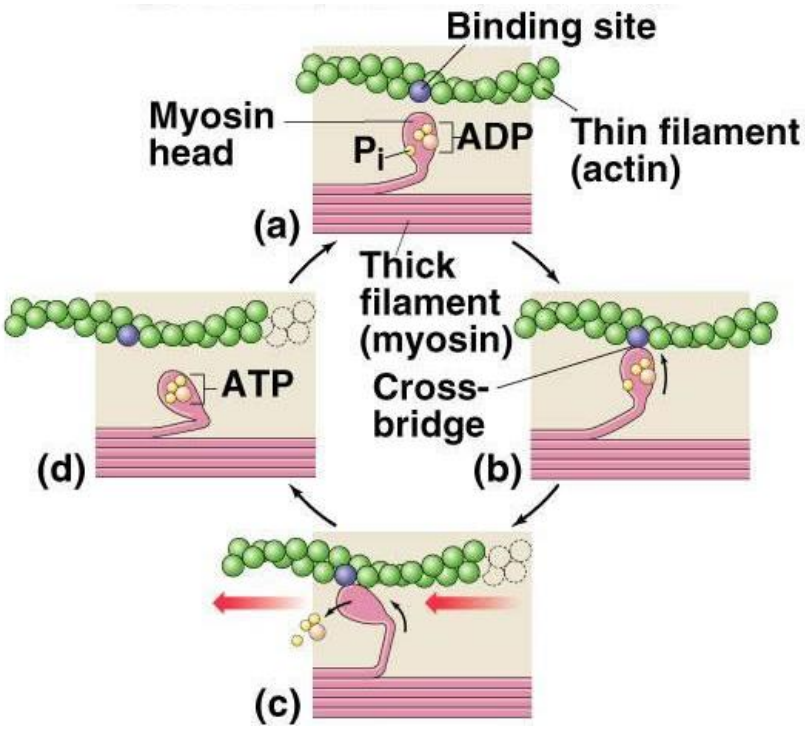

Figure 5. Depicting the chain of events that take place to perform a contraction; ATP guides the Actin/Myosin interactions to shorten the sarcomere.

2.2.1 Initiation of Contraction

Contraction is initiated by a motor-neuron, which when activated releases acetylcholine into the synapse. Acetylcholine binds to ligand-gated sodium channels on the myotube. Sodium rushes into the cell, rapidly depolarizing the cell membrane and initiating an action potential that travels along the length of the myotube. The action potential travels down deep protrusions into the myotube called T-tubules. T-tubules contain voltage-gated calcium channels that open in response to the depolarization caused by the propagating action potential. These voltage-gated calcium channels are directly coupled to calcium channels in the sarcoplasmic reticulum. Thus, when T-tubule voltage-gated calcium channels open, so do sarcoplasmic reticulum calcium channels, allowing the rapid influx of calcium ions into the sarcoplasm. Calcium influx allows dissociation of troponin from myosin-actin binding sites, initiating contraction via sliding filaments. A single brief contraction is termed a muscle twitch. A twitch sequence is proceeded

by a period of relaxation, followed by contraction initiated from a short duration of an electrical stimulation. A tetanic contraction is essentially a series of closely spaced twitch contractions, in which the electrical stimulations are so closely spaced that a continuous contraction occurs. Responses of muscle fibers are dependent on: stimulus strength, stimulus speed, and number of stimulations.

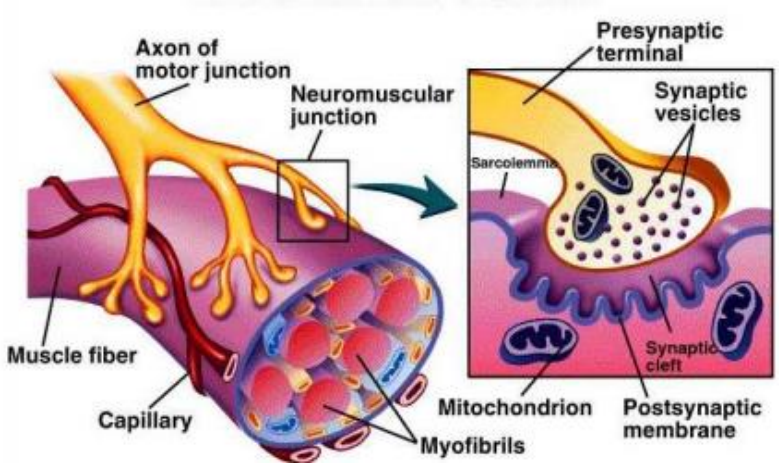

Figure 6. Depiction of a neuromuscular junction; showing the gross anatomy of a synaptic junction of a neuron and a muscle fiber [8].

2.3 Skeletal Muscle Development

Skeletal muscles play a crucial role from structural assistance to movement in living organism. There are more than 640 skeletal muscles in the adult human body [11]. They are multinucleated fibers that result from the fusion of many individual mononucleated progenitor cells. To deeper understand and perform In Vitro studies, one must completely understand the process of which skeletal muscle take to differentiate and mature in vivo; only then can tissue testing and analyzing be meaningful.

There are three different types of muscle found in the human body: cardiac, smooth, and skeletal. Cardiac muscle makes up the component of the heart; they are systemic contractile cells

able to generate a magnitude of force to pump blood throughout the circulatory system. They are involuntary and highly striated. Smooth muscles are muscle cells that surround and line the organs in the human body, for example the stomach, and blood vessels. Smooth muscles are involuntary, and aid in the movement of substances across the body. Skeletal muscles are the most abundant, and carryout all movement and support by binding to the exoskeleton. They are voluntary muscle cells that derive their mobility from somatic cerebrospinal nerves.

2.3.1 Skeletal Muscle Somitogenesis

During gestation, cells will begin to position and differentiate from the three germ layers that develop: the ectoderm, mesoderm, and endoderm. Mesoderms, after introduction of morphogen gradients, are induced to become somites; the first metameric structures in mammalian embryos. After somites leave the caudal region of the mesoderm, the cyclic expression of genes ceases, and retinoic acid increases; establishing polarity in the somite. From this polarized somite, the mesenchymal sclerotome forms from the most ventral part; the precursor to cartilage and bone. Skeletal muscle are derived of the structures that form from the most dorsal portion of the somite; which remain epithelial and becomes dermomyotome. From those dermomyotomes, the lips will mature to become myotome; the primitive muscle structure that contains the committed muscle cells [12]. Those muscle cells express high levels of MyoD and Myf5. Those expressions are the markers of terminal specification to the muscle lineage. For mature skeletal muscle cells to form, they must further differentiate; a process where a cell adapts a specific structure and function aided by specific growth factors, receptors, and transcription factors [13].

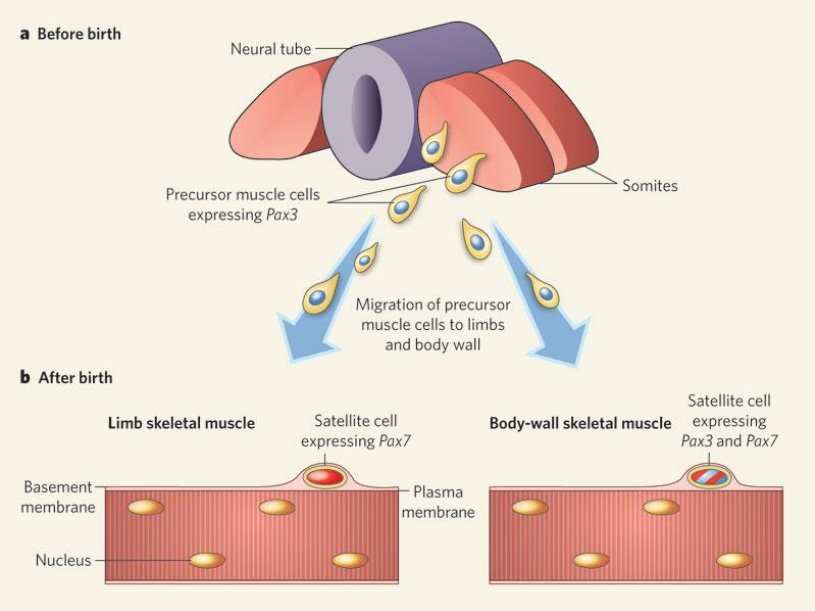

Figure 7. Shows precursor muscle cells becoming limb skeletal muscle and body-wall skeletal muscles after the expression of Pax7 and Pax3 [13].

2.3.2 Skeletal Muscle Myogenesis

The process in which a progenitor cell differentiate and grows into a skeletal muscle cell is called Myogenesis. This process is first seen during later stages of embryonic development, in which the mesodermal cells give rise to skeletal muscle cells. The first identifiable muscle cell is the myoblast, which is defined as the determination phase of myogenesis; a committed skeletal muscle lineage derived from progenitor cells. The myoblasts have the ability to synthesize myofibrillar proteins; actin and myosin. During the terminal differentiation phase, myoblasts are able to physically fuse with other myoblasts to form multinucleated cells, called myotubes/myotubules. Finally, the maturation phase is complete when the myotubes start linearly aligning to one another; growing in size to diameters of up to 100um.

For Myogenesis to take place, growth factors, enzymes, proteins, and signaling must interact with the differentiated cell to aid growth. It is due to the genetic transcription factors that allows for maturation to be achieved. Of the many factors, some are exceptionally important:

MyoD, Myf5, myogenin, and Mef2. MyoD is a single cDNA; a member of the DNA-binding proteins. In somites, when expressed, it is responsible for driving the growth that leads to body wall and limb muscles. Myf5 is another protein that is responsible for growing the trunk and intercostal muscles from the somites. When both these proteins are expressed, commitment of multipotent somite cells to the myogenic lineage takes place. Myogenin expression is an important aspect of the terminal differntiaion of myoblasts; however, dispensable for establishing myogenic lineage. Myogenin aids in the fusion of myoblasts to primary myotubes. This is aided by Mef2; a myocyte enhancer.

2.4 Tissue Regeneration

Muscle regeneration is a process that occurs in three steps: inflammation, repair and remodeling. When a muscle experiences trauma, the damage to the cells elicits an immune response that causes inflammation. Macrophages are released into the injury site and phagocytize the necrotic cells. Damage to the basal lamina due to myotrauma also activates satellite cells located peripherally to the myotubes. During this step, paired box protein 7 (Pax7+) satellite cells express MyoD which prevents the myotubes from undergoing apoptosis [14].

Satellite cells, mononucleated progenitor cells found under the basal lamina of myofibers, play a major role in the following repair and remodeling phases, especially in hypertrophy, the growth of myotubes occurring in response to an applied load or resistive force [15]. Satellite cells exist in a dormant state until activated by damage to the muscular tissues, or myotrauma. When the muscle experiences injury, the basal lamina is ruptured and the satellite cells undergo a cycle of activation, proliferation and then chemotaxis (migration to the injury site). Myotrauma causes the release of certain factors, such as insulin-like growth factors I and II (IGF-I and IGF-II), hepatocyte growth factors (HGF), fibroblast growth factors (FGF). These factors cause increased proliferation of satellite cells and, in turn, increased muscle mass. The amount of HGF

and FGF released by myotubes is proportional to the extent of the myotrauma [16]. After moving to the injury site, the satellite cells undergo determination and then turn into myoblasts. Once myoblasts, Pax7+ is downregulated and myogenin is upregulated in response [15]. The expression of myogenin causes the myoblasts to enter into terminal differentiation, causing them to differentiate into myotubes and fuse to the existing, healthy myotubes. The new myotubes will then mature into muscle fibers when undergoing axial straining due to movement and use of the muscle group [16].

After the formation of new myotubes, vascular endothelial growth factors (VEGF) are released to promote the formation of blood vessels to the myotrauma site; they will provide the new tissue with nutrients needed to promote maturation [17]. The new tissue will also become innervated, providing the electrical stimulation required to produce voluntary movement and exercise the maturing muscle.

During the later stages of the healing process, fibroblasts proliferate and undergo chemotaxis. These cells secrete collagen to form an extracellular matrix where the new myotubes are forming so that the new tissue has a scaffold to grow on [18]. In cases involving volumetric muscle loss, fibroblasts can release collagen at a rate faster than that of muscle regeneration; this will lead to dense scar tissue formation that can impede the healing process and could possibly cause the loss of muscle functionality in the injured area. At the end of the healing process, the new myofibers and ECM are reorganized and functionality to the injured area is restored once the cells are mature enough.

2.5 Clinical Significance

The skeletal muscle system is one of the most important organ systems in humans; it plays the major role in voluntary movement and facilitates respiration and the flow of lymph to the heart. Muscular disorders are serious medical conditions that profoundly affect the quality of

life of those afflicted; many have been known to leave patients paralyzed and with significantly shorter life expectancies. Muscular dystrophies, such as Duchenne's muscular dystrophy and Becker's muscular dystrophy, involve the progressive loss of muscle mass and function, leaving patients paralyzed, in severe pain and completely dependent on others for their care. Atrophies caused by disuse or stemming from neurogenic disorders also have similar effects and prognoses as muscular dystrophies. Dystrophies and atrophies are difficult for physicians to treat; most times doctors treat the symptoms since there has been little development for a complete cure. The afflicted patients are typically provided these treatments for the rest of their lives, accumulating expensive medical bills for their family members to pay. A tissue-engineered skeletal muscle could provide an in vitro means for pharmaceutical companies to test drugs for these disorders. These models would provide a cheaper, safer and more streamlined method for drug testing that could possibly eliminate the need for expensive animal and human trials. Skeletal muscle models could expedite the discovery of a cure for these disorders, giving those suffering these diseases much longer, high quality lives.

Muscular dystrophy is a category of genetic muscular disease characterized by the progressive deterioration of muscle mass. Although over thirty different variations currently exist, the most commonly occurring are Duchenne's muscular dystrophy (DMD) and Becker's muscular dystrophy (BMD) [19]. DMD is characterized by the deletion of the protein dystrophin, normally found in the sarcolemma of skeletal muscle. Dystrophin is responsible for making myofibers more mechanically stable in order to have smooth, coordinated voluntary movement. DMD is typically found in males with symptoms manifesting within the first five years of life [20]. The degradation of muscle occurs at an incredibly fast rate; most patients suffering from it do not survive past their twenties. BMD is another variation of muscular dystrophy that is

extremely similar to DMD, characterized by decreasing dystrophin levels. The main differences are that BMD progresses at a much slower rate and symptoms usually manifest first during adolescence or early adulthood [19].

There currently exists no cure for any form of muscular dystrophy, only treatment to slow its progress and alleviate its symptoms. Most patients afflicted with this disorder undergo physical therapy in the attempt to preserve muscle strength and tone. Eventually, all those with this disorder will lose their strength and will not be able to produce voluntary movement. Many will have difficulty breathing since they are not able to properly use their intercostal muscles to expand the thoracic cavity during inhalation, thus becoming dependent on respirators and supplementary oxygen in order to breathe. Physicians may also prescribe steroids and/or recommend surgery in order to treat the symptoms, however these interventions are only utilized to extend life and increase quality of life [21].

Muscular atrophy is characterized by the degradation of muscle caused by its disuse. Muscle atrophy most commonly occurs in bedridden patients who do not perform any voluntary movement. Some instances of atrophy have neurogenic origins, in which the nervous system cannot properly conduct action potentials to produce muscle contraction and thus movement [22]. Other factors that can lead to disuse include level of activity, weight and age. Mature muscles must undergo a minimum amount of force to maintain strength and tone. If muscles do not experience the minimum force required, the body also cannot build muscle mass. Prolonged disuse of muscles activates the Ub-proteasome pathway, which incites protein degradation within the skeletal muscles. In this instance, the muscles will degrade at a much faster rate than they will generate [23]. This will eventually lead to the loss of muscle stability and function, leading to the loss of voluntary movement.

Volumetric muscle loss is the significant dissection of muscle due to trauma or medical procedures. This significant muscle loss destabilizes the affected area, making voluntary movement difficult to impossible. When the body senses the loss of a large volume of muscle, rhabdomyolysis, the dissolution of skeletal muscle, takes place. The body will try to use the satellite cells to repair the damaged area, but if the amount of muscle lost is significant then fibroblasts will secrete high levels of collagen to form dense scar tissue [18]. Although the scar tissue fills the area missing skeletal muscle, it cannot provide the same functionality as muscle.

Currently, there are no viable disease models for most musculoskeletal diseases. The successful development of treatments for these diseases is contingent upon drug discovery, requiring predictive disease models. In vitro models of human skeletal muscle could represent a highly predictive disease modeling approach and may play a role in the pharmaceutical drug discovery process. The United States Food and Drug Administration requires that a potential drug to undergo a phased testing in order to determine its efficacy and biocompatibility. Phase 0 of testing involves no live test subjects, but Phases I through IV involve live animal and human test subjects. Those used in testing may be subjected to the negative side effects from the experiments. It also costs pharmaceutical companies millions of dollars to pay for the testing and compensation for human subjects. Skeletal muscle constructs that are biomimetic of human muscle can totally eliminate the need for animal testing and reduce the number of human subjects required to test potential drugs. The constructs may be able to save pharmaceutical companies millions of dollars and make the drug testing process more efficient and streamlined.

2.6 Tissue-engineering Of In Vitro Skeletal Muscle

Many approaches have emerged in the creation of biomimetic in-vitro models of skeletal muscle, which will be discussed in the next sections. First, various tissue-engineering methods will be discussed, followed by a discussion on cell selection and differentiation techniques.

2.6.1 Tissue-engineering Approaches

Decades ago, scientists began to realize the limitations of cell/tissue biology research on cells/tissues cultured on stiff two-dimensional surfaces [24]. Of particular difficulty was the formation of muscle tissue *in vitro*. 2D cultures often detached from the culture surface resulting in a free-floating monolayer that was difficult to maintain. In an attempt to combat these issues, researchers began to culture muscle cells on top of collagen hydrogel matrixes. This allowed the formation of neonatal-like myotubes, however these immature myotubes differed significantly from their in-vivo counterparts. The myotubes often expressed very little myofibriallar protein and were thus incapable of transition to adult-like mature muscle tissue [24].

Vandenburgh published a 1988 paper that described a new method for culturing primary skeletal muscle cells that allowed for the formation of more biomimetic tissue. Primary avian muscle biopsy cultures were suspended in a collagen matrix and set into circular molds surrounded by a stainless steel anchoring-mesh. While 2D cultured tissues only showed lamina formation at the cell-surface contacting site, these 3D cultured tissues in collagen allowed the formation of a biomimetic basal lamina around the entire periphery of the cell. The mesh allowed permanent tissue attachment, even after the construct detached from culture surface, thereby maintaining tension within the tissue. Tissues cultured with this new 3D collagen method showed increased protein expression and could maintain elevated levels for several weeks. This method provided key benefits over traditional 2D culture systems and produced myotubes that were more biomimetic than previously created. While the myotubes were still immature,

Vandenburgh's work set a platform for 3D skeletal muscle tissue-engineering research for years to come.

By 1997, the importance of uniaxial strain in the alignment of muscle fibers had been realized [25]. By combining this with his 3D collagen tissue-engineering method, Vandenburgh developed a tissue-engineering system in which collagen-embedded mammalian myoblasts were seeded into a rectangular mold with metallic mesh anchors on either end of the mold in Figure 8. As the myoblasts fused into aligned myotubes within the collagen matrix, the collagen gel was contracted and pulled away from the sides of the mold [25]. The tissue was left anchored only to the mesh anchors and thus passive uniaxial tension was established within the tissue-matrix constructs and myotube alignment was improved as a result.

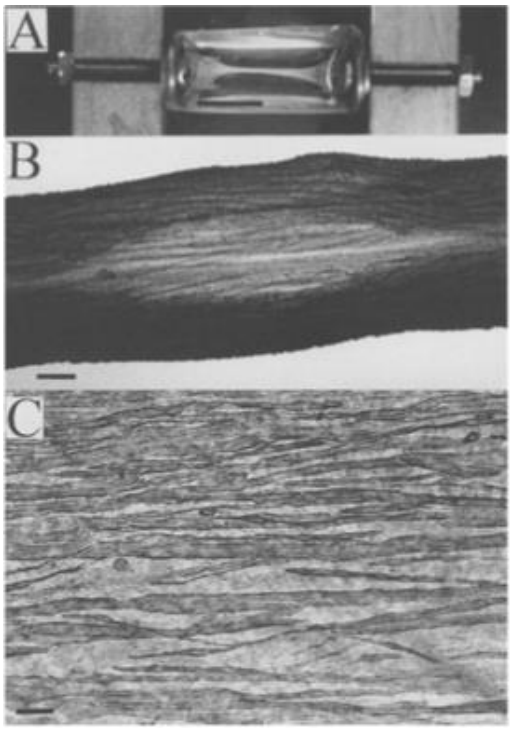

Figure 8. A: Engineered tissue anchored between mesh anchors. B: Whole construct showing aligned myotubes on surface. C: Magnified view of myotubes within construct [25]

By 2002, Vandenburgh and Powell had improved the 1997 collagen-assisted self-assembly method to utilize human cells and had termed their contracts Human BioArtifical Muscles (HBAMs) [26]. These constructs allowed for the formation of aligned human myotubes, however the myotubes were still immature. The myotubes had low diameters (~5μm) and only composed ~7% of the construct cross-sectional area (the rest was the non-native ECM collagen/Matrigel matrix) in Figure 9. In their 2002 paper, Vandenburgh and Powell incorporated mechanical stimulation into the tissue-engineering process in hopes to improve maturity and biomimicry of the HBAMs. The tissues were mounted on two pins that were connected to a uniaxial stepper motor and subjected to mechanical strain regimens. Mechanical stimulation of the tissues resulted in improvements in both myotube diameter (12% improvement from 6.4μmto 7.1um) as well as in myotube area percentage (40% improvement from 7.8% to 10.9%) [26]. However, when these values are compared to native tissue, the lack of biomimicry is strikingly apparent.

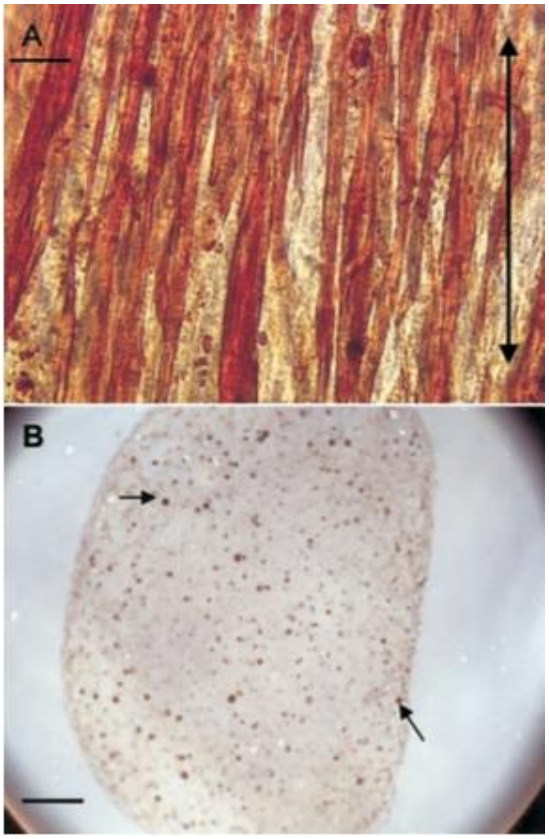

Figure 9: A: IHC staining of HBAM for scarcomeric myosin (Scale bar 20um). B: Cross-section of HBAM with myotubes stained brown (Scale bar 100um) [26].

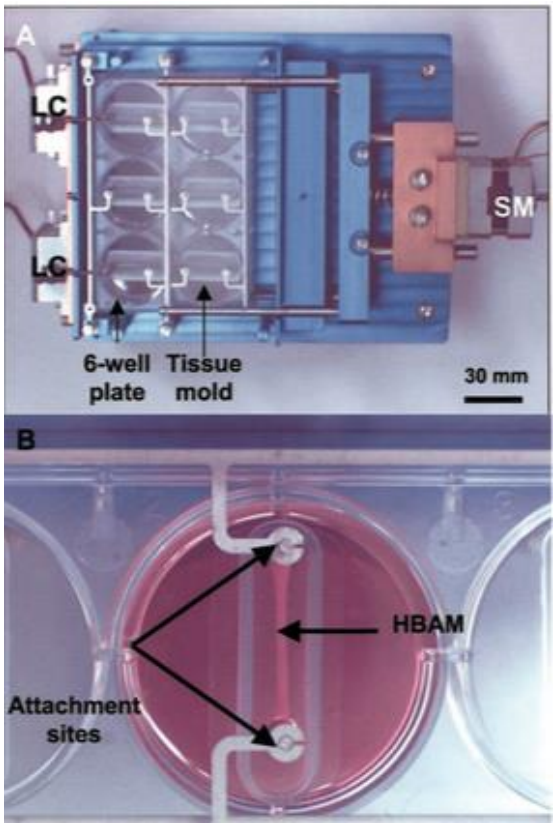

Figure 10: A: Mechanical stimulation platform, mechanical force transducers to quantify contractile force are labeled LC. B: Post mounted HBAM [26].

In a 2008 paper, Vandenburgh proposed a drug-screening platform based on his engineered "BAM" tissues [27]. For this system, miniature BAMs (mBAMs) were formed around two flexible PDMS post anchors (4 mm apart) in Figure 11. The method of tissue-engineering was almost identical to the HBAM method previously described, however the mBAMs were formed with primary mouse myoblasts rather than human primary cells. The flexible PDMS posts provided a means of contractile assessment. The post-mounted constructs were electrically stimulated to produce an isotonic tetanic contraction while a camera recorded post deflection. This analysis could then be used to calculate force production using a calibration curve. To prove the potential of this system as a drug-screening platform, Vandenburgh cultured tissues with IGF-1, a known anabolic. Promisingly, the IGF-1 increased myotube diameter as

well force production. Additionally, Vandenburgh showed that the system could identify compounds with deleterious effects on muscle function by culturing the mBAMs with a statin known to decrease muscle strength in patients. Encouragingly, the statin decreased mBAM contraction force, even at near-physiological levels.

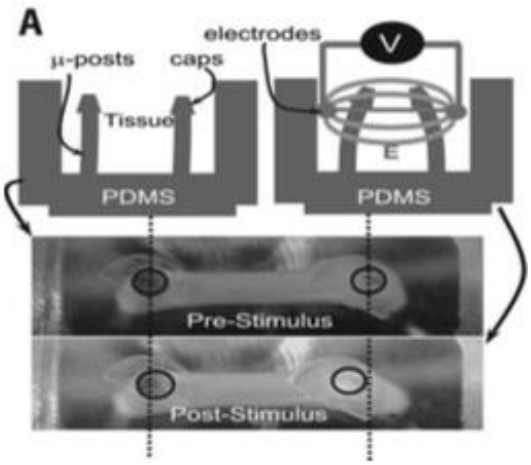

Figure 11: Summary of Vandenburgh's mBAM post-deflection approach for contractile assessment [28].

In 2010, Vandenburgh showed that this system could be created within standard 96-well plates in Figure 12 and thus could represent an extremely high-throughput and potentially automated drug-screening platform [28]. It should be noted however, that these mBAMS were still subject to a lack of biomimicry and tissue maturity.

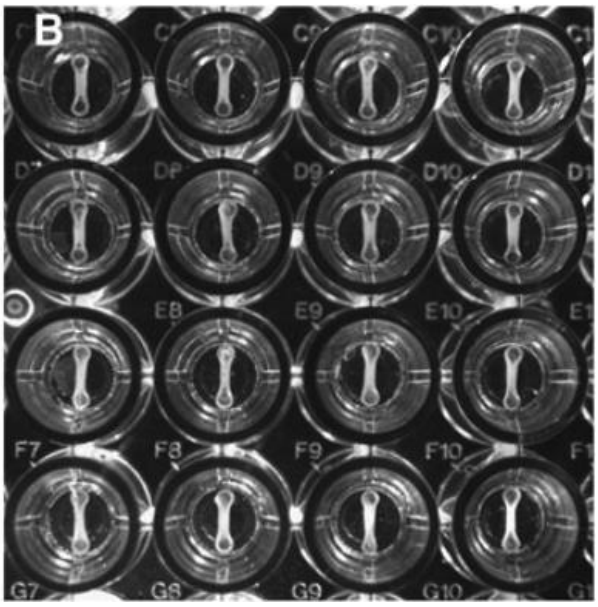

Figure 12: Representative image showing mBAMS mounted on PDMS posts within a 96-well plate [27]

Around the time Vandenburgh began his work with formation of skeletal muscle tissue in collagen matrixes in 1988, another group led by Strohman noticed that in-vitro formation of muscle tissue did not mimic in-vivo tissue formation due to lack of myotube transition to mature myofiber and the lack of critical tissue organization [29]. To try to combat this, Strohman seeded a primary avian culture of embryonic myoblasts and fibroblasts on top of Saran wrap fixed in place with metal pins. Upon formation of a monolayer of myotubes, the resulting tissue would detach from the Saran surface while remaining securely bound to the metal pins. The resulting tissue was highly contractile, dense, and myotubes were aligned in areas of near uniaxial stress. These myotubes expressed neonatal and adult forms of MHC, showing signs of enhanced maturation. Additionally, areas of what appeared to be connective tissue were present in the tissue, which the author attributed to the formation of the endomysium, perimysiem and epimysium [29].

Strohman's pioneering work inspired Dennis, who in 2000, noted that the mammalian skeletal muscle tissue constructs being generated by the Vandenburgh group necessarily required the addition of an exogenous ECM scaffold such as collagen or Matrigel [30]. The Dennis group was interested in characterizing contractile forces of tissue-engineered muscle constructs and believed that the use of exogenous ECM may interfere with force measurements. To accomplish the formation of exogenous-scaffold-free mammalian tissue constructs, the Dennis group plated primary rat myogenic biopsy cultures onto lamanin-coated PDMS. Inspired by the work of Strohman, the Dennis group used lamanin-coated silk sutures that were fixed to the plate to act as anchors. The fibroblasts within the biopsy culture were theoretically responsible for the deposition of ECM. Once confluency was reached and myotubes began to form, the monolayer delaminated from the underlying substrate, remaining attached to the anchors (Similar to the Strohman method). The delaminated monolayer subsequently rolled up to form a dense 3D tissue between the two anchors, shown in Figure 13. The Dennis group termed these constructs "myooids", as they resembled the structure and contractile function of native-muscle. However, these constructs produced a maximum force that was only 1% of native muscle capability. Additionally, myotubes did not express adult myosin isoforms and diameters were only between 5-20μm, again demonstrating the developmental block also observed in Vandenburgh's methods [30].

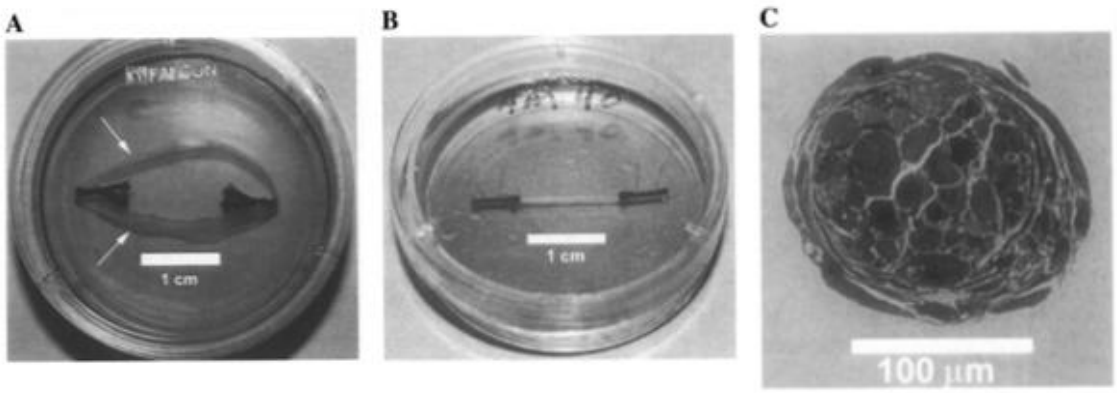

Figure 13: A: Representative image of a delaminating monolayer. B: Representative image of a rolled-up delaminated monolayer, remaining anchored to lamanin-coated suture anchors. C: Cross-section of a construct, showing similar structure to native muscle [30].

In a 2005 article, Huang and Dennis noted the primary weaknesses of his monolayer delamination tissue-engineering method [While these dense "myooids" were formed entirely of cell and cell produced products, they took up to a month to fully form due to the requirement of fibroblast secreted ECM. In an attempt to combat the excessive time required to form monolayer-delamination tissues, Dennis presented a system in which primary myoblasts were seeded onto a thin fibrin gel, which would subsequently contract around lamanin-coated silk suture anchors upon myotube formation. These tissues formed faster than Dennis's previous myooid constructs, however these fibrin-assisted self-assembled tissues showed poorer myotube density, similar to Vandenburgh and Powell's HBAMs that also used excess exogenous ECM. Typical of all current approaches to formation of skeletal muscle tissue, the fibrin-assisted self-assembled tissues were composed of small diameter immature myotubes (~10um) and were only able to produce a small fraction of native contraction force [5].

Dennis had shown that his fibrin-assisted self-assembled tissues did not allow for complete fibrin degradation and thus sufficient cell-cell contact was not achieved and the density and maturity of the tissue suffered. By 2011 Dennis showed that these tissues could be improved

by the incorporation of fibroblasts within the tissue constructs. However, the role of the fibroblasts remained unexplained [31]. Another group later conducted a study examining the role of fibroblasts in these fibrin-assisted self-assembled tissues. By forming constructs with Dennis' fibrin-assisted self-assembly method using primary mouse myoblasts and mouse embryonic fibroblasts, it was shown that fibroblasts maintained myotube viability, played a large role in fibrin scaffold degradation and remodeling, and assisted in the rolling of the delaminated cell-fibrin sheet [31].

The various shortfalls of existing tissue-engineering techniques for the formation of biomimetic skeletal muscle constructs led the Page Lab to develop a novel self-assembly process [32]. Primary myogenic cultures containing myogenic cells and fibroblasts are partially differentiated in 2D, and then suspended in media and cast into V-bottom ring molds. The tissues are left to completely differentiate and are capable of forming dense and highly organized skeletal muscle tissue in-vitro, shown in Figure 14. Additionally, the self-assembly method is capable of producing myotubes of up to 100μm in diameter, essentially identical in size to native myotubes. No other culture method has been able to produce myotubes with diameters above 20um. It should be noted that not all myotubes produced by the self-assembly method are of this large size, but the fact that it is capable of producing even one such fiber is a promising indicator of the potential of this method for producing mature tissues [32].

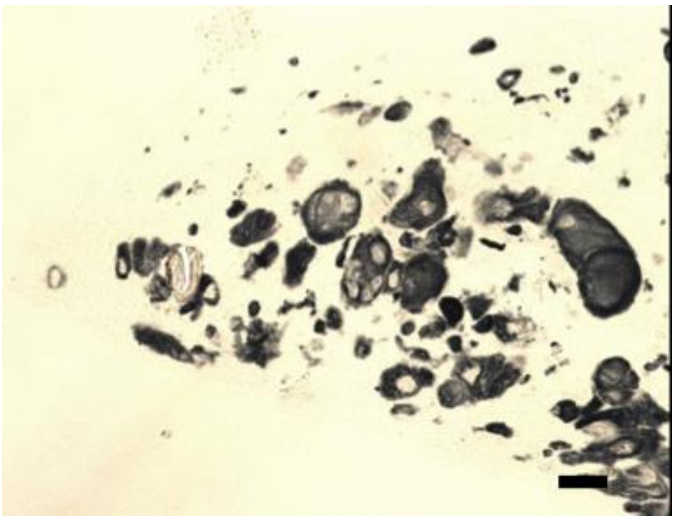

Figure 14: Representative cross-section of a self-assembled tissue-ring from the Page Lab. Black staining is for myosin [32].

2.6.2 Cell Selection

Researchers have used and tested a variety of cell types while attempting to construct tissue-engineered muscle. Early papers preferred the use of avian stem cells due to their ease of obtaining and relatively cheap cost. Mouse and rat cell lines such as C2C12 came into use due to their cheapness and ease of culturing [30]. They have the drawback of not perfectly mimicking primary cells, which is non-ideal because the ultimate goal of skeletal muscle tissue-engineering is to imitate natural muscle as closely as possible. Since 2000 rat and mouse primary cells have seen an increase in use as they form better biomimicry constructs [33, 31]. As technique for tissue-engineering improved Human primary cells came into use [33]. Human primary cells show similar alignment and density to rodent cells and bring tissue-engineering closer to the goal of truly biomimetic constructs. They have the drawback of being harder to obtain and therefore more expensive than rat and mouse primary cells.

Many of these papers use myoblasts only [28]. Some studies also co-cultured with fibroblasts to allow for self-assembled ECMs [30]. They either used primary fibroblasts from the

same animal [31], fibroblast like cells such as 10T1/2 [30], or primary biopsy culture containing both myogenic cells and fibroblasts [30].

2.6.3 Differentiation Techniques

Researchers have taken several different approaches to induce myogenic differentiation in vitro. Over the years research groups have continuously altered differentiation protocols as they refine their methods and use new cell types. Typically cells are seed and maintained in growth media than switched to differentiation media. Some groups switch to maintenance media after differentiation and some continue with differentiation media. Due to the high variance the differentiation methods are summarized in Table 1 below.

Table 2: Summary of various techniques for induction of myogenic differentiation.

Paper	Cell	Growth Media	Differentiation	Maintenance Media
Dennis and Kosnick II 2000	Primary rat myogenic co-culturing, no exogenous ECM, monolayer delamination	f12 with 20% FBS 3-8 days in growth media or until confluence	DMEM 7% Horse serum until monolayer delamination (2-3 weeks)	NA
Huang et al. 2005 (Dennis)	Primary rat myoblast only in fibrin	10% FBS 5 ng/ml FGS-2 in F12K media	6% heat-inactivated FBS in DMEM containing	NA
Vandenburgh 1997	Cells suspended in Matrigel collagen solution	20% FBS, HAMs F-10 media 3 days	High glucose DMEM 10% Horse serum for 3 days	high glucose DMEM, 10% Horse serum, 5% FBS, up to 4 weeks
Vandenburgh 2002	Primary human cells	mgm:skgm 15% FBS 3 days	High glucose DMEM 2% Horse serum for 5 days	high glucose DMEM, 10% Horse serum, 5% FBS, up to 4 weeks
Li 2011	Primary Mouse Myoblasts and Mouse Embryonic Fibroblasts	HAMs F-10 20% FBS, recombinant human fibroblast growth factor	DMEM with 5% Horse Serum	NA

2.7 Strategies for the Advancement of Engineered Tissues

All tissue-engineered skeletal muscle to date has shown a developmental block in tissue maturity. Namely, in the transition from neonatal myotubes to mature myofibers. Many groups have utilized mechanical or electrical stimulation in an attempt to improve tissue maturity, and their efforts are reviewed below.

2.7.1 Electrical Stimulation of In-Vitro Skeletal Muscle

It has been known for decades that muscular hypertrophy in skeletal muscle results in an increase in protein expression and decreases in protein degradation [34]. While contractions are

triggered by motor-neurons in-vivo, in 1976, a group demonstrated that the effects of hypertrophy could be mimicked in de-nervated skeletal in-vitro by stimulating differentiated myotubes electrically. Further, the group showed that the increased protein expression is due primarily to an increase in contractile protein synthesis, such as myosin heavy chain [34].

Proteins involved directly in contraction, such as myosin heavy chain, are not the only proteins essential for the process. One of the key pieces to muscle contraction is the transport of glucose into the cell to ultimately provide the ATP necessary for contraction. It has been shown that electrical stimulation is capable of up-regulating glucose intake through both insulin and GLUT4 dependent pathways [35]. Additionally, it has been show that embryonic-derived skeletal muscle further matures when stimulated in-vitro [36]. While unstimulated myotubes derived from avian embryos express an embryonic form of myosin heavy chain, stimulated myotubes express a form of late-embryonic myosin heavy chain, indicating a role of electrical stimulation in skeletal muscle maturation.

These observations led Dennis to evaluate the effects of electrical stimulation on his fibrin-assisted self-assembly tissue models, shown in Figure 15 [37]. Consistent with prior research, Dennis saw increased excitability and force production from electrically stimulated tissues, indicating an advance in maturity. Dennis raises some key points about the stimulation of 3D muscle tissue. The purpose of electrical stimulation is to mimic the function of motor-neurons, which trigger the propagation of an action potential across the myotube membrane, ultimately triggering release of calcium from the sarcoplasmic reticulum, thus triggering contraction. Dennis shows that electrical field strength effects force production and excitability significantly. Field strengths of 2.5 V/mm show the highest increase in excitability and force

production. Field strengths above 5 V/mm show detrimental effects on excitability and force production, likely due to electrochemical damage to the tissues.

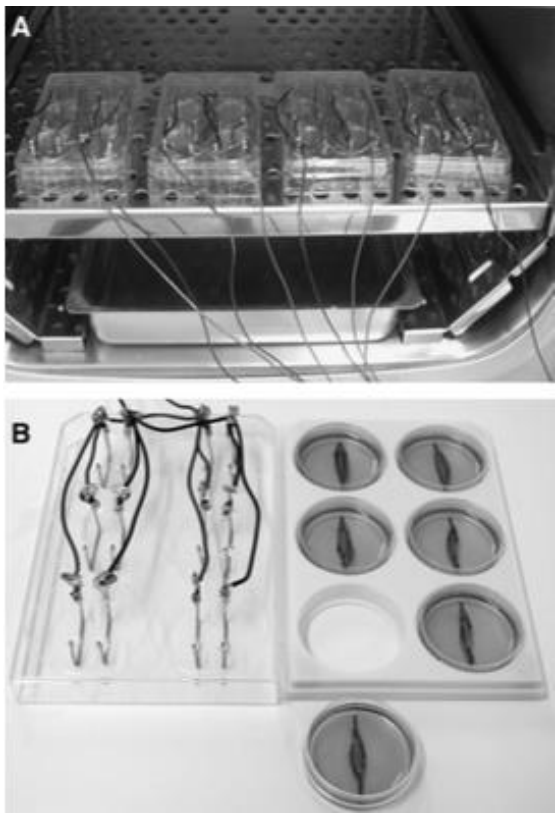

Figure 15: A: Representative image of Dennis's electrical stimulation platform in an incubator. B: Representative image of the electrode configuration with a 6-well plate [37].

2.7.2 Existing Platforms for the Electrical Stimulation of Skeletal Muscle Constructs

This section discusses various electrical stimulation platforms that are commercially available or available through the Page Lab. Only systems that could potentially stimulate 3D in-vitro skeletal muscle constructs are discussed.

IonOptix C-Pace EP Culture Stimulator for Chronic Pacing and C-Dish [38].

The IonOptix electrical stimulation platform consists of a multichannel programmable power box and custom C-Dish electrode plates that are compatible with standard 4-well, 6-well, and 8-well culture plate models in Figure 16. The system is capable of outputting pulses with 0.4-24 ms duration, a voltage of up to 40V, with frequency from 0.010-99Hz. This system has been used in various research applications including studies investigating the effects of electrical stimulation on skeletal myotubes [39,40]

Figure 16: IonOptix C-Pace EP prgrammable multi-channel power source and 6-well electrode plate lid [38]

In terms of the IonOptix system as an electrical stimulation platform for a high-throughput tissue-engineering system, the C-Pace falls short. The C-Pace EP system is not compatible with a 96-well plate, which limits its potential for high-throughput applications. Additionally, the C-Pace EP system cannot produce pulses with a duration of under 0.4 ms

Myomics MyoForce Analysis System (MFASTM) [41]

Vandenburgh's company Myomics used the MyoForce Analysis System (MFASTM) electrical stimulation platform. The platform was not designed to stimulate constructs for the purpose of maturation; rather it was designed to trigger tetanic contractions for the purpose of contractile assessment of mBAMs. The system could theoretically be used to provide electrical stimulation regimens for the purpose of tissue maturity enhancement, however the system is only capable of stimulating one tissue construct at a time. This, accompanied by the fact that the system functions outside of an incubator, means the MFASTM is unsuitable for the high-throughput stimulation of tissue-engineered skeletal muscle constructs.

MQP-RLP-1502 Electrical Stimulation Lid

A 2015 WPI MQP team, MQP-RLP-1502, was commissioned to address the lack of an existing platform for the high-throughput stimulation of tissue-engineered skeletal muscle constructs. The group created a 96-electrode stimulation lid (Figure 17). The lid is controlled by an Arduino Uno microcontroller, which allows for the programming of an automated customizable stimulation regimen. The device is EtO sterilizable, corrosion resistant, functional in an incubator, and is able to establish maximum of 4.8V across stainless steel electrodes. The device is designed for use in a in a 96-well plate, with stainless steel electrodes in each well attached to brass buss-bars. The lid is capable of establishing a maximum electric field of ~1.6 V/mm, however the field strength is adjustable using potentiometers [42].

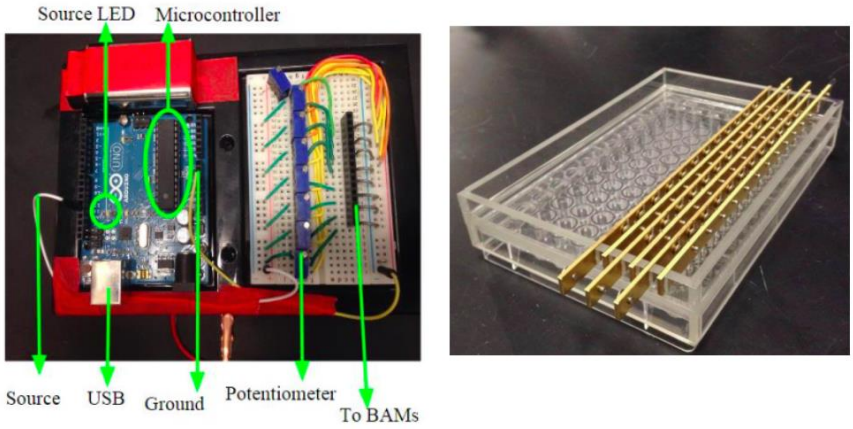

Figure 17: Left: Programmable Adriano Microcontroller and breadboard circuit. Right: Electrical stimulation lid with buss-bar-mounted electrodes [42].

This stimulation platform addresses the need for high-throughput stimulation, however there are areas for improvement. The MQP-RLP_1502 group stated that the lid is capable of establishing an electric field of 2 V/mm, which is close to the optimal 2.5 V/mm [37], however the system is currently incapable of actually establishing field strength of that magnitude. A DC-DC converter could be added to the system to allow for higher electrical field strength.

2.7.3 Mechanical Stimulation

It is concluded that bone elongation (2 mm/wk) initializes organogenesis. Over the years, it has been shown that mechanical stimulation is able to improve in-vitro skeletal muscle generation [26]. This is because mechanical stimulation mimics the elongation, movement, tension, and stresses caused on skeletal muscle cells; aiding in muscle maturity and hypertrophy. The passive tension applied to the skeletal muscle by the elongated bone influences its weight, length, and density (myofilament organization). Repetitive stretch and relaxation of avian and rodent skeletal muscle cells altered the structural organization of the engineering constructs tested on a rodent; bio-mimicking native tissue.

2.7.4 Existing Platforms for the Mechanical Stimulation of Skeletal Muscle Constructs

This section discusses various mechanical stimulation platforms that are commercially available or available through the Page Lab. Only systems that could potentially stimulate 3D in-vitro skeletal muscle constructs are discussed.

Mechanical Cell Stimulator, Version 4.0

The Vandenberg group developed a mechanical cell stimulator device to aid in mechanical stimulation of their constructs [26].

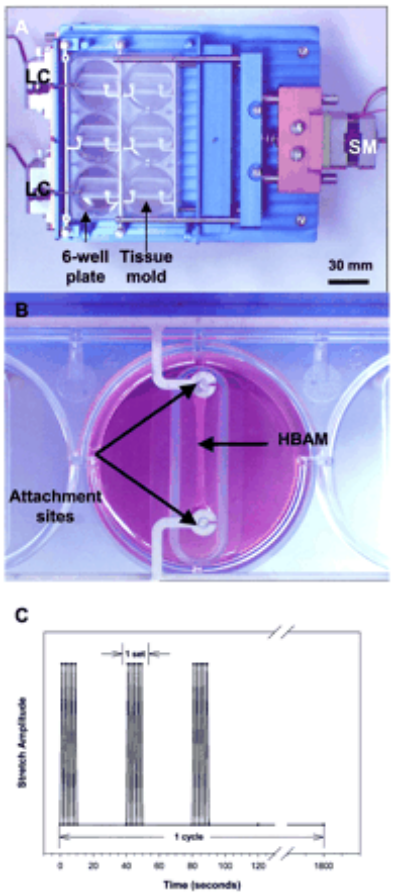

Figure 18. Vanderburg's mechanical stimulation device [26].

The system utilized designed well plates plate that experimented with exogenous ECM for human bio-artificial muscles (hBAM). A mechanical lid was designed to physically stretch and relax the BAMS. The system contained a stepper motor that is able to translocate a pin attached in each culture well. The device contained a transparent cover that was placed on top of the cultured wells for sterility and protection. Each well contained 2 attachment sites that the mechanical lid rested and anchored to. They induced 3 sets of 5 stretches/relaxation for 28 minutes. Of the original 20 mm construct length, a 5% strain was applied for 2 days, 10% strain applied for another 2 days, and lastly 15% strain applied for 4 days. The results showed an increase in myotube alignment, in which myotubes were taking a parallel configuration/orientation. A 12% increase in the myofiber diameter was also observed following the regimen; indicating that mechanical stimulation is vital to hypertrophy [26].

MQP-RLP-1501 Mechanical Stimulation Lid

Prof. Page's previous MQP team was able to develop a rotating-pin mechanical stimulation lid. The lid worked on a standard 96-well plate. The mechanical lid contained L-shaped rods that were placed on the inside of the lid; suspending the L shaped rods inside each well. The system worked with a hydraulic pump, in which a syringe automatic-pumper was used to adjust hydraulic pressures. The functionality of the lid worked on the premises that the tissue constructs within each well were surrounding PDMS posts; a PDMS post would protrude out of the well. The hydraulic pump system would create pressure that pushes on a rubber-plastic moving slider that induces the L-shaped rods to rotate; creating strain on the tissue construct that is around the PDMS post. As the PDMS post moves due to the rotating rods, mechanical stimulation of the construct takes place [43].

Figure 19. The designed hydraulic system that controls a mechanical stimulating lid; rotating L-shaped rods to induce mechanical stimulation [43].

Chapter 3: Project Strategy

This Chapter describes the various strategies utilized by the team to narrow the design space and set the stage for the rest of the design process. A revised client statement is defined and used to set various objectives, requirements, constraints, specifications, and functions. Approaches to management strategy are also discussed.

3.1 Initial Client Statement

The initial statement by the client asked for the design of functional in-vitro human skeletal muscle tissue constructs biomimetic of native tissue and capable of high-throughput production and testing. The constructs should eventually be able to recapitulate human muscular disorders to improve preclinical pharmaceutical testing. Furthermore, the constructs must be able to be assessed for contractile function and characterization of a variety of metrics including: fiber alignment, stimulation, maturation, cell density, and ECM composition.

This initial statement is extremely broad and allows for numerous approaches. While the vagueness of the initial client statement establishes a very "open" design space, further narrowing down of the design space was needed to allow the formation of an explicit project approach.

3.2 Revised Client Statement

Through research and discussion with the client, it was determined that many of the design requirements mentioned in the initial client statement are inherently built into the Myomics drug-screening platform. As previously mentioned, this system allows for the high-throughput production of human skeletal muscle tissue models that are anchored to flexible PDMS posts in 96-well plates. The system uses a custom automated plate handler to position each tissue construct between two electrodes that trigger tetanic contraction and allow for contractile assessment via post-deflection. The central disadvantage of the Myomics platform is

the biomimicry of the tissue constructs themselves. The tissues are less dense, less mature, and much weaker than native muscle. Thus, pharmaceutical companies are hesitant to adopt the technology. It was through this line of logic that allowed the establishment of a revised client statement with specific goals that explicitly defined the design space for this project:

"Engineer a device, or set of devices, capable of improving tissue biomimicry via electrical and mechanical stimulation. This device(s) should preserve the high-throughput nature of the Myomics system and should be compatible with the Myomics method of contractile assessment."

Thus, our device(s) should be compatible with tissues mounted on the PDMS posts used by Myomics. This will allow anchorage of the tissues in a way that mimics the myotendinous junction, and will allow high-throughput contractile assessment via post-deflection through use of the Myomics custom plate handler. Additionally, the team is not limited to the use of a fibrin-assisted self-assembly methods of tissue-engineering. While the mBAMs used in the Myomics platform are formed via this method, other tissue-engineering strategies are to be explored and evaluated for benefits over the traditional mBAM method.

The revised client statement allowed the team to generate a list of needs and wants in order to gain a deeper understanding of what must be accomplished by the design project. A desirable for the project can be classified as either a need or a want. A *need* is a feature required for the project while a *want* is a feature that can improve the final product but is not required/unobtainable. The team ranked each desirable on a needs scale of 1-10 in which the value 1 represents a feature that is completely not required and the value 10 represents a feature that is absolutely required. Desirables ranging from 8-10 were considered needs, while anything below was considered a want. The needs and wants of the sponsor are depicted in Table 2 below.

Table 3: Needs and Wants for the team's project assessed on scores from 1-10; 10 being an immediate need, and 1 being not required.

Desired Design Component/Function	Ranking (1-10)	Rationale	Need or Want
Viable Tissue Formation	10	Mature living tissue is necessary for any sort of assessment	Need
Mechanical Stimulation in Incubator	9	Enhances muscle cell maturation, expected to be essential in the formation of biomimetic tissue	Need
Electrical Stimulation in Incubator	9	Enhances muscle cell maturation, expected to be essential in the formation of biomimetic tissue	Need
Biomimetic Tissue Generation	7	Needed in order to create accurate skeletal muscle models, disease models; while compete biomimicry is ideal, we expect that this is largely unattainable	Want
High-Throughput Production	10	Listed as need in client statement; essential for use in pharmaceutical testing	Need
Contractile Assessment	10	As function of skeletal muscle tissue is contraction, this metric provides the only option for complete assessment of tissue integrity; also listed as need in client statement	Need
User Friendly	5	Due to lack of existing muscle construct systems, we expect that users will be willing to sacrifice usability for results	Want
Biocompatibility/Sterility	10	Materials must be biocompatible to ensure tissue viability. Must allow for maintenance of sterile conditions.	Need

Needs:

It should be noted again that some of these project needs are met by inherent qualities of the Myomics system, for which our design is to be used in. High-throughput production and contractile assessment are met by the Myomics system itself, and thus our design must simply preserve these traits. Four other *needs* were established. One of the most important outcomes is the production of viable tissue; the formation of living muscular fibers that are able to proliferate, metabolize, and have contractile functionality. Mechanical and electrical stimulation of the muscle construct is vital to the proliferation, differentiation, viability, and overall growth. Native muscles grow significantly due to mechanical stimulation; the ability to physically create stress and strain on a muscle fiber, aiding in hypertrophy [44]. As observed in almost all living organisms possessing skeletal muscle fibers, the more a muscle fiber is subjected to cyclic strain, stress, and relaxation periods, the bigger, thicker, and denser it is. This is caused by the shear stress that 'rips' muscle fibers, inducing a healing process utilizing satellite cells alongside proteins, and growth hormones; leading to denser muscle constructs. Not only has mechanical stimulation been shown to aid in tissue maturity, but uni-axial strain has been show to enhance fiber alignment [45]. Desired mechanical stimulation is within 10-15% of stretch/relaxation of original tissue length. Electrical stimulation is vital due to the fact that muscles cannot contract without an electrical charge/action-potential response. Muscles contract and release based on the activation/action-potentials generated by the peripheral nervous system; passing an electrical charge throughout the fibers along the axons/dendrites causing a contractile motion. To fully assess a viable biomimetic muscle construct, it must be mechanically stimulated for hypertrophy, and electrically stimulated for contractile assessment and proper growth. Both of these stimulation techniques should be implemented over long periods of time, and thus must function

in an incubator. Lastly, biocompatibility and sterility is crucial when working with live media, insuring that no cytotoxicity or contamination occurs in the system; causing adverse effects such cell death, slow growth, or sub-optimal tissues.

Wants:

The team determined two *wants* for the project. The first being the formation of perfectly biomimetic tissue constructs. While this would be ideal, and would represent a huge leap in the field of skeletal muscle tissue-engineering, this feat is expected to be largely unattainable and is outside the scope of this project. The constructs should merely be as biomimetic as is possible with the current technology, and should improve upon areas lacking in current approaches. The second *want* is ease of use of the device(s). Due to the lack of existing high-throughput tissue-maturing systems for skeletal muscle, the team reasons that potential clients will be willing to sacrifice ease of use. Additionally, tissue-engineering systems are often complex and require specialized technicians, and thus are not typically expected to be entirely user-friendly.

3.3 Technical Design Requirements

To meet the needs and wants of the client, the team can further breakdown the project into design objectives from which explicit functions and feasible means can be elucidated. By first deciding what the system must do in a broad sense, the team can then determine specific functions, brainstorm means, and conceptualize alternative designs.

3.3.1 Design Objectives

From the revised client statement, a set of three primary objectives for the project can be determined:

1) Enhance tissue maturity and density to form more biomimetic tissues
2) Compatible with Myomics drug-screening platform
3) Preserve high-throughput nature of Myomics drug-screening platform

Objective 1 states that our device(s) must be capable of enhancing tissue maturity, thus overcoming the main limitation of the Myomics drug-screening platform. As discussed in the literature review, the mBAM tissues used by Myomics lacked cell density (~6% myotube) when compared to native tissues (90% myofiber). The tissues also lacked maturity, with the mBAMs consisting of immature neonatal-like myotubes with diameters of only ~6μm. Compared to mature native myofibers with diameters of ~100um, the mBAM tissues clearly show a lack of maturity and thus a lack of biomimicry. Our device should help overcome the developmental block seen in Myomics' traditional mBAM tissues and should improve the above-mentioned metrics to values closer to those of native tissue.

Objective 2 states that our device(s) must be compatible with the Myomics drug-screening platform. This means that tissues must be anchored to flexible PDMS posts in 96-well plates. The device must also allow contractile assessment via post deflection as facilitated by the

existing Myomics MyoForce Analysis System, which uses two electrodes on either side of the tissue (parallel to tissue alignment) to trigger tetanic contraction.

Objective 3 states that our device(s) must preserve the high-throughput nature of the Myomics drug-screening platform. This means that our device must act upon all tissues within a 96-well plate at once and should provide tissue maturation techniques in a way that minimizes the required labor and time necessary for tissue maturation.

3.3.2 Design Requirements

From the objectives mentioned above, four main design requirements can be elucidated:

1) Use of most appropriate tissue-engineering method
2) Mechanical stimulation of tissue constructs
    a. Adjustable and customizable strain regimens
    b. Displace tissue anchorage (PDMS posts)
    c. Act upon all tissues in 96-well plate to preserve high-throughput capabilities of the Myomics system
3) Electrical stimulation of tissue constructs
    a. Adjustable and customizable electrical stimulation regimens
    b. Establish an electrical field capable of inducing contraction
    c. Act upon all tissues in a 96-well plate to preserve high-throughput capabilities of the Myomics system
4) Function in incubator
5) Biocompatible
6) Maintain sterility
7) Maintain user safety

Design requirement 1 states that the design should utilize the most appropriate tissue-engineering method, meaning that the team is not limited to the fibrin-assisted method of mBAM formation. The tissue-engineering method chosen for the final design should be best suited to the production of biomimetic tissues. Design requirement 2 states that the device(s) should provide mechanical stimulation to the tissues. As discussed in the literature review, mechanical stimulation has been shown to enhance tissue biomimicry by improving myotube alignment, improving tissue density, improving protein synthesis, and increasing myotube diameter. The device(s) should allow the implementation of customizable and automated strain regimens and should act upon all tissues in a 96-well plate. The tissues should be mechanically stimulated via the displacement of the PDMS posts to which the tissues are to be anchored. Design requirement 3 states that the device(s) should provide electrical stimulation to the tissues. As discussed in the literature review, electrical stimulation has been shown to enhance tissue maturity by mimicking skeletal muscle innervation and has been shown to improve myotube alignment, myotube diameter, and protein synthesis. The devices(s) should allow the implementation of an adjustable and customizable electrical stimulation regimen and should provide electrical stimulation to all tissues in a 96-well plate. Design requirement 4 states that the device(s) should function within an incubator environment. This requirement stems from the fact that mechanical and electrical stimulation regimens often span several hours. Since the tissues likely cannot survive outside of an incubator for such a long time period, the tissues must be conditioned within an incubator. Requirement 5 limits the materials used in the design(s). Any material that is to come into contact with cells or media must be biocompatible, meaning that it must not exhibit any cytotoxic effects. This will ensure the formation of healthy, functional tissue constructs. Requirement 6 stems from the fact that cells in culture must be kept sterile to prevent bacterial or

fungal contamination. Prevention of contamination ensures the formation of healthy, viable tissue constructs. Requirement 7 states that the device(s) must ensure the safety of the device operator; it must be in compliance with standards set to preserve the Health and Safety of the operator from hazards and risks.

3.3.3 Design Specifications and Design Constraints

From the design requirements described above, specifications for our device(s) can be elucidated:

Specifications

1) Physiologically relevant strain regimens (0-30%)
2) Electric Field strength from 0-0.3 V/mm [46]

Specification 1 states that the device(s) must be a capable of providing physiologically relevant strains, which range from 0-30% [47].

This specification stems from the fact that skeletal muscles typically experience strains of up to 30% in vivo, and thus strain values in this region are likely to play an important role in the development of mature skeletal muscle tissue. Specification 2 states that the device(s) must be capable of providing electric fields from 0-0.3 V/mm. This specification stems from the work of Ikeda et al, who observed significant improvement in tissue maturity when hydrogel-assisted self-assembled tissues were stimulated at 0.3 V/mm [46].

The design requirements discussed in the previous section also give way to various design constraints:

1) Compatible with PDMS posts
    a. Dimensions → 4 mm tall, 3.2 mm apart
    b. Tissue placement
2) Incubator environment

a. 37 ˚C

b. 95% humidity

c. 5% CO_2

3) Nutrient perfusion limits

a. Perfusion limit of 80-300 μm from nutrient source

4) Function in 96-well plate

a. Dimensions → 6.42 mm diameter, 11 mm depth

Constraint 1 is set by the requirement that the device(s) must act upon tissues mounted on PDMS posts. These posts are 3.2 mm apart and 4 mm in height. Constraint 2 stems from the requirement that the device(s) must function in an incubator environment. Incubators for conventional cell culture operate at 95% humidity, 5% CO_2, and 37˚C. Constraint 3 stems from the fact that cells can only survive when they are 80-300 μm from their nutrient source (i.e. the media). This sets hard constraints for our tissue size, meaning that a cylindrical tissue can have a maximum of a 300μm radius. If this limit is exceeded, cells in the center of the tissue may die. This would result in a necrotic tissue core, which could severely impact the tissues biomimicry. Constraint 4 stems from the requirement that the device(s) must be compatible with the Myomics drug-screening platform and must also preserve the high-throughput nature of that system. This means that the device(s) must function within a 96-well plate, with well dimensions 6.42 mm diameter and 11 mm well depth.

3.3.4 Design Functions

From the objectives, requirements, specifications, and constraints described in the previous sections, a list of design functions and sub-functions can be elucidated.

1. Appropriate tissue-engineering method
    - Produce the most biomimetic tissue constructs possible

- Compatible with dual-post anchorage system

2. Electrical stimulation of the tissue constructs
    - Stimulate tissue constructs, mimicking native electrical contraction inductions
    - Capable of accurate, controlled and automated stimulation regimens on a dual-post anchorage system
    - Cause no harm to neither the culturing method nor the tissue constructs
    - Function in a 96-well plate for high-throughput production
3. Mechanical stimulation of tissue constructs
    - Stimulates tissue constructs, mimicking native mechanical stretching and relaxation
    - Displace anchorage points
    - Capable of accurate, controlled and automated stimulation regimens on a dual-post anchorage system
    - Cause no harm to either the culturing method nor the tissue constructs
    - Function in a 96-well plate for high-throughput production

3.3.5 Design Standards

The design of the tissue-engineering system must adhere to various industry standards in order to ensure the safety and effective operation of the entire system. Below is a table of relevant industry standards as set by the FDA, ISO, and ANSI:

Table 4: Industry Standards

Tissue and Cell Culture	Biocompatibility	Sterility	Environment	Laboratory Equipment and Techniques
ISO 22442-2:2007 Sourcing, collection and handling of animals and tissues	ISO 10993-1:2009 Biological evaluation of biocompatibility of medical devices	ISO 11737-2:2009 Sterilization of medical devices	ISO 17422:2002 Plastic environment impact	ISO/NP 20391-1 Guidance on cell counting methods
ISO 13022:2012 Management of viable human cells				ANSI SLAS Microplate Standard: Dimensions of 96-well plate
ISO 22432-1:2007 Management of animal tissues and their derivatives				ISO 7712:1985 Use of disposable micropipettes
				ISO 7550:1985 Use of disposable serological pipettes

The tissue and cell culture standards ensure that the design will meet the safety requirements associated with tissue culture. They will also ensure that accurate results can be produced, and that poor cell handling, or improper culture technique does not affect those results. Biocompatibility standards will ensure the device does not damage the cells or affect their growth negatively. If the cells are damaged during device operation our results will be inaccurate. These standards provide clear methodology to ensure that the device materials are

indeed biocompatible. Sterility standards will ensure that the device will be able to be properly sterilized to prevent cross contamination during use. These standards, like the tissue culture standards, will ensure the health of the cells and tissues on which the device operates. Environment standards help prevent environmental damage. These standards provide methodology to evaluate the impact of the device and device materials on the environment. These standards also advise on the safe use of hazardous substances, as well as recommend ways to avoid material waste. The laboratory equipment standards will ensure we produce accurate assessment of our device's efficacy. They also make ensure the device is built to the standards of other laboratory equipment such as the 96-well plate.

The American National Standards Institute, Inc, ANSI, has set specific standards for the production and manufacturing of 96-well plates. The wells of a 96-well plate should be arranged as eight rows by twelve columns. The distance between the left-outside edge of the plate and the center of the first column of the well must be 0.5661in (14.38 mm). The left edge of the part will be defined as the two 12.7 mm areas (as measured from the corners) as specified in SBS-1; while maintaining 9mm (0.3543in) for each following column from the left outside edge of the 96-well plate. The distance between the center of the first row of wells and the top outside edge of the plate must be 0.4425in (11.24 mm). The top edge of the part is defined as two 12.7 mm measured from the corners; following the standards from SBS-1. Each following row shall be an additional 9mm (0.3543 inches) in distance from the top outside edge of the plate. The positional tolerance of the well centers will be specified using so called "True Position". The center of each well will be within a 0.70 mm (0.0276 inches) diameter of the specified location. The plate would be marked with the letter A or numeral 1 located on the left-hand side of the well. The top well of the place can be marked with a numeral 1 located on the upper side of the well.

In order for users to effectively utilize this device, several applicable electrical standards were employed during the design process. IEC 61010-031 specifies the safety requirements for electrical equipment within the laboratory setting and includes a provision on handheld probes. IEC 61010-2-030 goes further and specifies the safety requirements of equipment having testing and/or measuring circuits. IEC 61243-3 gives the safety requirements for working with live voltages. IEC 61010-2-081 was especially important in respect to this project because it specified the requirements for automatic and semi-automatic laboratory equipment, a major component of the final design. IEC 61010-2-101 was also employed for its requirements regarding *in vitro* diagnostic medical equipment.

Chapter 4: Design Process

Each of the three design functions described in the previous section has its own set of sub-functions, and thus each function was approached as an individual 'functional block'. The design process was conducted on each functional block separately, the details of which will be described in the following order:

1. Tissue-engineering
2. Electrical Stimulation
3. Mechanical Stimulation

4.1 Tissue-engineering

To determine the tissue-engineering method best suited to form the most biomimetic tissue constructs, the team reviewed literature and discussed with members of the Page Lab. Three main approaches for the formation of tissue-engineered skeletal muscle constructs have emerged over the years, each of which are thoroughly described in Chapter 2. Briefly, the first method is hydrogel-assisted self-assembly tissue-engineering. Tissues of this type are formed from myoblast-only or myoblast-fibroblast co-cultures that are seeded within an exogenous matrix material such as collagen or fibrin. The cell-gel mix is set in the well of a tissue culture plate around a set of anchors (e.g. PDMS posts). As the cell-gel mixtures are cultured, the cells begin to digest the exogenous matrix material, causing the developing tissues to contract around the anchors, forming 'double-ended box-end wrench' shaped skeletal muscle constructs. This is the method used to form the mBAMs traditionally used in the Myomics drug-screening platform. The second tissue-engineering method is monolayer delamination. Tissues of this type are formed from a myoblast-fibroblast co-culture that is allowed to form a monolayer at the bottom of a tissue culture plate. When anchors (e.g. lamanin-coated sutures) are placed on the monolayer, the monolayer rolls up around itself, remaining anchored to the sutures. The third

tissue-engineering method is self-assembly, developed in the Page Lab by graduate student Jason Forte. Tissues of this type are formed from myoblast-fibroblast co-cultures that are seeded into V-shaped channels and are allowed to self-assemble into skeletal muscle tissue constructs.

4.1.1 Selection of Tissue-engineering Method

Table 4 was used to rank the tissue-engineering methods in regards to their ability to produce biomimetic tissues. Various tissue maturity metrics were assessed for each method and compared to native values. Each method was assigned a ranking (1-10) for each tissue maturity metric based upon how the metric compared to the native value.

Table 5: Tissue-engineering method comparison to native metrics.

	Native	Hydrogel-Assisted Self-Assembly	Monolayer Delamination	Self-Assembly
Myotube Alignment	0-10˚ deviation from axis of alignment (Rank 10)	0-10˚ deviation from axis of alignment [4] (Rank 10)	0-30˚ deviation from axis of alignment [31] (Rank 6)	0-20˚ deviation from axis of alignment [32] (Rank 9)
Myotube Diameter	100 μm (Rank 10)	7μm [4] (Rank 2)	5-20 μm [6] (Rank 3)	5-100 μm [32] (Rank 7)
Tissue Density (% area comprised of myotube)	90% myotube (Rank 10)	12% myotube [4] (Rank 2)	70-90% myotube [6] (Rank 9)	50-80% myotube [32] (Rank 8)
Rank	30	14	18	25

From Table 5 it was determined that the self-assembly tissue-engineering method held the most promise for the formation of biomimetic tissue constructs. While hydrogel/mold systems and hydrogel-assisted self-assembly systems generated tissues with poor cell density, the self-assembly method forms tissues with densities comparable to native human skeletal muscle. Additionally, the self-assembly method is capable of producing myotubes of up to 100 μm in diameter, essentially identical in size to native myotubes. No other culture method has been able

to produce myotubes with diameters above 15 μm. It should be noted that not all myotubes produced by the self-assembly method are of this large size, but the fact that it is capable of producing even one such fiber is a promising indicator of the potential of this method. The team hypothesizes that if self-assembled tissues are formed under uniaxial tension on PDMS posts and are subjected to mechanical and electrical stimulation, the biomimicry of the constructs could be greatly improved. The resulting tissue constructs could potentially represent the most biomimetic in-vitro model of human skeletal muscle to date.

4.1.2 Self-Assembly Tissue-engineering Means

As mentioned in the revised client statement, the tissues must be compatible with the Myomics drug-screening platform and must thus be formed around PDMS posts in a 96-well plate. Unfortunately, there currently exists no way to create self-assembled tissues anchored between two PDMS posts in a 96-well plate. To address this issue a functions-means table was created in order to help the team to generate conceptual designs that will allow the formation of self-assembled tissues anchored to PDMS posts in a 96-well plate. The two main self-assembly-specific functions are:

1) Provide a mold or channel in which to seed the myogenic co-culture
2) Allow removal of mold/channel material after tissue formation

Function 1 stems from the fact that this method of tissue-engineering necessarily requires a channel in which to seed cells in order to create a dense ‘double-ended box-end wrench’ shaped tissue construct. Function 2 stems from the fact that any material used to form a mold or channel must be removed after tissue formation in order for the tissue to be freely suspended and anchored only to the PDMS posts. Additionally, any material used to create a channel or mold will be in contact with the PDMS posts themselves, and thus may interfere with post-deflection

based contractile assessment. A functions-means table corresponding to these two functions can be seen in Table 6.

Table 6. Function/Means for tissue-engineering method.

Function	Means		
Mold/Channel	V-Shaped	U-Shaped	Flat-Bottom Shape
Removal of Mold/Channel	NIPAAm	Low-Melting Point Agarose	Manual Material Removal

4.1.3 Self-Assembly Tissue-engineering Conceptual Design

From conversations with Professor Page and Jason forte, it was determined that a mold/channel with a V-shaped geometry is best suited to produce highly dense self-assembled tissues. Thus, the team decided that the design concepts must form V-shaped channels in 96-well plates. As the molding material must be removed upon successful tissue formation, the team evaluated the various means proposed in Table 5. The first proposed material is poly(N-isopropylacrylamide) (NIPAAm). NIPAAm is a unique polymer due to its lower critical solution temperature of 32˚C; above this temperature the material is solid and will change to a liquid state when the temperature drops below this. Additionally, NIPAAm does not allow cellular adhesion and thus the cells would only be able to adhere to the PDMS posts. This characteristic would enable the cells to be seeded and cultured in a solid mold, which could then be removed once the tissue has formed by cooling the mold quickly to liquefy it, followed by careful aspiration of the NIPAAM, leaving the post-anchored muscle construct suspended in media. The second material evaluated was low-melting point agarose, which has a gel point of ~30˚C. Unfortunately, the gel point differs from the melting point in these types of material, with the melting point of low-melting point agarose being ~65˚C. This means that if the team were to use this material to form molds or channels in a 96-well plate, the gel would have to be heated to 65˚C in order to liquefy

and allow easy removal. This material was abandoned immediately as temperatures above 40˚C can cause cell death and extensive tissue damage. The third way of removing the mold material was manual removal in which the device operator would remove the mold material manually from the 96-well plate. This method was abandoned because the tissue constructs are fragile and may be damaged during material removal. Additionally, removal of molding material from a well of a 96-well plate may be physically difficult as these wells are very small and do not provide much room for maneuvering. From the rationale described above, the team generated a conceptual design that could form V-shaped channels around PDMS posts in NIPAAm in 96 well plates. A single well unit of this design is depicted in Figure 20.

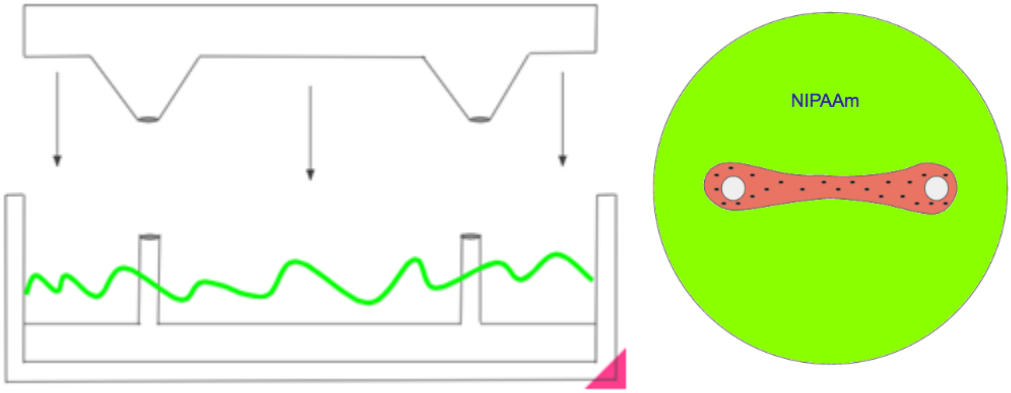

Figure 20. A single-well unit of the NIPAAm molding process

The mold would fit over the PDMS posts and would form a V-shaped 'double-ended box-end wrench' channel geometry in NIPAAm, which would be heated to 37˚C to solidify before the mold was removed. The cells could be seeded into this channel and tissue would be allowed to form before the NIPAAm is removed via cooling to at 4˚C and subsequent aspiration.

4.1.4 Self-Assembly Tissue-engineering Method Feasibility Study

The team had various concerns about this method. The first and foremost concern was that the post-holes would be too loose and would allow NIPAAm to seep into the holes, resulting in NIPAAm-coated posts which would be unable to support cellular adhesion. Another concern

stemmed from the size of the mold device itself. The mold device must fit into a well of a 96-well plate and therefore cannot exceed 6.8 mm in diameter. The well size and the PDMS post dimensions also restrict the channel dimensions. The channel must be established between posts that are only 3 mm apart and 4 mm in height, and result in a tissue construct that is suspended off of the well bottom. Additionally, the channel must be "double-ended box-end wrench" shaped and have a V-shaped cross-sectional geometry. The small size of this mold could present a challenge from a manufacturing perspective. Traditionally, molds are 3D printed in the Page Lab, however the small geometry of this particular mold may present a challenge for the 3D printers on Campus.

To determine the feasibility of 3D printing our mold, we created a SolidWorks model of a function mold unit, shown in the left panel of Figure 21, and had it printed on the most accurate 3D printer available to us, the Objet260 Connex Rapid Prototype Machine. The mold was printed with MED610, a biocompatible rigid polymer. The resulting mold is depicted in the right panel of Figure 21. A top view of the mold can be seen in the left panel of Figure 22, and the mold fit on top of a set of PDMS posts can be seen in the right panel of Figure 22.

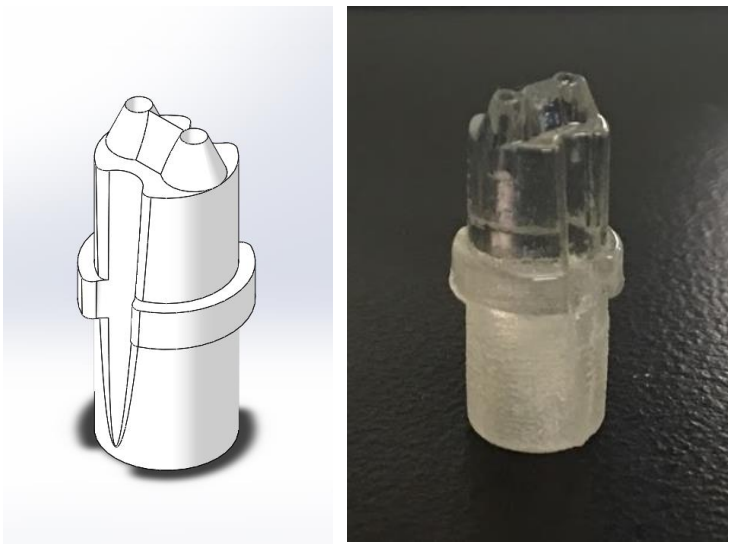

Figure 21. Left panel: CAD model of V-shaped NIPAAm mold. Right panel: image of 3D printed mold.

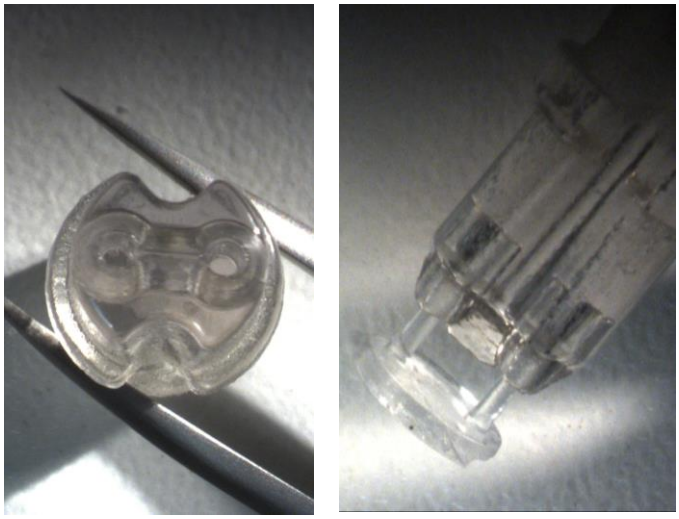

Figure 22. Left panel: Top view of 3D printed mold. Right panel: 3D printed mold with PDMS posts.

As can be seen in Figure 21, the mold was printed successfully. The team next assessed the feasibility of NIPAAm as a molding material by making a NIPAAm solution according to protocols provided by the Page Lab. Briefly, NIPAAm was dissolved in cold PBS to a

concentration of 2% and allowed to set in an oven at 47˚C for 30 minutes. Unfortunately, the resulting NIPAAm 'gel' did not have a consistency that would render it capable of holding a shape. The gel took the form of a viscous liquid, which, if left in the oven, formed a two-phase mixture. The two-phase mixture consisted of a loose and 'sticky' white NIPAAm material and a top liquid phase that was predominately PBS as seen in. The left panel of Figure 23 shows the NIPAAm dissolved in cold PBS, and the right panel of Figure 23 shows the 'clumped' NIPAAm after 20 minutes at 47˚C. From these observations, the team concluded that this conceptual design was non-viable.

Figure 20. Left panel: NIPAAm dissolves in cold PBS. Right panel: Clumping of NIPAAm solution after 20 minute at 47˚C

It was at this point that the team decided to revert back to the Tissue-engineering method conventionally used to create the mBAMS in the Myomics drug-screening platform; hydrogel-assisted self-assembly. This choice stemmed from the fact that this method is already tailored to the formation of tissue constructs mounted on PDMS posts in 96-well plates. Although this mBAM method yields tissues that are less biomimetic than self-assembled tissues, the team

hypothesized that mBAM biomimicry could be improved through the introduction of mechanical and electrical stimulation, and thus could meet the objectives set by the revised client statement.

4.2 Electrical Stimulation

As described in Chapter 2, native skeletal muscle tissue is innervated. Motor-neurons communicate with myofibers, sending chemical signals to initiate electrical action potentials thus stimulating myofiber contraction. The innervation of skeletal muscle has been shown to be critical for tissue integrity with non-innervated muscle tissue showing signs of atrophy and loss of function. One simple strategy to combat this issue when attempting to form tissue-engineered in-vitro models is to electrically stimulate the tissue, mimicking the electrical impulses and subsequent myofiber contractions that are facilitated by motor-neurons. Electrical stimulation has been shown to enhance differentiation and maturity of in-vitro muscle tissue by increasing expression of contractile proteins such as MHC [48,49].

4.2.1 Electrical Stimulation Means

The electrical stimulation device designed by the team must meet the functions described in Chapter 3, which are restated below:

1) Stimulate tissue constructs, mimicking native electrical contraction inductions
2) Capable of accurate, controlled and automated stimulation regimens on a dual-post anchorage system
3) Cause no harm to neither the culturing method nor the tissue constructs
4) Function in a 96-well plate for high-throughput production

A functions-means table corresponding to these functions can be found below in Table 7.

Table 7. Function/Means table for Electrical Stimulation.

Function	Means		
Stimulate Tissues	Metallic electrodes	Polymer electrodes	Contactless pulse delivery
Accurate and controlled regimen	Arduino Microcontroller	Raspberry Pi Microcontroller	Programmable Wave-generator
No harm to tissues	Stainless steel electrodes	Platinum electrodes	Contactless pulse delivery
Function in 96-well plate	96-electrode lid	Contactless pulse lid	

4.2.2 MQP-RLP-1502 Electrical Stimulation Lid

It should be noted that a previous MQP group, MQP RLP 1502, developed an electrical stimulation lid that meets the above functions. The stimulation lid is controlled by an Arduino Uno microcontroller, which allows for the programming of an automated customizable stimulation regimen. The device, shown in Figure 24, is EtO sterilizable, corrosion resistant, and is able to establish maximum of 4.8 V across stainless steel electrodes. When used in a 96-well plate, the lid is capable of establishing a maximum electric field of ~1.6 V/mm. However the field strength is adjustable using potentiometers.

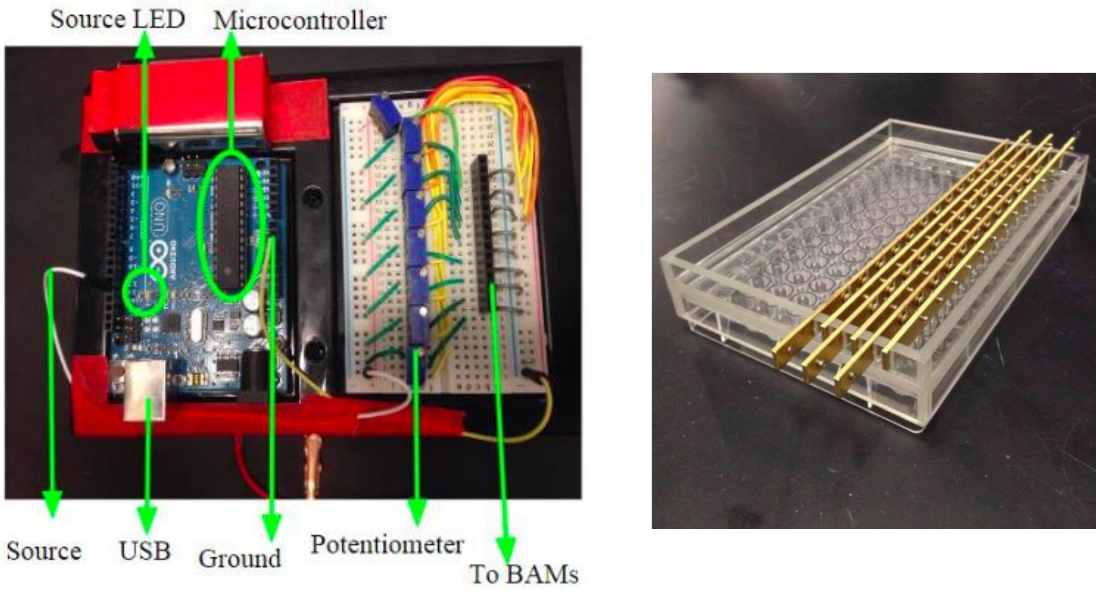

Figure 24: MQP-RLP-1501 Electrical Stimulation Lid

This stimulation lid provided a promising means to address our design need of electrical stimulation, thus before consideration of alternatives the team first validated the performance of the device. To accomplish this, the team assembled the device and bypassed the potentiometers in order to achieve a maximum electrode voltage of 4.8 V. A test regimen was programmed into the device. The test regimen consisted of five pulse trains delivered 100 milliseconds apart with individual pulse lengths of 10 seconds. The frequency of pulses within each train was 10 Hz. Using an oscilloscope wired across a single electrode, the team was able to detect a waveform that matched the programmed regimen perfectly. This simple study confirmed the ability of the device to deliver programmed electrical stimulation regimens at the required voltage.

It should also be noted that this lid is designed to stimulate hydrogel-assisted mBAM constructs mounted on PDMS posts in a 96-well plate, and thus is compatible with the Myomics drug-screening platform.

The team determined that this electrical stimulation lid presents a viable means to provide electrical stimulation for our tissue constructs. Not only will the lid perform its intended function

within our tissue-engineering system, but also the use of this pre-fabricated lid will save the team valuable time and resources that would otherwise be dedicated to the development of a new electrical stimulation system. For these reasons, the MQP-RPL-1502 electrical stimulation lid, or a variation of it, was chosen as a final system design component.

4.3 Mechanical Stimulation

As discussed in the literature review, skeletal muscle is subjected to mechanical forces during development. As such, mechanical stimulation has been used as a strategy to enhance tissue-engineered skeletal muscle maturity. Mechanical stimulation has been shown to increase muscle maturation, aiding in the betterment of myofiber alignment and increasing myofiber diameters and contractile protein production [26]. These factors improve overall tissue biomimicry of the cultured tissue, including contractile force.

4.3.1 Mechanical Stimulation Means

The team's mechanical stimulation device must meet the functions and sub-functions described in Chapter 3, which are restated below:

1. Stimulates tissue constructs, mimicking native mechanical stretching and relaxation
2. Displace anchorage points
3. Capable of accurate, controlled and automated stimulation regimens on a dual-post anchorage system
4. Cause no harm to either the culturing method nor the tissue constructs
5. Function in a 96-well plate for high-throughput production

A functions-means table corresponding to these functions can be seen below in Table 8.

Table 8: Functions/Mean for Mechanical Stimulation.

Function	Means				
Stimulate tissue constructs (force production and transfer)	Hydraulic system	Pneumatic system	Stepper-motor assembly	Brake cable assembly	Sliding Magnetic rack
Displace anchorage points	Sliding 'comb' rack	Magnetic Posts	'Balloon' post platform		
Accurate and automated stimulation regimens	Arduino microcontroller	Programmable syringe sump	Programmable air compressor	Raspberry Pi Microcontroller	
Cause no harm to tissues	No contact with cells or media	Biocompatible materials			
Function in 96-well plate	Sliding 'comb- rack with 96 combs	Magnetic Posts	96-balloon modification of 96-well plate		

4.3.2 MQP-RLP 1501 Mechanical Stimulation Lid

It should be noted that a previous MQP group, MQP-RLP-1501, made a lid capable of mechanically stimulating PDMS post-mounted tissue constructs in a 96-well plate. The lid uses a sliding frame, to which L-hooks are attached via rubber wheels. As the frame slides, the wheels rotate, and the L-hooks displace the PDMS posts. The force for the system is provided by a hydraulic system consisting of two syringes, a section of plastic tubing, and a programmable syringe pump. The lid was designed to be capable of actuating the posts to strain the tissue constructs 5-15%. Figures 25 and 26 show the design parts as well as the final assembly.

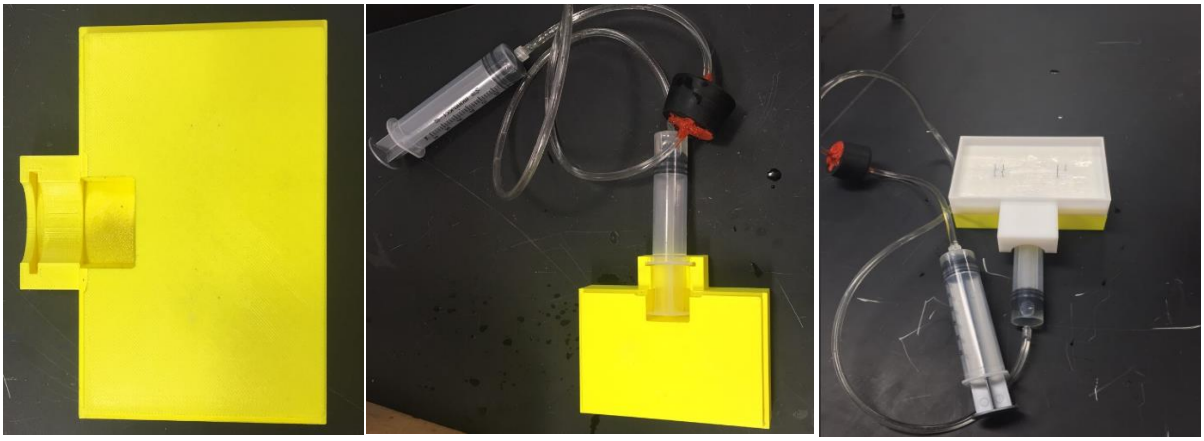

Figure 25. On the left is the top part of the mechanical lids; acting as a cover for the system. Center image shows the hydraulic system and lid assembly. Right image sows the completely assembled device.

Figure 26. Shows the mechanical lid's bottom piece; housing the L Shaped rods. Bottom-up on the left, top-down view on the right

This MQP-RLP-1501 lid represented a promising means to the mechanical stimulation objective of our tissue-engineering system, and thus before alternatives were considered, the MQP-RLP-1501 mechanical lid was tested by the team for feasibility as a final design component for our system.

To conduct a feasibility study, the system was tested for repeatability and accuracy. The bottom lid's L rods were first adjusted facing the same directional alignment; adjusted to be at 0 degrees for assessment, depicted below:

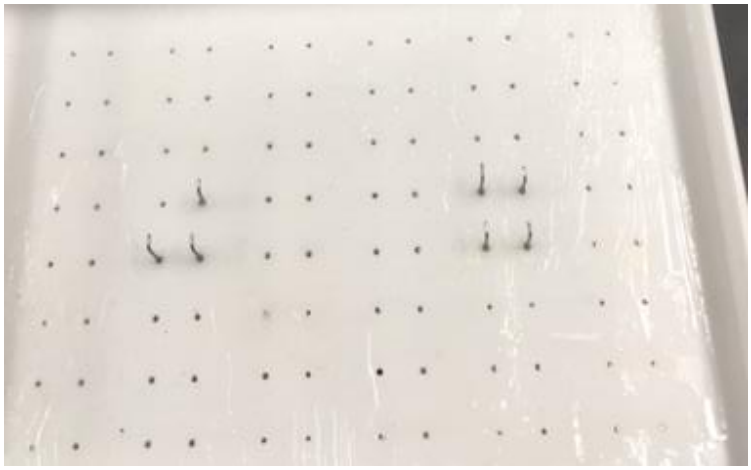

Figure 26. The bottom lid's L Shaped rods alignment along the horizontal access, adjusted to be 0 degrees

The lid was operated using a syringe pump adjusted to move the pins half a rotation. The pins should have moved 180 degrees clockwise. The feasibility test was run 5 times, and data was collected to quantify the accuracy and repeatability of the system. Below is a picture of the 4th trial:

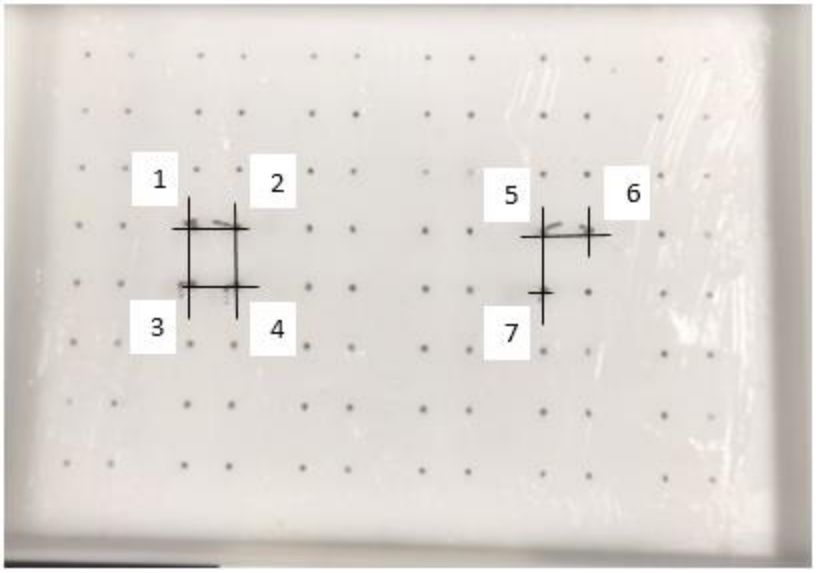

Figure 27. Shows the 4th trial of L-shaped rotation angles

The L shaped rods were never on sync throughout the 5 trials, nor did some of them fully move 180 degrees. The table below shows the 5 trials, including the angles that the L shaped rods rotated after adjusting to 0 degrees each trial:

Table 9: Angles corresponding to L Shaped rods for 5 trials.

Pin Number	1	2	3	4	5	6	7
Angles, each row represents a different trial	50	280	180	180	80	275	200
	40	290	170	170	75	280	200
	50	200	170	170	90	310	180
	50	240	190	180	60	290	180
	40	270	180	180	70	290	190

The inaccuracy and poor reproducibility is likely the result of varying levels of friction between the sliding rack and the rubber wheels, which would cause some L-rods to rotate more

or less than others. Another potential source of the poor accuracy and reproducibility could be poor precision within the hydraulic system itself. The syringes used were large, and thus had large rubber stoppers, which likely compress and decompress during the operation of the system. The results of this feasibility study suggest that the MQP-RLP-1501 mechanical stimulation lid may not represent a viable means to the mechanical stimulation functional block, and thus this lid was abandoned as a final design component.

4.3.3 Mechanical Stimulation Conceptual Designs

Using the functions-means table described in the previous section, the team generated three conceptual designs to meet the mechanical stimulation function black requirements:

1. Magnetic Posts with Magnetic Sliding Rack
2. 'Balloon' Assembly
3. Sliding 'Comb' Rack

Conceptual Design 1: Magnetic Posts with Magnetic Sliding Rack

The first conceptual design that the team generated relied on magnetic force production to actuate the tissue anchorage points. Magnetic iron particulate would be embedded within the PDMS posts themselves, and a magnetic lid would slide over the 96-well plate, theoretically displacing the posts to which the tissue would be mounted. The sliding magnetic rack could be displaced with a hydraulic system of a brake-cable assembly, which would allow function in an incubator. A preliminary model of the system is depicted in Figure 28 below.

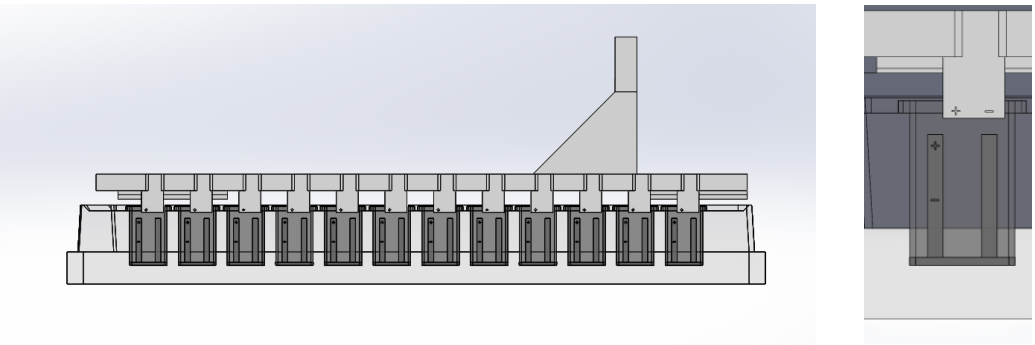

Figure 28. Preliminary model of Magnetic Posts with Magnetic Sliding Rack. Left panel: The Sliding Magnetic Rack on 96 well plate. Right Panel: Single well view.

Conceptual Design 2: 'Balloon' Assembly

The second conceptual design that the team generated relied on the inflation of small balloons to which PDMS posts would be mounted. An array of 96 interconnected balloons would be inflated by a pneumatic system, which would allow functionality inside an incubator. The inflation of the round balloons would tilt the posts away from one another, resulting in an increase in the post-to-post distance and thus a mechanical stretching of the tissue constructs. A preliminary model of the system is depicted in Figure 29 below.

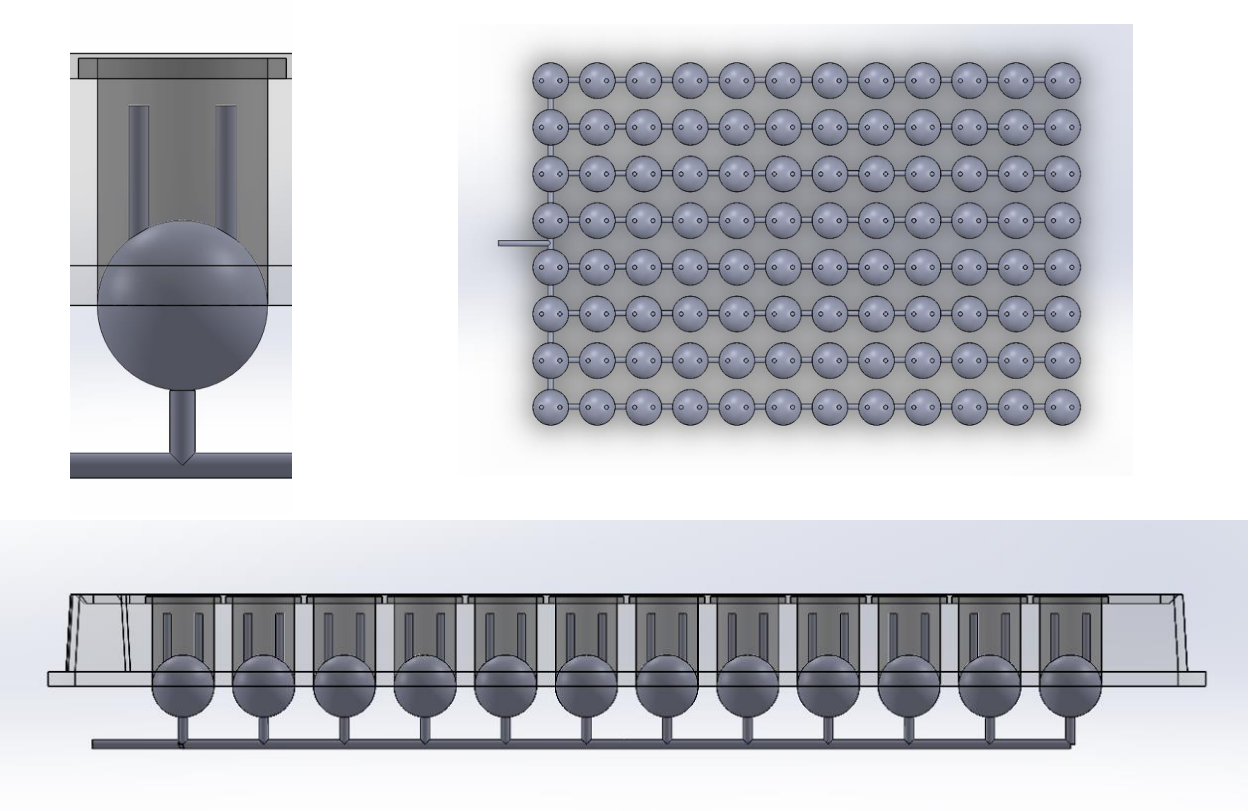

Figure 29. Preliminary model of the Balloon Assembly conceptual design. Top left panel: Shows single well view. Top right panel shows the array of the 96 Balloons. Bottom Panel: shows the Balloon assembly in the 96-well plate.

Conceptual Design 3: Sliding 'Comb' Rack

The third conceptual design generated by the team relied on direct actuation of the anchorage points with comb-like paddles mounted to a sliding rack. The paddles would extend into the well of a 96-well plate and would physically push the PDMS posts to which the tissues would be mounted. The sliding comb rack could be displaced using a hydraulic system or a brake-cable assembly, which would allow for operation in an incubator. A preliminary model of the system can be seen below in Figure 30.

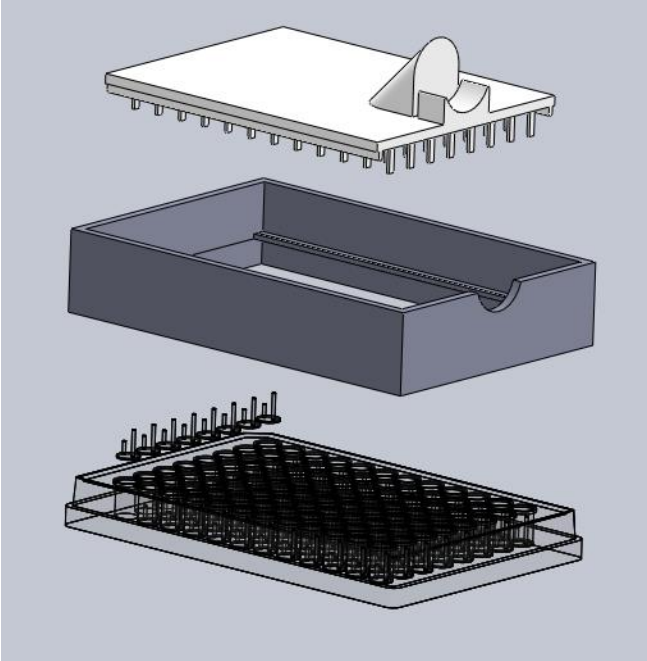

Figure 30. Preliminary model of the Sliding Comb Rack conceptual design.

4.3.4 Feasibility of Mechanical Stimulation Conceptual Designs

To test the feasibility of each conceptual design, crude and cheap prototype models were created for each design. Simple tests were performed with each prototype model in order to assess the potential of each device to meet the various design objectives and requirements associated with the mechanical stimulation functional block.

Feasibility of Conceptual Design 1: Magnetic Posts with Magnetic Sliding Rack

The team had various concerns with the Magnetic Posts with Magnetic Sliding Rack conceptual design. Firstly, the team was concerned that an array of 96 magnets may interfere with each other's magnetic fields, thus creating unequal forces on the particulate-filled PDMS posts. For example, while the horizontal displacement of the magnetic lid should ideally trigger a horizontal displacement of the PDMS posts, it is possible that a given post may be drawn towards the magnet in the well above it, which may cause some sort of diagonal actuation. Additionally, the team was concerned that incorporating iron particulate into the PDMS posts

may allow for the leaching of cytotoxic iron ions into the culture media, which could adversely affect tissue health.

To test the feasibility of the design, the team conducted an experiment to determine if a magnet is capable of effecting two PDMS post models. The PDMS posts were modeled using syringe needles that were densely packed with iron shavings. A relatively weak refrigerator magnet was used to actuate the post models. First, a single post model was placed needle-side-down in some putty. The magnet was then moved forwards and backwards over the post, causing deflections as seen in Figure 31.

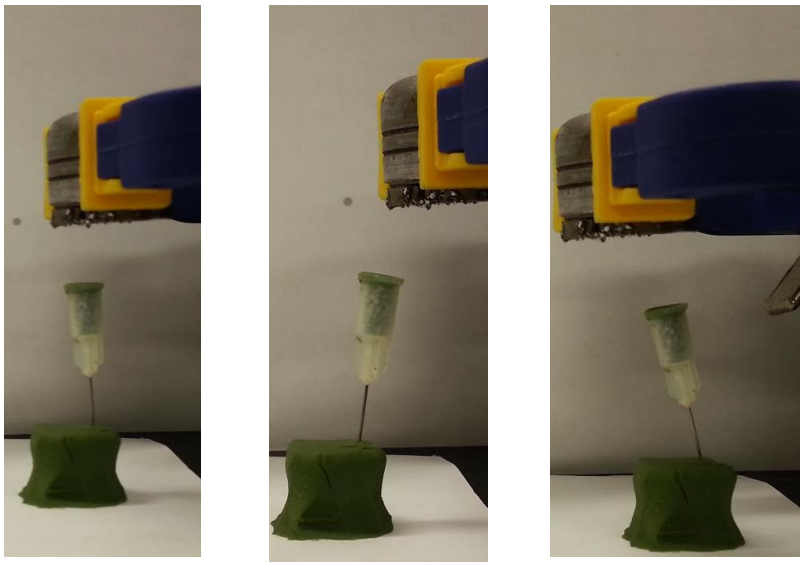

Figure 31. Feasibility study of magnetic post conceptual design.

To test the ability of a single magnet to effect the displacement of more than one post, two post-models were placed needle-side-down in putty. The post models were placed 9mm apart, which is the distance between wells in a 96-well plate. As can be seen in Figure 32, a single magnet was able to deflect both post-models. While this is a crude feasibility study, it does highlight the fact that an array of 96-magnets on a sliding rack would create a non-uniform

magnetic field, and could potentially compromise the accuracy and precision of the device. For this reason, as well as the concerns about cytotoxic iron ions, this conceptual design was abandoned as a candidate for the mechanical stimulation functional block.

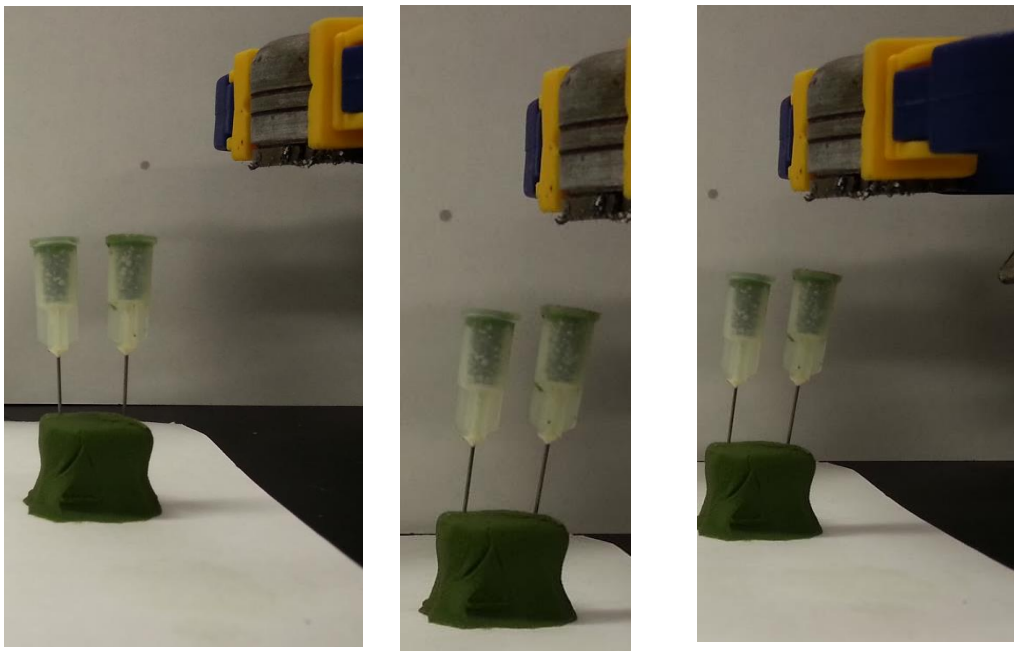

Figure 32. Feasibility study of the magnetic post conceptual design.

Feasibility of Conceptual Design 2: 'Balloon' Assembly

The Balloon Assembly conceptual design also raised a few concerns. Foremost, the team hypothesized that slight variations in balloon thickness and elasticity could cause unequal air distribution during inflation, and thus some tissues may be strained more than others. Additionally, this conceptual design requires the manufacturing of new 96-well plates, or extensive modification of existing 96-well plates to allow for the placement of balloons at the bottom of each well.

To test whether an array of interconnected balloons would be subject to unequal air distribution, a simple prototype was created using silicone tubing, balloons, and a balloon pump as shown in Figure 33.

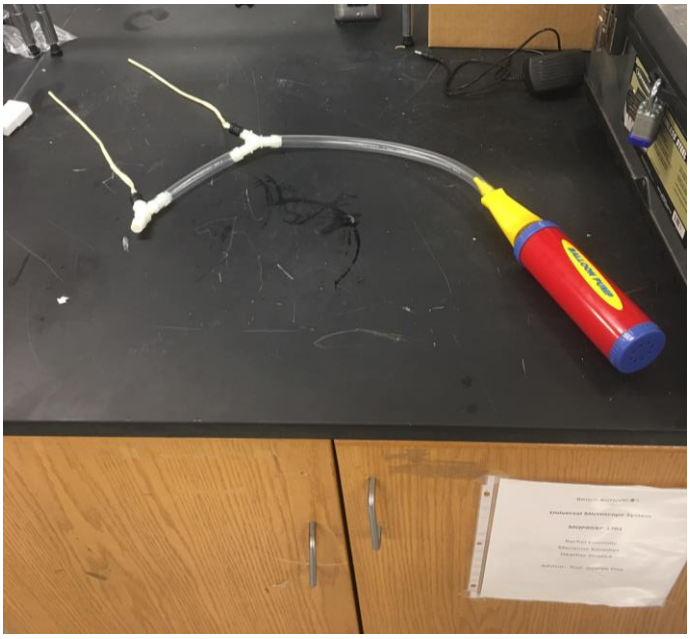

Figure 33. Setup for Balloon Assembly feasibility study.

As air was pumped into the system, only one balloon began to inflate, with the other balloon remaining completely deflated as seen in the left panel of Figure 34. Only when the inflated balloon was about 75% inflated was the system pressure great enough to begin inflating the second balloon as seen in the right panel of Figure 34.

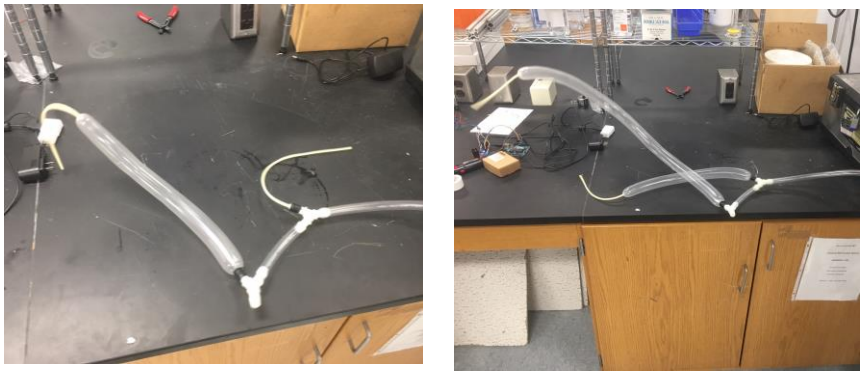

Figure 34. Feasibility study for Balloon Assembly conceptual design.

This phenomenon is likely due to minute differences in the thickness of each balloon, making one balloon easier to inflate than the other. Once one balloon begins to inflate, the stiffness of that balloon is decreased, making it even easier to inflate. Thus, one balloon tends to inflate before the others. This simple study validated the concerns of the team, and highlighted the possibility of unequal air distribution in the 'Balloon" Assembly conceptual design.

Feasibility of Conceptual Design 3: Sliding 'Comb' Rack

The team was confident using this alternative design. The team hypothesized that the system will operate linearly since it is solely composed of mechanical components that are in direct link with one another; reducing the source of error and maintaining linearity throughout the system. To prove the concept, the team tested the proposed alternative to confirm its ability to fulfill the requirement. Using a 96-well plate, the team placed an array of 200 µm pipette tips inside the wells; in a vertical orientation such that the tips are pointing up. This is show in Figure 35.

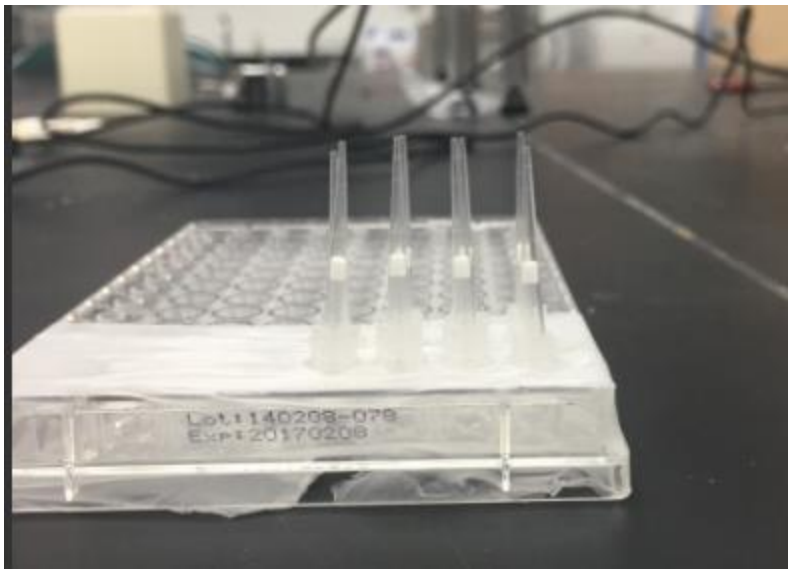

Figure 35. Setup of feasibility study for sliding comb Rack conceptual design.

This setup mimics the 96-well plate that would be used in in the design; where the pipette tips act as the PDMS post. Using the same idea, a second 96-well plate was made; this would act as the sliding 'comb' rack's protrusions shown below in Figure 36.

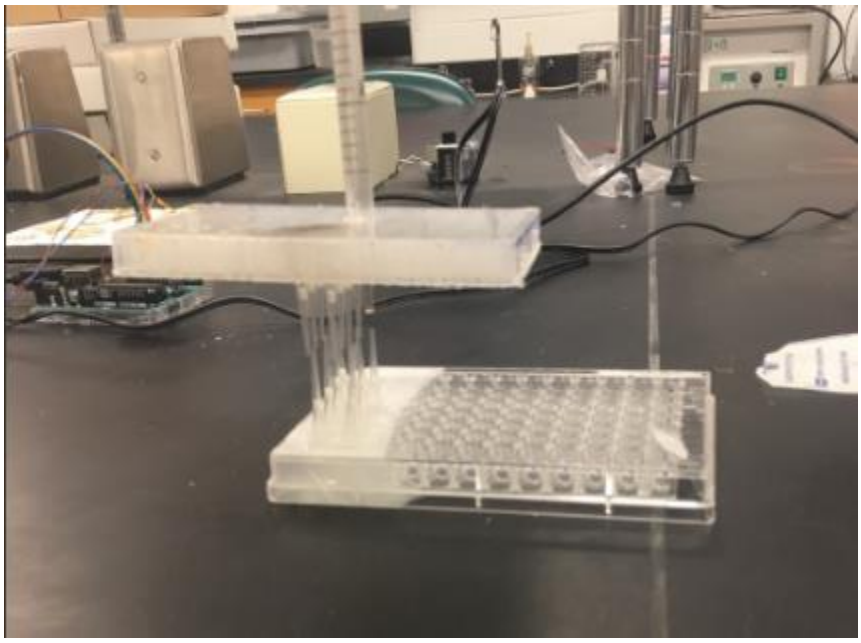

Figure 36. Feasibility study for Sliding Comb Rack conceptual design.

While the top 96-well plate, acting as the comb rack, moved back and forth, the tips of the bottom 96-well plate moved in the same direction all-together, shown in Figure 37 below:

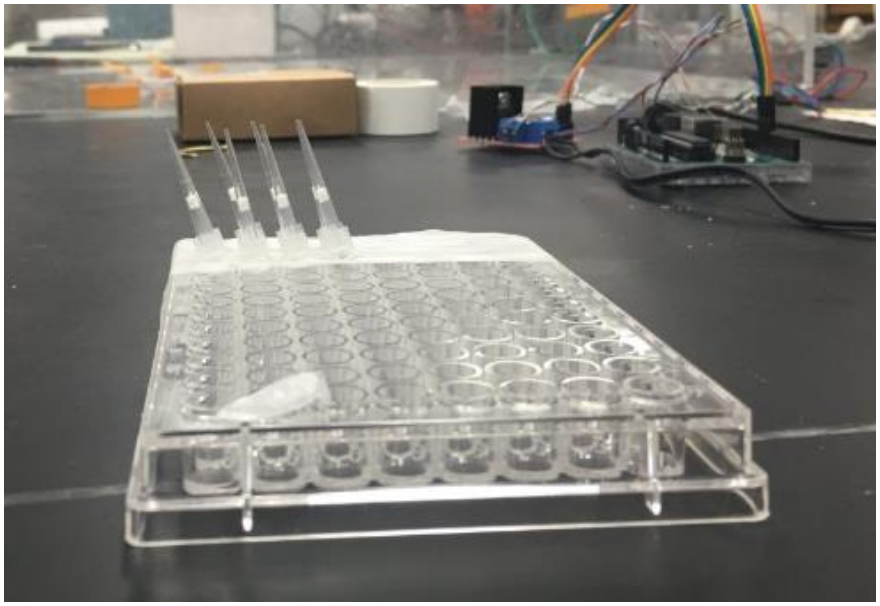

Figure 37. Results of feasibility study for Sliding comb Rack conceptual design.

This feasibility study confirmed the alternative design since the pipette tips would be acting on the 'comb' rack's protrusions that would act on the PDMS posts to induce mechanical stimulation.

4.3.5 Final Mechanical Stimulation Design Selection

To select the final design from the aforementioned conceptual designs, the team utilized the Pugh method of conceptual design selection. The Pugh method involves the identification of essential design requirements and functions, followed by the weighting of these requirements and functions on a scale of 1-5, with '1' being a minimally important requirement and '5' being a highly important requirement. Next, a baseline is established representing current approaches to the mechanical stimulation of skeletal muscle tissue constructs. For each requirement, each conceptual design is scored with a -1, 0, or 1, with a -1 score representing the likelihood for the

design to fall short of the baseline, a 0 score representing the likelihood of the device to meet the baseline, and a score of 1 representing the likelihood of the device to exceed the baseline. The Pugh matrix can be seen below in Table 10.

Table 10. Pugh Method for concept selection.

Design Requirement/ Function	Baseline	Rank	Magnetic Posts with Magnetic Sliding Rack	'Balloon' Assembly	Sliding 'Comb' Rack
Stimulate tissue constructs	0	5	0 (0)	0 (0)	1 (5)
Displace anchorage points	0	5	0 (0)	0 (0)	1 (5)
Accurate and automated stimulation regimens	0	4	0 (0)	-1 (-4)	1 (4)
Cause no harm to tissues	0	5	-1 (-5)	0 (0)	0 (0)
Function in 96-well plate	0	5	-1 (-5)	-1 (-5)	1 (5)
Score			-10	-9	19

Each Design requirement/function analyzed in the Pugh method was weighted as either a 4 or a 5 because every requirement is essential to the success of the device. The device must necessarily stimulate the tissue constructs, and must do so via displacement of the anchorage points, thus these requirements were given a score of 5. The ability of the device to offer accurate and controlled strain regimens was scored a 4 because this function is not absolutely necessary. Some degree of inaccuracy can be tolerated and it is not absolutely necessary that the regimens be automated; however these features are highly desired. The device must not cause harm to the tissues, as this could negatively impact the biomimicry of the tissue constructs. As such, this requirement was given a score of 5. Finally, the device must function in a 96-well plate

in order to be compatible with the high-throughput Myomics drug-screening platform, and thus this requirement was scored as a 5 as well.

As the conceptual designs were scored using the Pugh method, the results of the feasibility studies were taken into consideration. The Magnetic Post conceptual design would not likely outperform the baseline, as the non-uniform magnetic field may cause variations in PDMS displacement and the iron particulates may cause tissue damage. The 'Balloon' Assembly conceptual design was also predicted to underperform the baseline, as uneven air distribution may cause unequal post deflection and would require the manufacture of modified 96-well plates. The Sliding 'Comb' Rack conceptual design was predicted to vastly outperform the baseline. This concept is much simpler than the others, and relies merely on a plastic 'paddle' to push on a flexible PDMS to displace it. Additionally, this system relies on only one moving part, thus increasing the likelihood that this design will provide accurate and controlled strain regimens. The sliding rack is compatible with both hydraulic systems and brake-cable assemblies, both of which can be made using a programmable syringe pump to provide precise and automated strain regimens. This combined with the prediction that the device could be fabricated out of biocompatible materials to avoid cytotoxicity, lead to selection of this conceptual design for further development into the final design.

4.3.6 Modification and Finalization of Final Design

The initial model of the 'Comb' Rack concept is shown below in the left panel of Figure 38, and the right panel shows the finalized device. The following sections describe how the team arrived at the final design. The functionality of each feature of the final design will also be discussed in these sections. The sections will be organized by design component, which will be discusses in the following order:

1) 96-well plate
2) Elongated PDMS Posts
3) Support Frame
4) Post Fixation Frame
5) Sliding Comb Rack
6) Electrical Components
7) Cover
8) Force Production System (not depicted in Figure 38)

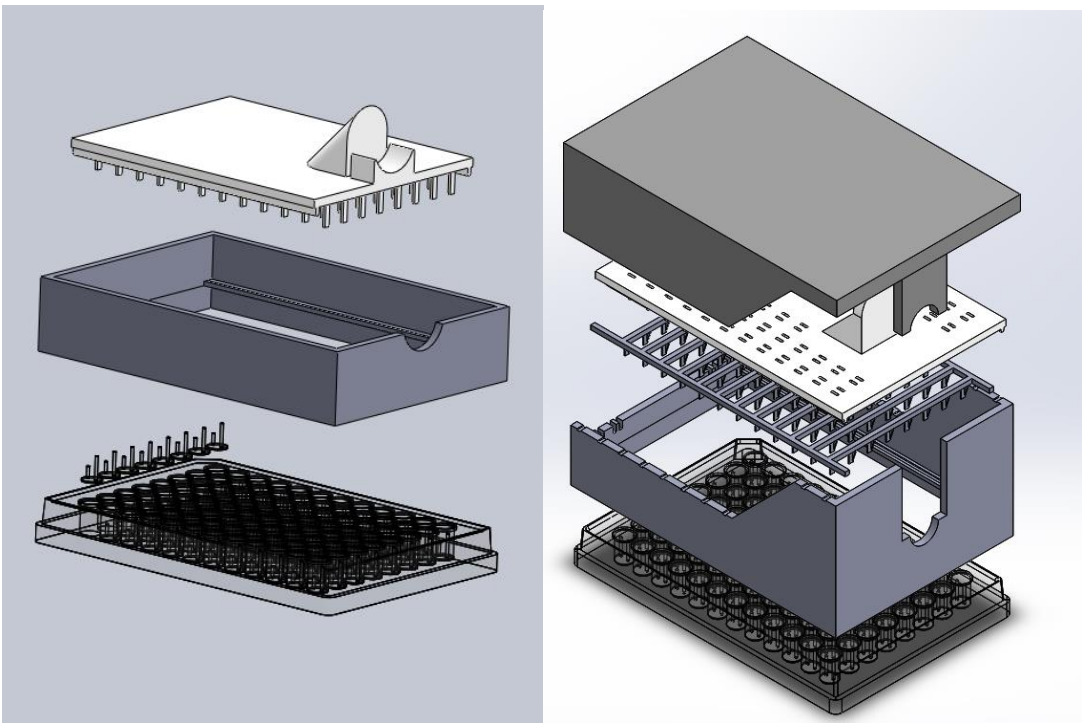

Figure 38. Left panel: Preliminary model for sliding comb Rack conceptual design. Right panel: Final design for Sliding Comb Rack

Component 1: 96-well Plate

Figure 39 shows a CAD model of a standard 96-well plate. While this plate is not something that was designed or modified by the team, it is included as a design component for clarity, as this is the plate in which our device was designed to function.

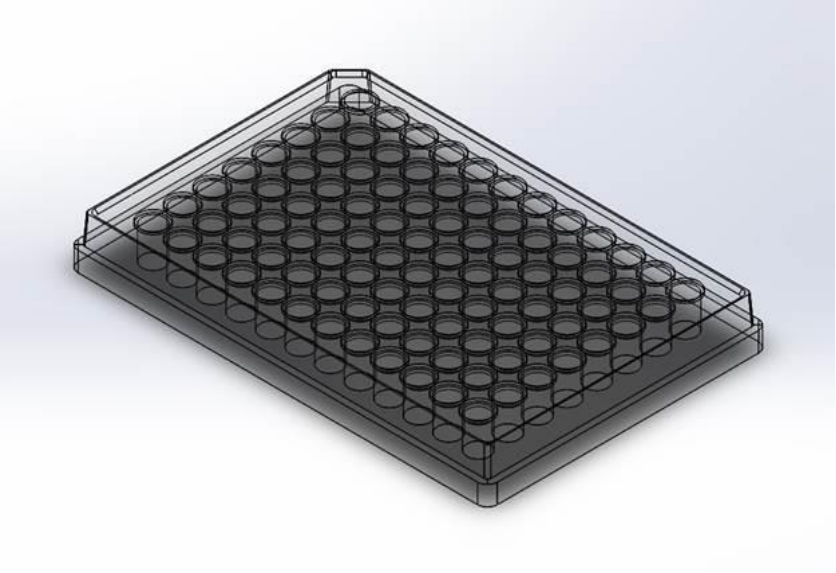

Figure 39. CAD model of 96-well plate

Component 2: Elongated PDMS Posts

The PDMS posts traditionally used in the mBAM Tissue-engineering method for the Myomics drug-screening platform are 4 mm tall and have caps on the tops of the posts, as shown in the left panel of Figure 40. In order for the Sliding Comb rack to displace the PDMS posts from above, the PDMS posts needed to be elongated. As the mold used to fabricate the PDMS posts is very expensive, the team opted to use a PDMS post modification technique inspired by the MQP-RLP-1501 team, in which the caps of detached posts are glued to the caps of another set of PDMS posts as seen in the right panel of Figure 40. The modified PDMS posts are now able to be displaced by the Sliding Comb Rack from above.

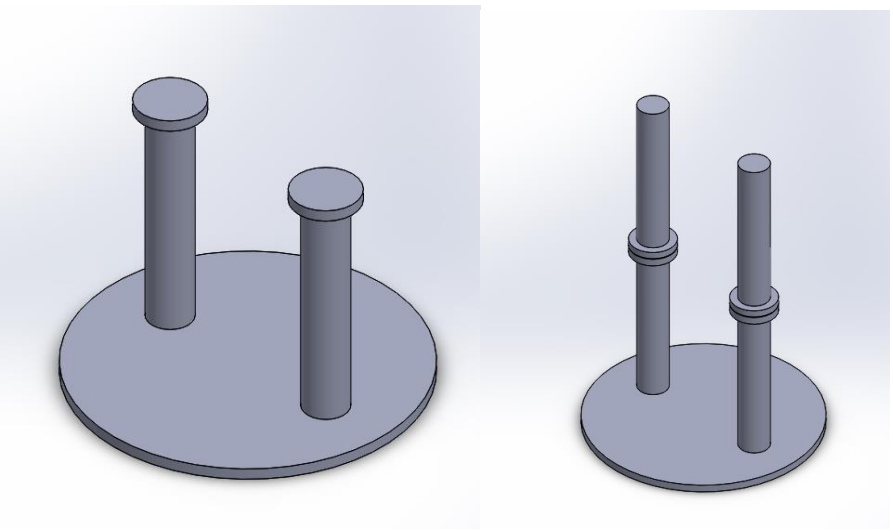

Figure 40. Left panel: Unmodified PDMS posts. Right panel: Modified PDMS posts

Component 3: Support Frame

The left panel of Figure 41 shows the final version of the Support Frame, which fits directly over a standard 96-well plate, as shown in the right panel of Figure 41. The purpose of the Support Frame is to provide rails on which the sliding Comb Rack can sit. The preliminary support frame proposed for the conceptual design was substantially modified, resulting in the final version of the support frame depicted in Figure 41. Firstly, the height of front of the frame was increased, to allow room for the sliding comb rack and cover, which we be discussed later. Next, small divots were placed around the perimeter of the frame in order to allow gas exchange between the internal device environment and the outside incubator environment. This is essential for tissue viability, as cultured cells require an environment in which carbon dioxide and oxygen gases can flow freely. Lastly, small grooves were placed on the back of the support frame, which was to allow the incorporation of electrical components from MQP-RLP-1502's electrical stimulation lid, which will be discussed later.

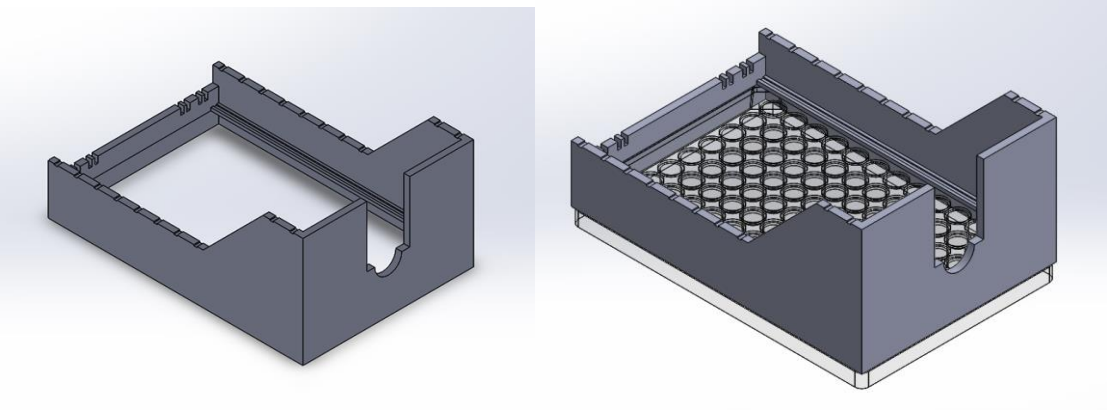

Figure 41. Left panel: Support Frame alone. Right panel: Support Frame on 96-well plate.

Component 4: Post Fixation Frame

This component was not included in the preliminary conceptual design and is thus a modification unique to the final version of the design. The Post Fixation Frame, depicted in the top left panel of Figure 42, fits directly into the Support Frame as shown in the top right panel of Figure 42. The Post Fixation Frame is designed to hold a single PDMS post in place. The need for this component stems from the idea that when tissue is anchored to both flexible PDMS posts, the displacement of one of the posts will likely cause the other post to deflect as well. This could lead to a scenario where the team thinks that the tissues are being strained a given amount, but in actuality they are being strained much less because both posts are moving. The Post Fixation Frame solves this problem by fitting over the non-actuated PDMS post, preventing any unwanted movement. An in-well view of the Post Fixation Frame and its interaction with the PDMS posts can be seen in the bottom panel of Figure 42.

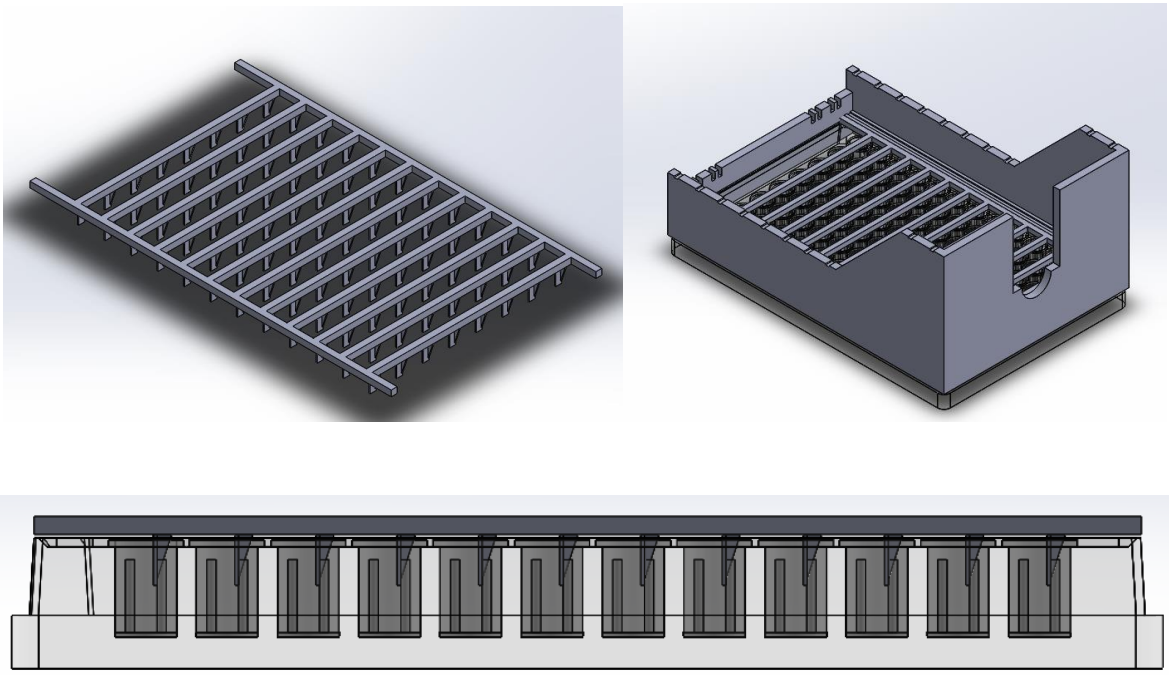

Figure 42. Top left panel: Post Fixation Frame alone. Top right panel: Post Fixation Frame with Support Frame on 96 well plate. Bottom panel: in-well side view of Post Fixation Frame

Component 5: Sliding Comb Rack

The top left panel of Figure 43 shows a top-down view of the final version of the Sliding Comb Rack and the top right panel shows a bottom-up view. The bottom left panel of Figure 43 shows how the Sliding Comb Rack fits into the Support Frame over the Post Fixation Frame (not visible). The purpose of the Sliding Comb rack is to physically displace a single PDMS post in each well in a horizontal direction. The protrusion on the top of the Rack is a backstop for which the force production system to interface with the Sliding Comb Rack, which will be discussed later. The bottom right panel of Figure 43 shows an in-well view of the Sliding Comb Rack and Post Fixation Frame. The dark grey 'paddle' is part of the Post fixation Frame, holding one of the PDMS posts in place, while the light grey 'paddle' is part of the Sliding Comb Rack, which when moved horizontally will displace a single PDMS post, stretching the tissue as a result. A

major modification to this component is the inclusion of elliptical slots, for which electrodes to fit, which will be discussed later. Additionally, the rails on the bottom of the Rack were shortened to reduce friction between the Sliding Comb Rack and the Support Frame. Another modification was the removal of ‘paddles’ on certain parts of the Rack. This allows the team to use the device as an experimental model, where four experimental conditions can be created in a single 96-well plate: Control (no stimulation), Mechanical Stimulation only, Electrical Stimulation only, or both Mechanical and Electrical Stimulation.

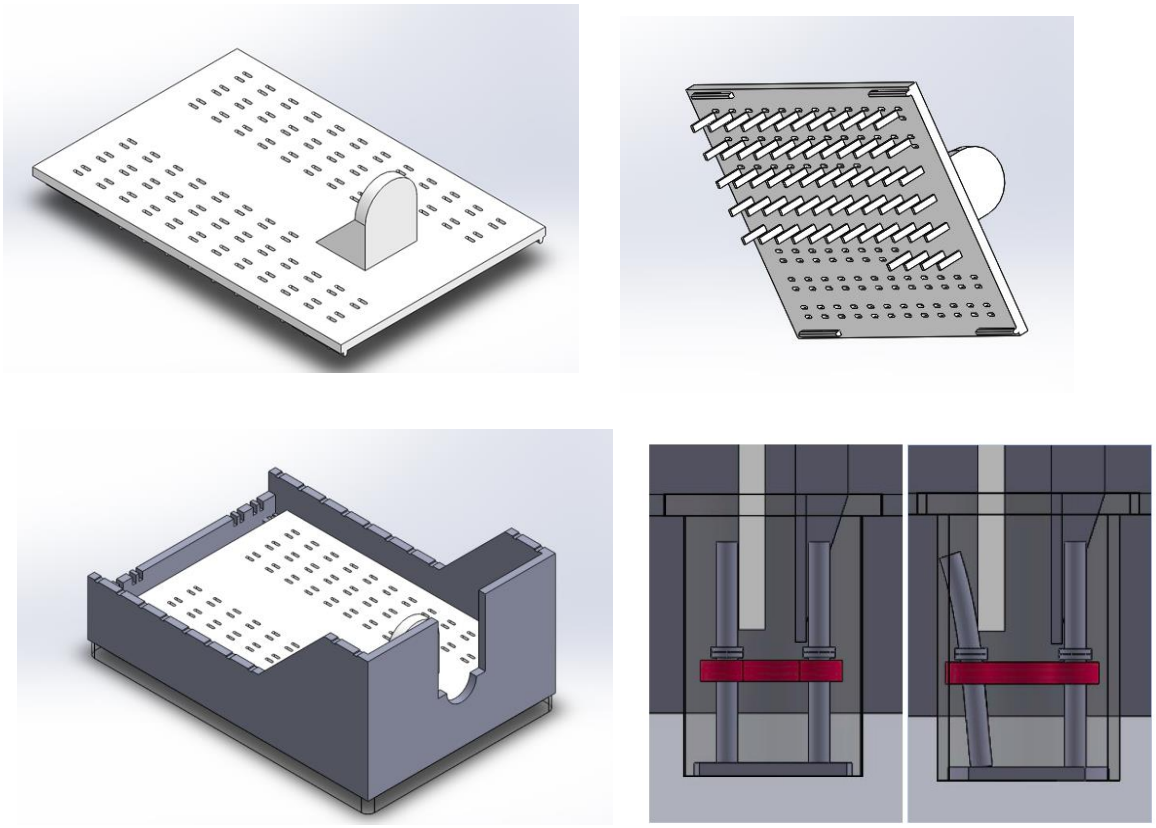

Figure 43. Top left panel: Isometric view of the Sliding Comb Rack. Top right panel: Underside view of the Sliding Comb Rack. Bottom left panel: Isometric view of the Sliding Comb Rack in assembly with Post Fixation Frame, Support Frame, and 96 well plate. Bottom right panel: In well view of mechanical stimulation.

Component 6: Electrical Component

A major modification leading to the final version of the design was the inclusion of electrical components adopted from MQP-RLP-1502's Electrical Stimulation Lid. The brass busbars and stainless steel electrodes, depicted in the left panel of Figure 44, were removed from the MQP-RLP-1502 lid and used in the team's final device. The brass busbars fit into the slots created in the Support Frame, and the electrodes fit into the elliptical holes in the Sliding Comb Rack as shown in the right panel of Figure 44. This allows for the Sliding Comb Rack to be horizontally displaced, with the electrodes remaining stationary within the well. The busbar-mounted electrodes are able to operated using MQP-RLP-1502's Arduino circuit and program.

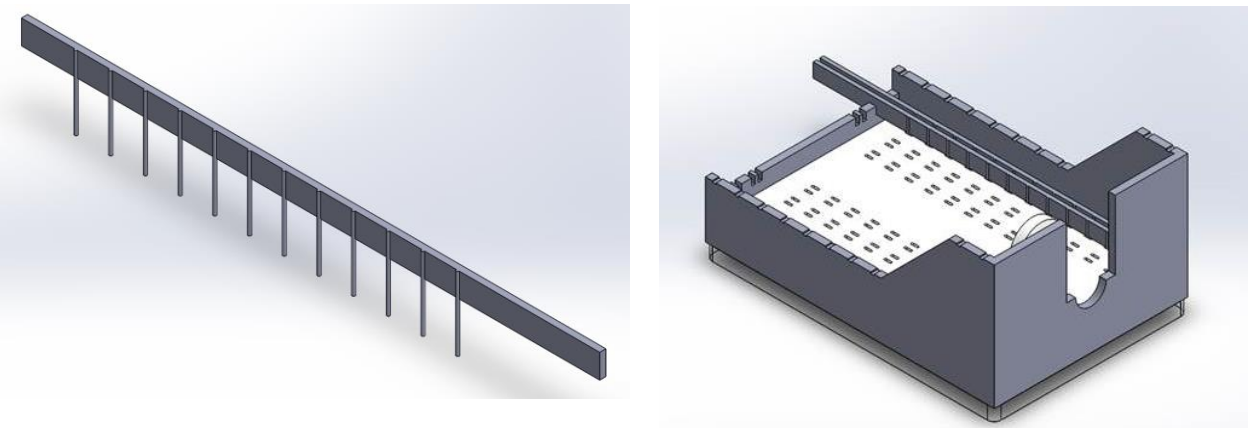

Figure 44. Left pane: Busbar and associated electrodes. Right panel: Busbars incorporated into the final design assembly.

Component 7: Cover

This component, depicted in Figure 45, is also an entirely new addition to the preliminary design and is thus a modification unique to the final version of the design. The cover simply serves to close off the internal system environment from the outside environment in order to maintain sterility during device function. As previously noted, shallow divots were placed on the Support Frame to allow gas exchange, even when the cover was placed on the device.

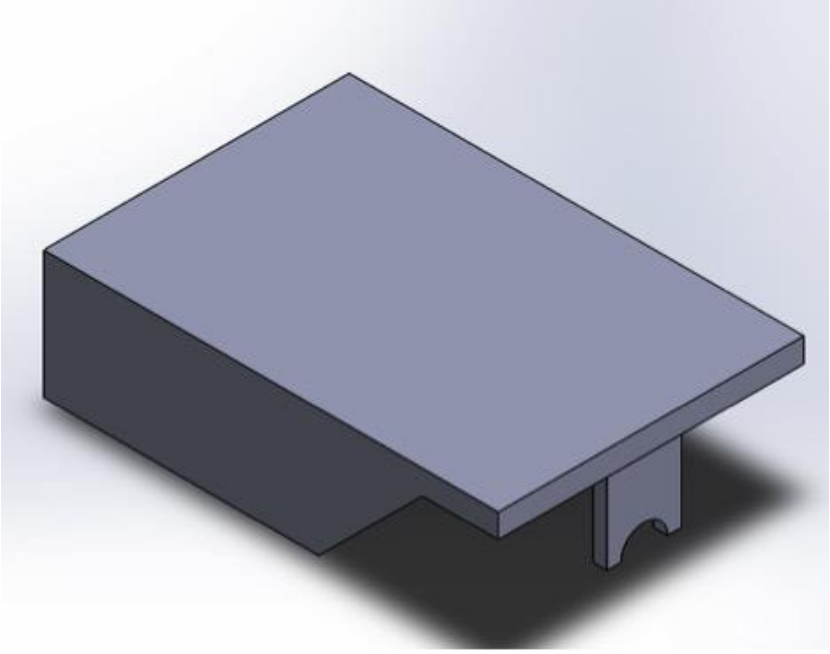

Figure 45. Isometric view of the Cover.

Component 8: Force Production System

As described earlier in Chapter 4, the team noted that either a hydraulic system or a brake cable assembly could actuate our Sliding Comb Rack design. The team first decided to pursue a hydraulic system, based on the fact a previous MQP groups had shown success with such systems. Silicone tubing connected two plastic 5 mL syringes, and the system was filled with degassed mineral oil. Thus, the displacement of one plunger should cause an equal but opposite displacement of the plunger of the other syringe. The hydraulic system was to be operated using a programmable NE-4000 syringe pump, which is capable of precise fluid infusion and withdraw. This initial prototype is shown in Figure 46.

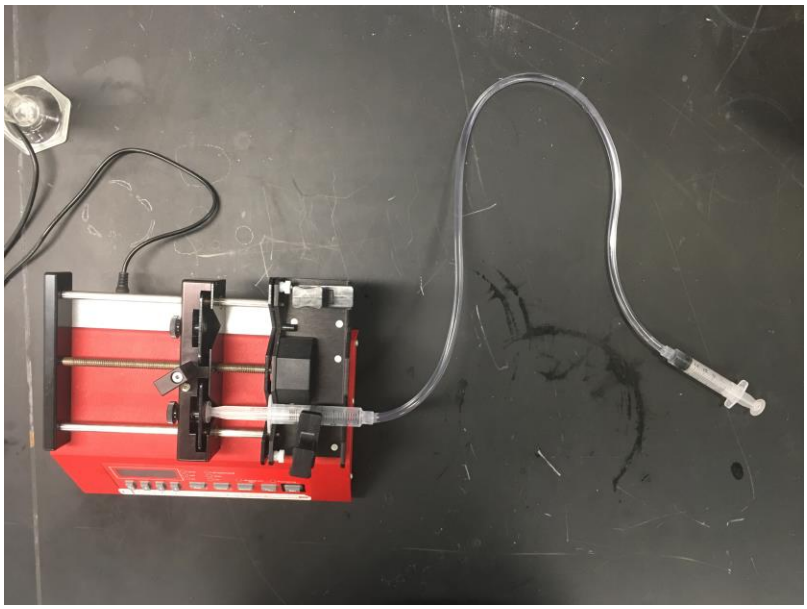

Figure 46. Setup of hydraulic system in NE4000 Syringe Pump.

By experimenting with the system, the team was able to rule out the feasibility of a hydraulic system. The plunger displacement needed to actuate the PDMS posts is on the order of microns, specifically 320μm for a strain of 10%. This displacement corresponded to a volume of 36.13 μL. The infusion and withdrawal of this small volume is well within the capabilities of the NE-4000 syringe pump, however the team saw no plunger movement when this volume was dispensed. The team hypothesized that the elasticity of the rubber syringe plungers and silicone tubing was responsible for absorbing the pressure created by the infusion of this 36.13 μL volume, thus preventing motion. The team was able to overcome the lack of motion by dispensing 100 μL into the system, however this caused an overshoot of plunger displacement. The team also created a modified hydraulic system with gas-tight glass syringes provided by the Page Lab, however this modified system failed as well. For these reasons the team abandoned the use of a hydraulic system as a means of force production for the actuation of the Sliding Comb Rack

The team next explored the use of a brake cable assembly as a means of force production for the actuation of the Sliding Comb Rack. A brake cable and brake cable housing was purchased from a sporting good supply store, and was attached to the NE-4000 syringe pump in the same way as the hydraulic system, as shown in Figure 47. Through various validation studies, the brake cable assembly and NE-4000 syringe pump were determined to meet the needs of the team. These verification studies, as well as the method for lid-cable interface, will be discussed in Chapter 5.

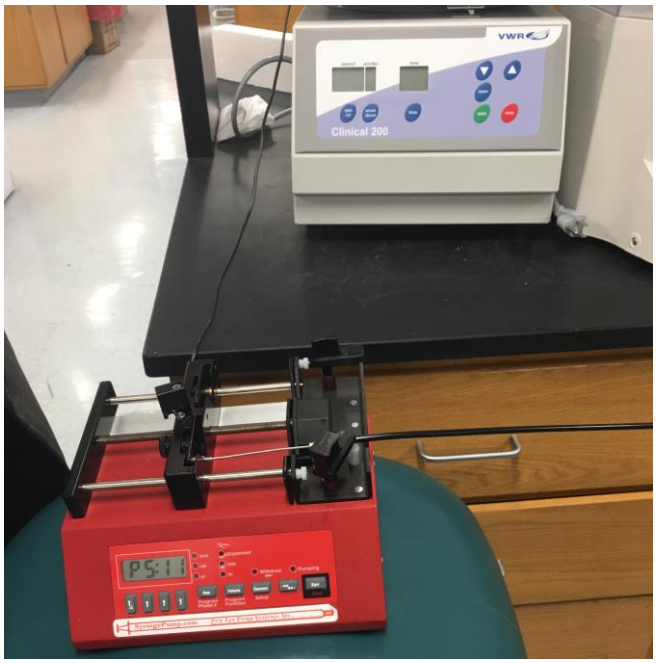

Figure 47. Brake cable assembly in NE4000 Syringe Pump.

Chapter 5: Design Verification and Validation

This Chapter details the various experiments that were performed in order to confirm the ability of the final design to meet the previously mentioned design objectives and requirements. Each functional block called for its own set of experiments, and thus the experiments will be organized by functional block and will be discussed in the following order:

1. Tissue-engineering
2. Electrical Stimulation
3. Mechanical Stimulation

5.1 Tissue-engineering Verification

The following section describes the verification and validation of the ability of the system to satisfy design requirement of maintaining sterile conditions during operation.

5.1.1 Sterilization and Maintenance of Sterility During Operation

As stated in the design requirements, the mechanical and electrical stimulation device must maintain sterility during operation in order to ensure the production of healthy, viable tissue constructs. If sterility is not maintained, bacterial or fungal contamination could occur.

The mechanical and electrical stimulation lid was fabricated using a rapid prototyping technique called 3D printing. The Support Frame was printed on the Dimension rapid prototyping machine and was fabricated out of ABS, a non-biocompatible rigid plastic. This plastic is sterilizable by ethylene oxide (EtO) treatment. All other parts of the lid were fabricated out of MED610, a biocompatible rigid polymer. MED610 is not sterilizable by EtO treatment, and has a melting point too low for autoclave sterilization. For these reasons, a new sterilization technique that is compatible with all parts of the lid was developed. This method involved the submersion of the lid in 70% isopropanol followed by submersion in 3% hydrogen peroxide, proceeded with a 15 minute PBS bath to rinse off excess isopropanol/hydrogen peroxide. To test the ability of this

method to completely sterilize the lid, as well as to test the ability of the lid to maintain sterile conditions in a 96-well plate, a sterility study was performed. Briefly, the lid was submerged in 70% isopropanol for 15 minutes in a tissue culture hood. The lid was then allowed to dry in the hood for 15 minutes to promote the evaporation of the alcohol. The lid was then submerged in 3% hydrogen peroxide for 15 minutes, and again allowed to dry inside the hood for 15 minutes. The lid was then submerged in sterile PBS for 15 minutes, and again allowed to dry inside the hood. The lid was then assembled and placed on top of a 96-well plate with antibiotic-free media-filled wells. Open holes in the lid, which would otherwise be filled by electrode busbars or components of the force production system, were taped over for this experiment. A control plate was also created with a single row of wells filled with antibiotic free media. The lid-test plate and control plate were then placed in an incubator for five days. An image of the experimental setup can be found in Figure 48. The results from this experiment will be discussed in Chapter 7.

Figure 48. Setup for Sterility Study.

5.2 Electrical Stimulation Verification

The experiments discussed in this section correspond to the electrical stimulation functional block. The experiments aimed to verify the ability of the electrical components to satisfy the design requirements relevant to this functional block, namely the ability of the system to provide automated, accurate, and customizable regimens as well as the ability of the system to act upon all wells of a 96-well plate.

5.2.1 Accurate, Automated, and Customizable Stimulation Regimens

To test the ability of the electrical components of the system to deliver accurate, automated, and customizable electrical stimulation regimens, a simple study was conducted. The four brass busbars and associated stainless steel electrodes were removed from MQP-RLP-1502's stimulation lid and were connected to the Arduino Uno that was used and programmed by the MQP-RLP-1502 team. An oscilloscope was attached to a single electrode and used to monitor the voltage over that electrode. The Arduino Uno was programmed to deliver electrical pulses of 4 ms width at a constant frequency of 1Hz; the resultant oscilloscope plot is depicted in Figure 49. The results from this experiment will be discussed in Chapter 7.

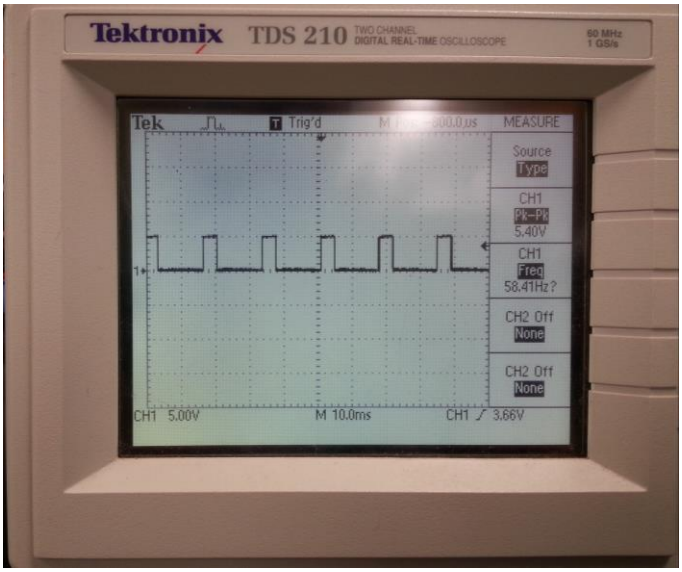

Figure 49. Oscilloscope display for electrical component validation and verification.

5.2.2 Act Upon All Wells of a 96-Well Plate

To confirm that the stimulation regimens observed over a single electrode by the oscilloscope in the previous experiment could be delivered by all of the electrodes in the system, a simple study was conducted. The MQP-RLP-1502 lid only had four busbars, which allowed for the stimulation of two rows of a 96-well plate. To confirm the ability of current to be delivered by all electrodes on the busbars, the electrodes were placed into 1M HCl filled wells of 96-well plate. When current is passed through the HCl solution, the liquid should bubble and turn yellow. The first four electrodes of the second row were removed to serve as controls. When a constant 5V was supplied across the busbars, current was delivered to all electrode-occupied wells as evidenced by the bubbles and yellow colorization in these wells as shown in Figure 50. The results from this experiment will be discussed in Chapter 7.

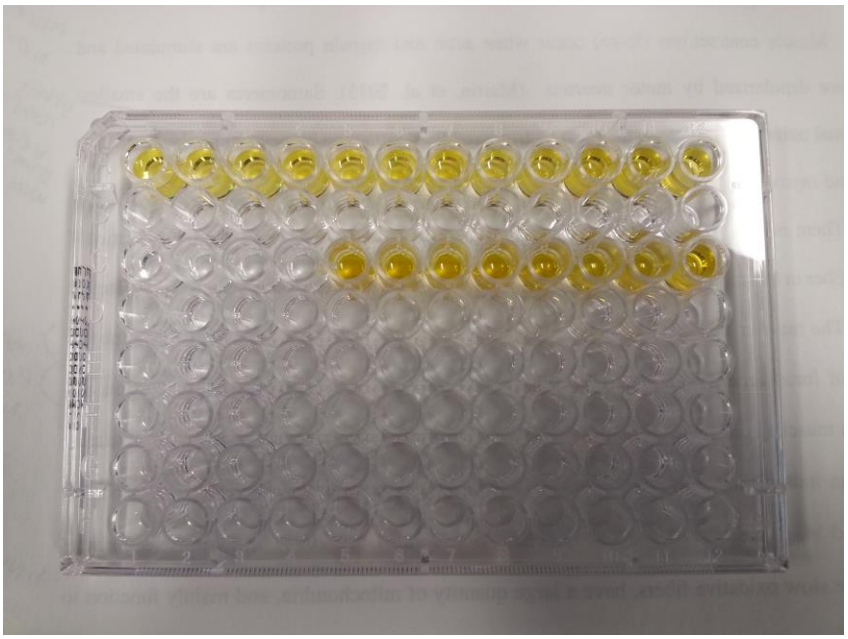

Figure 50. Results of HCL study for Electrical Component validation and verification.

5.3 Mechanical Stimulation Verification

Once the design was prototyped, the team conducted a series of experiments to verify the ability of the mechanical stimulation design component to meet the desired objectives.

5.3.1 Mechanical Stimulation Verification

The team next explored the use of a brake cable assembly as a means of force production for the actuation of the Sliding Comb Rack. Using the same setup described above for the hydraulic system, a break cable was used instead of a syringe. One of the break cable's ends was mounted on the NE4000; acting as a force production device that would displace the cable's end. To test the system, the team ran a feasibility study to correlate volume dispensing to distance; hoping to achieve a linear result that would be used as the mean of force production. The testing setup is show below in Figure 51.

Figure 51. Setup for Brake cable assembly validation and verification.

The cable was stretched to reduce the source of errors from curving; placed on the green chair and mounted to the NE4000 perfusion pump. The other end of the break cable was mounted on the NE4000 pump, shown near the microscope above. The break cable was attached to a Pasteur pipette that contained a fine needle tip at the end; shown below in Figure 52. The needle was placed under the microscope and above a hemocytometer grid to gather displacement values using ImageJ; the setup is show below in Figure 52.

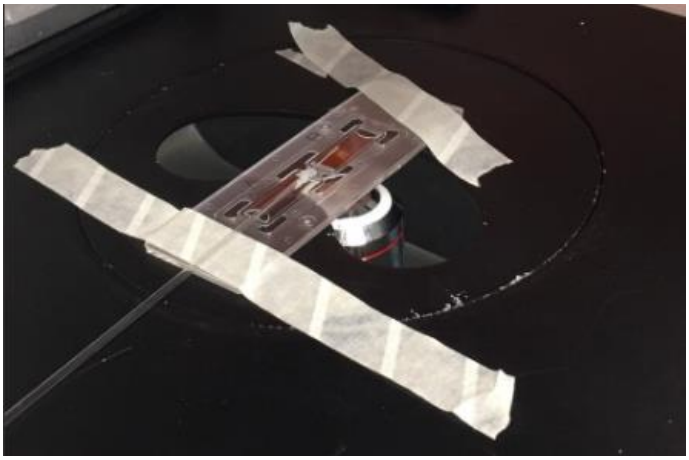

Figure 52. Setup of hemocytometer scaling setup under microscope.

Initially, calculations were conducted to derive the perfusion rate and dispensed volume that the NE4000 requires; the system was modelled using the inner diameter of a 5 mL syringe. The test calculated the distance of travel (infusion) and distance of return (withdrawal) of the needle tip from a known reference point. The test used 4 different dispensed volumes that corresponded to various theoretical distances. Each volume was dispended over a period of 5 seconds. Table 11 below shows the different volumes dispensed, and actual values of distance.

Table 11. Results from brake cable validation and verification study.

Theoretical Distance (µm)	Dispensed Volume (µL)	Average Experimental Distance (µL) (Dispense)	Average Experimental Distance (µL) (Withdrawal)	Error of return after withdrawal (µm)
500	56.5	387.64	389.05	-1.41
1000	112.4	1028.77	1027.04	1.72
1500	169.4	1646.61	1652.06	-5.45
2000	225.8	2258.87	2260.25	-1.38

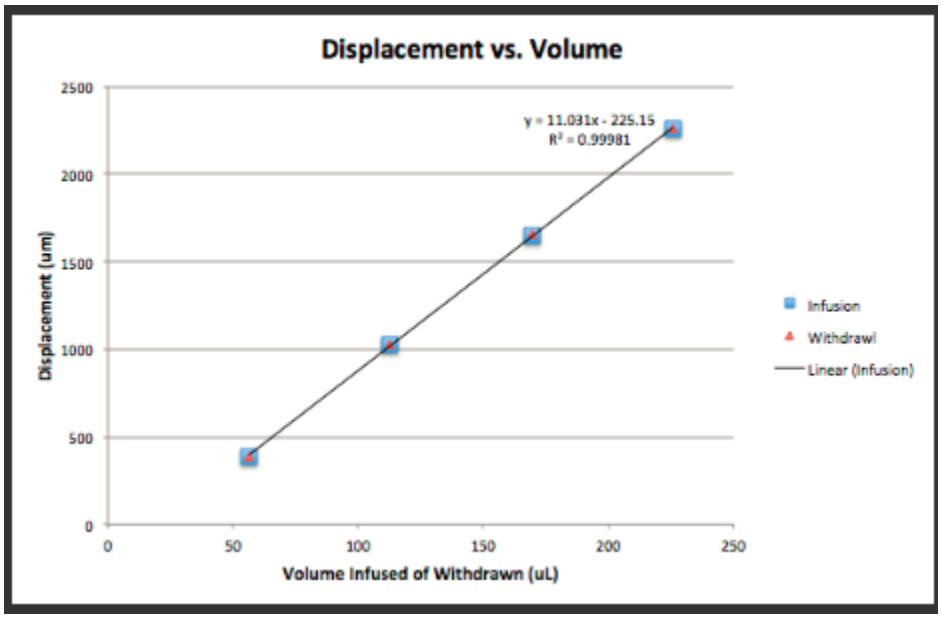

Figure 53.Relationship between brake cable displacement and syringe pump infusion/withdrawal volume.

Figure 53 above shows the trends attained from the feasibility study. The results of this experiment will be discussed in Chapter 7.

Next, the correlation between the displacement of the break cable and the actual strain experienced by the PDMS posts was determined. A 96-well plate was cut horizontally such that the PDMS posts in the front row of the plate were directly visible. PDMS posts were glued in each well and marked with a black sharpie for better visualization upon deflection. It should be mentioned that the PDMS posts were only 4 mm in height, however, another 4 mm post was glued on top to reach the needed 8 mm dimensions. A cell phone was set in focus to record the movement of the sliding comb rack and the deflection PDMS post upon contact. Three wells were tested in the experiment and the images were analyzed with ImageJ. Data corresponding to this experiment can be seen in Figure 54. The results of this experiment will be discussed in Chapter 7.

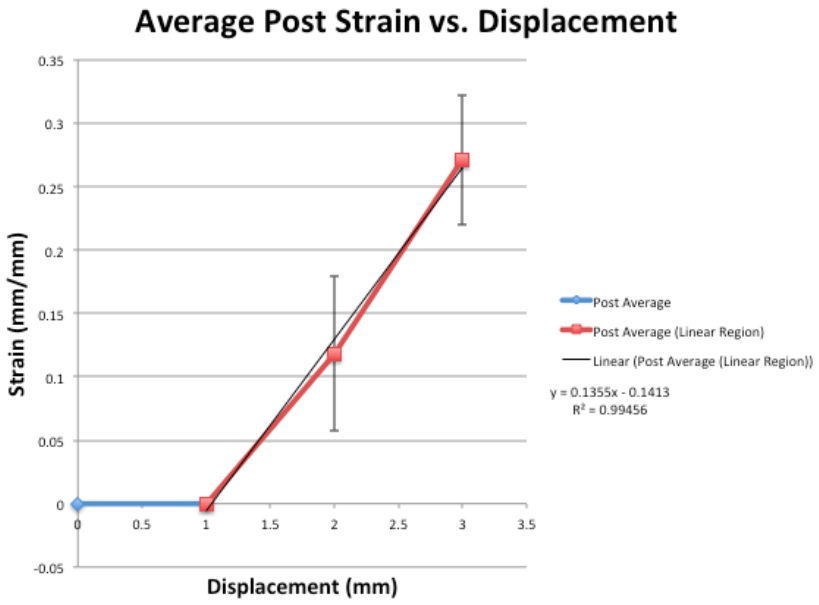

Figure 54. Relationship between post strain and brake cable Displacement.

5.4 Final Experiment

Once the function of the device was verified by the studies described in the previous sections, the team conducted a final experiment to assess the ability of the device to enhance the maturity of hydrogel-assisted self-assembled tissues. Briefly, modified PDMS posts were glued with un-cured PDMS to the well bottoms of a 96-well plate. The plate and electrical busbars were sterilized via EtO, and the sliding comb rack device was sterilized using baths of isopropanol and hydrogen peroxide as previously described.

Mouse myoblasts (C2C12s) and human primary fibroblasts (CRL2097) were cultured in culture media (DMEM, 10% FBS, 1X GlutaMAX) and maintained in a standard incubator environment. The C2C12s were maintained under 70% confluency to prevent premature differentiation and loss of myogenic potential. C2C12s and CRL2097s were combined in a 3:1 ratio, with 400,000 cells per tissue. Before seeding, 85µL of NIPAAm was pipetted into the bottom of each well and allowed to solidify in a 47˚C oven for 30 minutes. This layer of NIPAAm helps elevate the cells such that tissue forms around the caps of the modified PDMS posts. The cells were then suspended in the appropriate volume of 2 U/mL thrombin/DPBS(-). 60µL of this cell/thrombin/DPBS(-) solution was pipetted across the top of the solidified NIPAAm layer and subsequently mixed with 60µL of a 10% fibrinogen/DPBS(-) solution via gentle repeat pipetting. The plate was placed in an incubator for one hour to allow polymerization of the fibrinogen into fibrin. After the one hour incubation, 95µL of growth media (DMEM, 10% FBS ,1X GlutaMAX, 1% tranexamic acid (TEX), 5% aprotonin) was piptetted on top of the polymerized fibrin. The plate was placed back into the incubator overnight. After 12-16 hours of incubation, the plate was cooled to 4˚C for 30 minutes to facilitate the transition of NIPAAm back into a liquid. The NIPAAM and media were then

aspirated out of the wells and the tissues were rinsed once with cold media to remove excess NIPAAm. 200uL of growth media was pipetted into the wells and the tissues were allowed to remain in the growth phase for one more day, with media being changed daily. After a total of 3 days in growth media, the tissues were placed in differentiation media (DMEM, 2% HS ,1X GlutaMAX, 1% tranexamic acid (TEX), 5% aprotonin) for an additional 3 days.

After 3 days of differentiation, a stimulation regimen began using the sliding comb rack device. The rationale for the chosen stimulation regimen stems from the adoption, modification, and combination of two successful regimens from the literature, one for mechanical stimulation and one for electrical stimulation. The mechanical regimen was adopted from Heher et. al who statically strained hydrogel-assisted-self-assembled tissues to 10% strain for 18 hours followed by a static 3% strain for 6 hours. This regimen was ran continuously for 6 days. While this regimen showed better enhancement of tissue maturity than previously described cyclic regimens, the team reasoned that cyclic regimens were more physiologically relevant than static strain regimens. Additionally, since muscle is subjected to up to 30% strain during contraction, the team reasoned that a 20% strain, rather than a 10% strain, may show better enhancement of tissue maturity. Thus, a mechanical stimulation regimen was created that hoped to combine the benefits of static strain with the physiological relevancy of cyclic strain regimens. This modified regimen consisted of a climb to 20% strain over a period of one minute. 20% strain was maintained for 5 minutes before a decline to 0% strain over a period of one minute. This was followed by a 15-minute relaxation period during which electric stimulation took place before the mechanical cycle began again.

The electrical stimulation regimen was adopted and modified from Ikeda et al. who stimulated hydrogel assisted self-assembled tissues with an electric field of 1.5 V/mm with a 4

ms pulse width at 1Hz continuously for 7 days. This regimen yielded better results than similar approaches that used higher frequencies and lower pulse widths and thus was adopted by the team. Five minutes into the 15 minute relaxation period between mechanical cycles, the tissues were stimulated with five minutes of electrical stimulation of 1.5 V/mm with a 4 ms pulse width at 1Hz. A summary of the stimulation regimen can be found in Figure 55.

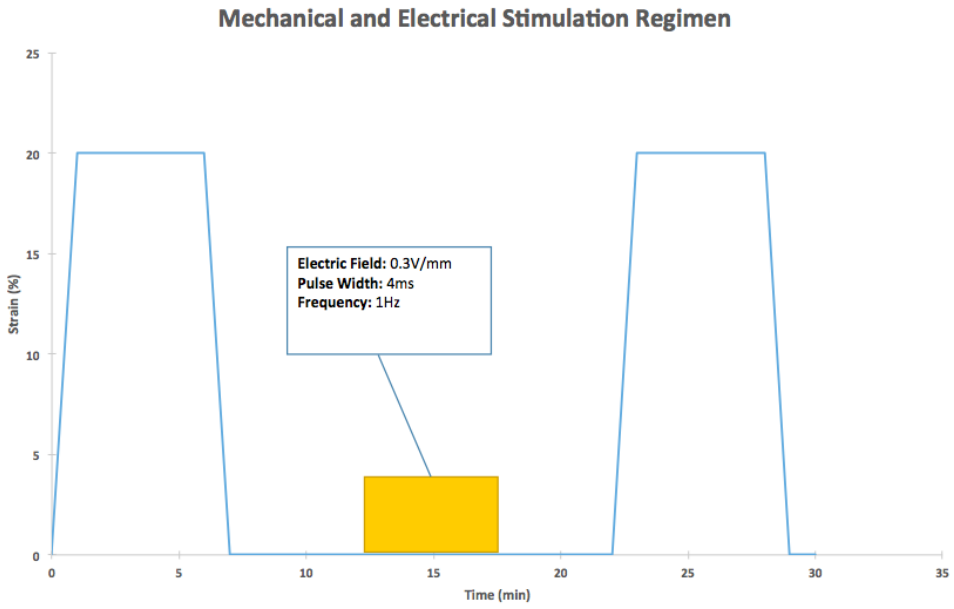

Figure 55. Mechanical and Electrical stimulation regimen.

For the final experiment, four experimental groups were created in order to properly assess the effect of the device. These four groups consisted of a control group with no stimulation, an electrical-stimulation-only group, a mechanical-stimulation-only group, and an electrical-and-mechanical-stimulation group. After 7 days of stimulation the tissues were assessed for contractile ability using the Myomics MyoForce Analysis System housed in Professor Page's laboratory. None of the tissues showed evidence of any contractile ability. The tissues were then collected for histological analysis. Briefly, the tissues were fixed in 4% paraformaldehyde, processed, and embedded in paraffin wax. The tissues were cut into 6 µm-

thick longitudinal sections using a microtome and subsequently stained using hematoxalin and eosin. The histological results from this experiment can be seen in Figure 56. These results will be discussed in Chapter 7.

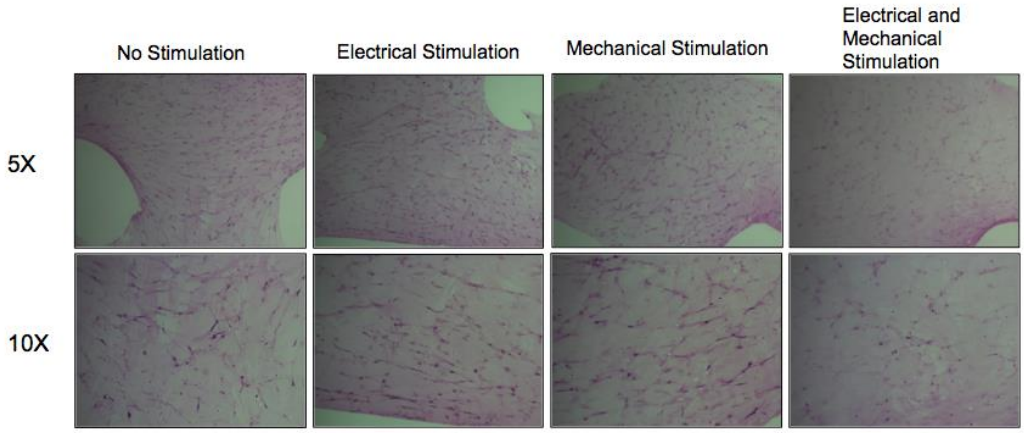

Figure 56. Histological results from final experiment.

Chapter 6: Final Design and Validation

This Chapter serves as the user manual for the device, giving insightful details on safety, operation, and control.

6.1 Device Overview

This section will discuss the use and assembly of the device, as well as the operation of the Arduino electrical system and the NE-4000 pump mechanical system.

6.1.1 Assembly of 96-well Plate and PDMS Posts

In a sterile beaker, prepare a 1:10 mixture of PDMS Curing Agent to PDMS. Obtain premade 4 mm PDMS posts; taking into account the number of experiments desired to be run. From the extra 4 mm PDMS posts, cut each 4 mm post to separate from the base. Using the prepared PDMS solution, apply a small amount of solution on the capped 4 mm PDMS post and place it on the cap of an uncut PDMS post system; this will allow the PDMS posts to reach 8 mm in height and maintain the caps in the middle. Furthermore, to adhere a 8 mm PDMS post to the 96-well plate wells, apply the solution to the base of the 96-well plate and the base of the 8 mm PDMS and gently place the PDMS posts in a horizontal orientation with the length of the plate.

6.1.2 Device Assembly

To assemble the device, the user must wear all protective gear that protects against biohazards and risks. The device should be assembled in a biosafety cabinet rated for tissue culture; the cabinet must be sterile. Bring the components of the device inside the hood, and follow the sterilization protocol in Section 5.1.1. When sterile, place the fixation frame on top of the support frame. Next, place the sliding comb-rack atop of the fixation frame and the support frame; the comb-rack should have mobility to slide along the track of the support frame. Place the buss-bars inside the designated holes and bar-supporter on the support frame; ensure that the buss-bars are not touching one another. Insert the break cable in the designated slot that

originates from the sliding comb-rack. Lastly, place the cover over the support frame to close the system and protect it from contamination. Use tape to cover any unfilled holes, such as buss-bar slots that are not being used.

To use the device on 96-well plates, uncover the well plate and place the lid aside. Place the assembled device on the 96-well plate; ensuring proper position of the comb-rack paddles, fixation plate, and the PDMS posts with tissues. At this stage, the system is ready to be connected to the mechanical force producing pump and the buss-bar electrical connectors.

6.1.3 Placing the Device in the Incubator

Remove the rubber stopper in the back of the incubator. Place the assembled device inside the incubator; sliding the free end of the break cable through the hole and outside of the incubator. Additionally, place the electrical alligator clips through the same hole. Attach the alligator clips to the buss-bars; following electrical convention. Place the rubber stopper back in the hole, and wrap the rubber stopper with Parafilm to preserve humidity. As this step, the device is ready to provide mechanically and electrically stimulation.

6.1.4 Mechanical Stimulation

Attach the break cable that is within the device assembly on the syringe backstop slot inside the NE-4000 Syringe Pump. Program the syringe pump to the desired regimen following the Pump Operation Manual. If problems arise programming the pump, call the service operator for NE Syringe Pumps; technical staff will assist if needed.

6.1.5 Electrical Stimulation

To operate the Arduino board, utilize the MQP-RLP-1502's program on the computer with the Arduino IDE. Plug in the USB connector to the PC. At this step, the alligator clips should have already been connected to the buss-bars. Open the serial monitor and input the

various parameter for the chosen electrical regimen when prompted. This will initiate the electrical regimen throughout the buss-bars via the alligator clips.

6.1.6 Full System Assembly

At this stage, the system should be in full operation utilizing both mechanical and electrical stimulations while maintaining sterility. To change the 96-well plate or to implement change, turn off the mechanical pump and the electrical simulation program. Detach the break cable from the syringe pump. Uncover the rubber stopper in the back of the incubator, and detach the alligator clips from the buss-bars. Remove the device and place in a biosafety cabinet and remove the 96-well plate.

6.2 Design Validation

This section discusses how the final design adheres to industry standards, as well as the impact of the project.

6.2.1 Industry Standards

The system was designed to follow industry standards in order to ensure user safety, biocompatibility and the correct handling of biological substances. ISO 22442-2:2007, ISO 13022:2012 and ISO 22432-1:2007 are all standards incorporated to ensure the correct sourcing and management of both animal and human cells used in the experiments. Standards ISO 18458:2015 and ISO 18459:2015 both give the frameworks for how to produce biomimetic tissue constructs. ISO 10993-1 and ISO 10993-5:2009 give the industry standards for the biological evaluation of medical device biocompatibility and the *in vitro* cytotoxicity of medical devices, respectively, which were followed via the use of only biocompatible materials during tissue culturing. In order to follow the standard on sterility, ISO 11737-2:2009, the system was sterilized using isopropanol and hydrogen peroxide. ISO/NP 20391-1 gave guidance on proper cell counting technique and ISO 7712:1985 was followed when correctly using and disposal of

plastic micropipettes. 96-well plates following the ANSI SLAS microplate dimensions were used to ensure accuracy and precision while applying mechanical and electrical stimulation to the tissue constructs. ISO standard 17422:2002 was also followed to ensure that the system does not have any significant negative impacts on the environment.

6.2.1 Economics

The device would have very little direct or immediate impact on the general economy or everyday living. In the future it might pave the way toward increased living conditions of people suffering from muscular dystrophy and would allow faster and cheaper development of drugs.

6.2.3 Societal Impact

The system the team created could potentially have significant impact on society once further development is continued. A system that could successfully grow and stimulate biomimetic human muscular tissue would streamline the drug-screening process for pharmaceutical companies, leaving them with additional money and enabling them to produce drugs at a faster rate. The money and time saved by the system could mean discovering a cure for muscular disorders such as DMD and atrophy faster. The finished system could also be modified to culture other human tissues *in vitro* to advance research in other diseases and disorders.

The completed system could also be responsible for the dissolution of human and animal testing popularly used by drug companies, both of which have ethical and economic considerations. Animal testing is currently the most efficient method to quickly test the efficiency of potential drugs, however as technology advances its use has been becoming more and more unpopular.

6.2.4 Political Impact

The successful creation of this system could cause some political implications in the United States, especially in the realm of healthcare and pharmaceutics. In the present political

climate, there could possibly be much objection from political parties that benefit from the manner pharmaceutical companies are ran now. If successful, the device could create a significant amount of income; a major change that could create political unrest within the government. There are also social and religious groups who believe that the creation of parts of the human body within a laboratory are violations to nature and will not support the use of this system.

6.2.5 Ethical Concerns

The creation of this system should actually have less ethical implications than the present methods of testing potential drugs. The system would firstly render these methods obsolete, since it will be more cost effective. The eradication of the present screening process would mean that animal testing would no longer be needed. Animal testing has become more and more controversial as investigators have uncovered a significant number of animal abuse cases from both pharmaceutical and cosmetic companies. The system would hereby create a more ethical way to develop necessary drugs. The system could also eliminate the need for human trials when testing potential drugs for muscular disorders. Although patients must sign up for drug trials by their own free will, they are still subjected to the potential side effects and complications that come with foreign compounds interacting with the body's cells. The use of this system could prevent future harm in people who wish to participate in test trials or it could eliminate the need for human trials all together.

6.2.6 Health and Safety Issues

The present system will not have any potential health or safety issues. The syringe-pump system, mechanical stimulation platform and the biological materials used all do not present any dangerous risks to users. Several ISO standards were strictly followed in order to ensure the

safety of its users (see Chart or earlier section). The system could only be used to harm if used in a way that it is not intended to be used.

Chapter 7: Discussion

This chapter serves as a platform for the discussion of results obtained from the verification experiments described in Chapter 5. Verification results will be used to provide evidence for the superiority of the team's design over current gold standards. These results will also be used to provide evidence that the team has met the initial design objectives and constraints.

7.1 General Discussion

This section describes conclusions drawn from the results of the verification experiments described in Chapter 5.

7.1.1 Sterilization Verification

As described in Section 5.1.1, an experiment was conducted to verify the ability of the device to maintain sterility during operation. A 96-well plate was loaded with media and the device was placed onto the plate, as it would be during operation. A control plate was also filled with media and set into the incubator with the standard 96-well plate cover as shown in Figure 48. After five days in the incubator there was no evidence of contamination in either the control plate or the test plate as evidenced by pinkish-red media coloration and absence of bacteria and fungi observed under a microscope. It was thus concluded that the new isopropanol/hydrogen peroxide sterilization method was capable of completely sterilizing the lid, and that the lid was capable of maintaining sterile conditions in an incubator. This means that the device should prevent all contamination and ensure the health of the tissues during stimulation.

7.1.2 Electrical Stimulation Verification

As described in Section 5.2.1, an experiment was conducted to verify that the electrical stimulation components were delivering the expected stimulation regimen. A simple regimen of 4 ms pulses of ~4.8V at 1Hz was programmed into the Arduino and the voltage across two opposite buss-bars was recorded in real time using an oscilloscope. The Voltage vs. Time plot

generated by the oscilloscope, depicted in Figure 49, confirms the ability of the system to deliver the regimen as expected. It can thus be assumed that any regimen programmed into the Arduino will be delivered to the tissues accurately.

Also described in section 5.2.1 is an experiment conducted to verify that all electrodes across the buss-bars were operational and capable of establishing an electric field within the wells of a 96-well plate. 1M HCL was pipetted into the wells of a 96-well plate and the buss-bars and electrodes were assembled on the plate. Four control wells were created by removing the electrodes corresponding to these wells. ~4.8V was established across the buss-bars and the HCL solution in the electrode-housing wells bubbled and turned yellow as seen in Figure 50. This confirms the ability of all electrodes along the buss-bars to establish an electric field and shows that the system has no poor connections.

7.1.3 Mechanical Stimulation Verification

As described in Section 5.3.1, an experiment was conducted to correlate the infusion/withdrawal volume of the syringe pump with the displacement of the opposite end of the brake cable. As seen in Figure 53, the variation between trials is comparatively small; indicating that the system is reproducible. It is seen that the infusion and withdrawal distances are right on top of each other; showing that the system is linear and not subject to drift. It should be noted that error bars are plotted in the graph, however, the error bars are too small to be seen; confirming the reproducibility and precision of the system. However, since the cable has a small degree of a flexible range of motion within its rubber housing; the Y-Intercept was not at 0. These results confirm the ability of the brake cable assembly to provide accurate, customized, and automated stimulation regimens.

Also describe in Section 5.3.1 is an experiment conducted to correlate the displacement of the brake cable with the actual strain experienced by the PDMS posts within the wells of the

96-well plate. The results shown in Figure 54 show a near-linear correlation of the strain the posts would induce on the tissues as the perfusion/withdraw rates increase. There was significant variation in strain between posts, due to small errors in device dimensions and variability of PDMS post placement within each well. Again, the initial flat portion of the calibration curve is due to the movement of the brake cable within its rubber housing.

7.1.4 Final Experiment Discussion

As described in Section 5.4, a final experiment was conducted to verify the ability of the device to function on living tissue and improve tissue maturity and overall biomimicry. Hydrogel-assisted self-assembled tissues were formed and subjected to stimulation regimens. It should be noted that no signs of contamination were observed over the course of this experiment, confirming both the efficacy of the sterilization protocol as well as the ability of the device to maintain sterility during operation.

This experiment yielded tissues incapable of contraction when assessed using the Myomics Myoforce Analysis System housed in Professor Page's laboratory. To investigate possible causes of the lack of contractile ability, the tissues were analyzed histologically and the results can be seen in Figure 56. All tissues did indeed consist of myotubes, however the myotubes were entirely thin, short, and lacked density. There did seem to be some slight qualitative improvement in alignment in electrical-stimulation-only and mechanical-stimulation-only groups when compared with the control group. However, both types of stimulation combined yielded tissues with even less density and fewer myotubes, perhaps caused by tissue damage via over-stimulation.

The lack of contractile ability and the presence of thin and short immature myotubes were likely caused by a cell density issue that occurred during tissue formation. The lack of cell density could be attributed to errors in cell counting. It could also be attributed to the fact that the

team had difficulty getting the NIPAAm layer to solidify, and thus the majority of cells could have sunk down to the bottom of the well, rather than being incorporated into the fibrin matrix. It should also be noted that the levels of matrix compaction were sub-optimal and thus the tissues were larger than expected, which could have also negatively impacted cell density. Another possible source of the lack of contractile ability and the presence of short and this immature myotubes is the fact that C2C12s were used for myoblasts, rather than primary human myoblasts. C2C12s typically have less of an ability to degrade matrix when compared to primary human myoblasts. This lack of degradation ability could have prevented the myoblast from migrating within the tissue and thus could have limited myoblast-myoblast fusion, which could explain the short and thin myotubes. Additionally, lower matrix degradation could have negatively impacted matrix compaction, as degradation plays a role in the compaction process.

With that being said, even though this final experiment failed, these results do not refute the ability of the stimulation device to function as intended. The Sliding Comb Rack has been shown to operate as intended as evidenced by the numerous verification studies described in Chapter 5. The results of this final experiment merely suggest that further work must be put into the optimization of the tissue engineering process and the stimulation regimens used.

7.2 Comparison to Gold Standard

The Sliding Comb Rack design offers numerous advantages over current 'gold standard' devices. Most industry devices, like the MagneTissue Bioreactor system and IonOptix C-Pace EP are designed to mechanically or electrically stimulate large tissue constructs, and are thus generally unsuited to high-throughput applications. Additionally, there exists no platform that both electrically and mechanically stimulates tissue constructs. The Sliding Comb Rack design overcomes both of these limitations by operating on tissues in a 96-well plate and by incorporating both mechanical and electrical stimulation capability into a single device.

Numerous other WPI MQPs have been tasked to overcome the aforementioned issues with commercially available devices, and the most successful iterations have been MQP-RLP-1501 and MQP-RLP-1502. These designs stimulate PDMS post-mounted tissues in a 96-well plate and are thus suited to high-throughput applications. However, each of these designs only utilizes a single type of stimulation, with the MQP-RLP-1501 device providing mechanical stimulation and the MQP-RLP-1502 device providing electrical stimulation. The Sliding Comb Rack design incorporates both electrical and mechanical stimulation into a single platform and thus offers the unique advantage of allowing integrated stimulation regimens, which would not have been possible before this design.

Overall, this device has the potential to become the gold standard in the electrical and mechanically stimulation of PDMS post-mounted engineered tissues, specifically skeletal muscle constructs. With the ability to stimulate tissues in a high-throughput manner, and with the incorporation of both electrical and mechanical stimulation capabilities into a single platform, the Sliding Comb Rack design could be used to enhance tissue maturity of skeletal muscle models. These models could play roles in bio-actuation, developmental research, or pharmaceutical applications. Most notably, this device could be used to mature engineered tissues used in drug-screening platforms such as that used by the Myomics company. With improvement in tissue maturity and overall biomimicry, these engineered skeletal muscle models could prove to streamline preclinical drug testing for musculoskeletal disorders.

7.3 Comparing Final Design to Initial Objectives and Constraints

This section discusses how the final design meets the initial design objectives, requirements, specifications and constraints. Rationale supporting the fulfillment of these objectives, requirements, specifications, and constraints will be provided via reference to various

design features and results from verification experiments.

7.3.1 Fulfillment of Design Objectives

At the onset of this project, three primary objectives were determined as described in Section 3.3.1. These objectives are listed below:

1) Enhance tissue maturity and density to form more biomimetic tissues

2) Compatible with Myomics drug-screening platform

3) Preserve high-throughput nature of Myomics drug-screening platform

Objective 1 states that the device must enhance tissue maturity and density in hopes of improving tissue maturity and overall biomimicry. While our final experiment did not yield significant improvements in tissue maturity, this was likely due to errors in tissue formation. The device has been shown to function as intended, and significant amounts of evidence suggest that mechanical and electrical stimulation do improve tissue maturity. Thus it is concluded that the final design is capable of meeting the objective of improved tissue maturity, provided that the tissue engineering and stimulation regimens are optimized.

Objective 2 states that the final design must be compatible with the Myomics drug-screening platform. This means that tissues must be formed around PDMS posts, and that these tissues must be able to be assessed for contractile ability via post-deflection analysis. Indeed, our system uses the same tissue engineering method as the Myomics platform and thus produces tissues anchored to PDMS posts. Additionally, our system yields tissues that can be assessed using the Myomics MyoForce Analysis System, which was used to assess the contractile ability of the tissues produced during the final experiment.

Objective 3 states that the final design must preserve the high-throughput nature of the Myomics platform. To meet this objective the final design was made to simultaneously act upon 96 tissues in a 96-well plate.

7.3.2 Fulfillment of Design Requirements

The three primary objectives described give way to various design requirements, detailed in Section 3.3.2. These requirements are listed below:

1) Use of most appropriate tissue engineering method

2) Mechanical stimulation of tissue constructs

3) Electrical stimulation of tissue constructs

4) Function in incubator

5) Biocompatible

6) Maintain sterility

7) Maintain user safety

Requirement 1 states that the team must use the most appropriate tissue engineering method. This method should be chosen on its ability to yield mature biomimetic tissue. Through a comparative analysis described in Section 4.1.1, the team chose the self-assembly engineering technique as the most appropriate. Unfortunately, attempts to create self-assembled tissue around PDMS posts in a 96-well plate failed, and the team reverted to the hydrogel-assisted self-assembly engineering method. Thus, this requirement was not met, as the most appropriate engineering method was abandoned for a less appropriate engineering method. It is recommended that future work be put into forming self-assembled tissues that are compatible with the final design.

Requirement 2 states that the final design must mechanically stimulate the tissue constructs. Through the results of the verification studies described in Section 5.3.1 and discussed in Section 7.1.3 it is clear that the final design is capable of providing mechanical stimulation. This stimulation has been shown to be accurate and relatively precise, and is capable of automation and customization.

Requirement 3 states that the device must electrically stimulate the tissue constructs. Through the results of the verification studies described in 5.2.1 and discussed in section 7.1.2, it is clear that the final design is capable of providing electrical stimulation. The components of MQP-RLP-1502's design that were adopted into this MQP's final design were shown to provide accurate, automated, and customizable stimulation regimens.

Requirement 4 states that the system must function in an incubator. Both the Arduino system that controls electrical stimulation as well as the syringe pump that controls mechanical stimulation are housed outside of the incubator, and thus the incubator environment does not interfere with the function of these systems. As further evidence for the fulfillment of this requirement, no compromise of device function was observed during the final experiment in which the device functioned inside an incubator environment for a full week.

Requirement 5 states that device must be biocompatible. This requirement was achived by ensuring that any material that would contact cells or media was rated highly for biocompatibility. Thus, the sliding rack and the post fixation frame were made of a biocompatible polymer MED610. Additionally, the stainless steel electrodes adopted from MQP-RLP-1502's device were shown by MWP-RLP-1502 to be biocompatible and corrosion resistant during operation. Additionally, these electrodes were sterilized using EtO to prevent corrosion that could occur during autoclaving.

Requirement 6 states that the final design must maintain sterility during operation. Through the results of the sterilization method verification study described in Section 5.1.1, it is clear that the sterilization method used is capable of initially sterilizing the device. Further, no contamination was observed during the final experiment and thus the device is capable of maintain sterility during operation.

Requirement 7 states that the system must maintain user safety. No operator injury was sustained during the fabrication or operation of this device. Proper aseptic technique and use of proper PPE during tissue culture prevents tissue culture associated risks. The Ardunio and circuit used to control electrical stimulation do have exposed wires, however the board is cable of outputting a maximum of only 5V, which is harmless when touched with bare hands. Also, if the device were ever to be manufactured and distributed commercially, all electronics would be properly housed and up to industry standards and thus would pose no threat to user safety.

7.3.3 Fulfillment of Design Specifications

The design requirements give way to various design specifications, discussed in Section 3.3.3. These specifications are listed below:

1) Physiologically relevant strain regimens (0-30%)

2) Electric field strength up to 0.3 V/mm

Specification 1 states that the final design should be capable of straining the tissues to strain values between 0% and 30%. From the verification studies described in Section 5.3.1 and discussed in Section 7.1.3, it is clear that the device is able to strain tissues from 0% to 30% as evidenced by the data presented in Figure 54. While this study was conducted on PDMS posts free of tissues, it can be assumed that tissues will experience real-life strain values on this order during operation because one PDMS post is held in place by the fixation frame.

Specification 2 states that the system must be able to establish an electric field strength of at least 0.3 V/mm during electrical stimulation. This specification is inherently fulfilled by MQP-RLP-1502's device, as it operates under an Arduino output of ~4.8V with an electrode separation of 3mm. This corresponds to a maximum electric field strength of 1.6 V/mm. Further, the design allows adjustment of field strength via potentiometers and thus is capable of establishing a field strength from 0 V/mm to 1.6 V/mm.

7.3.4 Fulfillment of Design Constrains

The design requirements also give way to various design constraints, discussed in Section 3.3.3. These constraints are listed below:

1) Compatible with PDMS posts

2) Incubator environment

3) Nutrient perfusion limits

Constraint 1 states that the system must be compatible with the PDMS posts used in the Myomics platform. The entire system was designed with this constraint in mind, and is designed to actuate modified PDMS posts of 3.2 mm post separation and 8mm post height. As evidenced by the results of verification studies described in Section 5.3.1, the device is able to function on these PDMS posts as expected.

Constraint 2 states that the device will be subjected to an incubator environment of 37˚C, 95% humidity, and 5% CO_2. Thus all materials and electronics must be able to function in this environment. As previously discussed, the device was capable of meeting this constraint.

Constraint 3 states that the design is limited by nutrient perfusion limits of 80-300 μm. Because the engineered tissues lack a vascular system, nutrients must passively perfuse into the tissue. Cells that are more than 300 μm from the nutrient source (i.e. media) are likely to die. The small tissues formed by the hydrogel-assisted self-assembly technique are small enough such that most cells are within this perfusion limit. Indeed, no evidence of necrosis was observed from the histological analysis of the tissues produced during the final experiment.

Chapter 8: Conclusions and Recommendations

8.1 Conclusions

In conclusion, a device was created that met the objectives, requirements, specifications, and constraints set by the client statement. The device is able to simultaneously mechanically and electrically stimulate 96 tissue constructs, allowing for high throughput testing and production. Through rigorous testing and analysis the device proved to perform the intended functions and accomplish the set project goals. Overall, this device has the potential to become the gold standard in the electrical and mechanically stimulation of PDMS post-mounted engineered tissues, specifically skeletal muscle constructs. While commercially available stimulation platforms lack high-throughput capabilities and the integration of both mechanical and electrical stimulation, this Sliding Comb Rack design overcomes these limitations. The unique advantages of this design equip the device with a potential to enhance the maturity and overall biomimicry of skeletal muscle models used for drug screening. As previous iterations of this drug screening technology, such as the Myomics platform, have been plagued by lack of maturity, this design could play a role in breaking down the maturity barrier that limits overall biomimicry.

8.2 Recommendations

During and after the process of designing the device the team came up with improvements that could be made to the device.

A major improvement to the system would be the optimization of tissue-engineering. As discussed in Chapter 4, self-assembly tissue constructs could be used to have greater tissue maturity. The V-shaped mold that the team developed could theoretically be used to accomplish this, provided that the issues with NIPAAm are resolved or a different material is used.

A unified control system could be created to ensure calibration between the mechanical and electrical stimulation regimens. Currently the electrical stimulation is managed by an Arduino and the mechanical by a programmable syringe pump. This requires two parallel programs to be run and calibration between them depends on human input at beginning of regimens. In addition knowledge is required of both systems which makes them harder to use. If a single control system was used for both systems it would simplify use and reduce error.

Several mechanical improvements could be made to improve the durability, usability, and functionality of the device. The lid currently blocks a top down view of the posts. By either using a more clear material or creating material free paths top down observation of the posts during mechanical and electrical stimulation could be conducted and post deflection measured. Post deflection measurements would allow for higher throughput testing of BAMS.

Currently the lid is made of materials that need different sterilization techniques. ABS needs to be ETO sterilized, and MED610 requires a 15 min 70% isopropanol bath followed by a 15 minute hydrogen peroxide bath. Sterilization needs to occur before each culture. If materials were selected that could both be sterilized with a single technique it would simplify the culturing process and reduce costs. For example, the entire device could be made out of polystyrene, the material which tissue culture plates are made out of. This would allow sterilization of the whole system by EtO. Additionally, polystyrene is optically transparent, and would allow the use to see directly into the tissue culture plate.

The entire comb rack of the lid is currently made of MED 610. MED610 is expensive. Use of a different material or materials in the lid would allow several lids to be manufactured and different mechanical strains and lid designs tested more easily.

To reduce sources of error and maintain reproducibility, the PDMS mold system should be modified to produce the desired dimensions of the PDMS Posts. At the current state, the mold is only capable of producing PDMS posts that are 4 mm in height and a cap on post. This proposed mold would be 8 mm in height and integrate two caps within the PDMS post. This will ensure that the PDMS posts are in union. The current method to produce 8 mm PDMS posts require adhering two 4 mm posts together. This typically produces variations within each post, which leads in an overall lesser reproducibility of the system.

The team would like to integrate a mechanical motor that fully operates an incubator. Due to budget constraints, the team had to propose an alternative to mimic the performance of a motor. This motor must produce forces to move the comb-rack back and forth to stimulate tissues; the motor must be precise and accurate in displacing the comb-rack. Additionally, the motor must be able to function in an incubator; having shielding from the humidity that interferes with the electrical components of motors.

References

[1] N. Shanks, R. Greek and J. Greek, "Are animal models predictive for humans?", *Philos Ethics Humanit Med*, vol. 4, no. 1, p. 2, 2009.

[2] D. McNeil, C. Davis, D. Jillapalli, S. Targum, A. Durmowicz and T. Coté, "Duchenne muscular dystrophy: Drug development and regulatory considerations", *Muscle & Nerve*, vol. 41, no. 6, pp. 740-745, 2010.

[3] J. Manning and D. O'Malley, "What has the mdx mouse model of duchenne muscular dystrophy contributed to our understanding of this disease?", *J Muscle Res Cell Motil*, vol. 36, no. 2, pp. 155-167, 2015.

[4] C. A. Powell, B. L. Smiley, J. Mills, and H. H. Vandenburgh, "Mechanical stimulation improvestissue-engineered human skeletal muscle," *American Journal of Physiology-Cell Physiology,* vol. 283, pp. C1557-C1565, 2002

[5] Y. Huang, "Rapid formation of functional muscle in vitro using fibrin gels", *Journal of Applied Physiology*, vol. 98, no. 2, pp. 706-713, 2004.

[6] R. Dennis And P. Kosnik, Ii, "Excitability And Isometric Contractile Properties Of Mammalian Skeletal Muscle Constructs Engineered In Vitro", *In Vitro Cell Dev Biol Anim*, Vol. 36, No. 5, P. 327, 2000

[7] Gillies AR, Lieber RL. Structure and Function of the Skeletal Muscle Extracellular Matrix. *Muscle & nerve*. 2011;44(3):318-331. doi:10.1002/mus.22094.

[8] Skeletal Muscle | Anatomy and Physiology", *Opentextbc.ca*, 2017. [Online]. Available: https://opentextbc.ca/anatomyandphysiology/chapter/10-2-skeletal-muscle/. [Accessed: 17- Jan- 2017]

[9] C. Duance, D.J. Restall, H. Beard, F.J. Bourne, A.J. Bailey, The location of three collagen types in skeletal muscle, FEBS Letters, Volume 79, Issue 2, 15 July 1977, Pages 248-252, ISSN 0014-5793, http://dx.doi.org/10.1016/0014-5793(77)80797-7.

[10] "Judith Brown CPD", *Judithbrowncpd.co.uk*, 2017. [Online]. Available: http://www.judithbrowncpd.co.uk/Skeletal%20Muscle.pdf. [Accessed: 17- Jan- 2017].

[11] "SEER Training:Muscle Groups", *Training.seer.cancer.gov*, 2017. [Online]. Available: https://training.seer.cancer.gov/anatomy/muscular/groups/. [Accessed: 16- Jan- 2017].

[12] Arnold SJ, Robertson EJ. 2009. Making a commitment: Cell lineage allocation and axis patterning in the early mouse embryo. Nat Rev **10**: 91–103.

[13] Pownall ME, Gustafsson MK, Emerson CP Jr.. 2002. Myogenic regulatory factors and the specification of muscle progenitors in vertebrate embryos. Annu Rev Cell Dev Biol **18**: 747–783 http://jap.physiology.org/content/91/2/534.full

[14] M. Buckingham, "Myogenic progenitor cells and skeletal myogenesis in vertebrates," *Current Opinions in Genetics & Development,* vol. 16, pp. 525-532, 10// 2006.

[15] B. Blaauw, G. Pallafacchina & S. Schiaffino, "Role of satellite cells in muscle growth and maintenance of muscle mass," *Nutrition, Metabolism and Cardiovascular Diseases,* vol. 23, pp. S12-S18, 2013.

[16] T.J. Hawke and D.J. Garry, "Myogenic satellite cells: physiology to molecular biology," *Journal of Applied Physiology,* vol. 91, pp. 534-551, 2001.

[17] M. Juhas and N. Bursac, "Engineering skeletal muscle repair," *Current Opinion in Biotechnology,* vol. 24, pp. 880-886, 10// 2013

[18] B. Sicari, V. Agrawal, B. Siu, C. Medberry, C. Dearth, N. Turner and S. Badylak, "A Murine Model of Volumetric Muscle Loss and a Regenerative Medicine Approach for Tissue Replacement", *Tissue Engineering Part A*, vol. 18, no. 19-20, pp. 1941-1948, 2012.

[19] E. Mercuri and F. Muntoni, "Muscular dystrophies," *The Lancet,* vol. 381, pp. 845-860, 2013.

[20] E. Hoffman et al, "Dystrophin: the protein product of Duchenne muscular dystrophy locus," *Cell,* vol. 51, pp. 919-928, 1987.

[21] American Thoracic Society, "Respiratory care of the patient with Duchenne muscular dystrophy," vol. 170, ed. 2004.

[22] J. Campellone (2014, 10/6/15) *Muscle Atrophy*

[23] J. Bailey et al, "Multiple types of skeletal muscle atrophy involve a common program of changes in gene expression," *The FASEB Journal,* vol. 18, pp. 39-51, 2004.

[24] H. Vandenburgh, P. Karlisch and L. Farr, "Maintenance of highly contractile tissue-cultured avian skeletal myotubes in collagen gel", *In Vitro Cellular & Developmental Biology*, vol. 24, no. 3, pp. 166-174, 1988.

[25] J. Shansky, J. Chromiak, M. Del Tatto and H. Vandenburgh, "A simplified method for tissue engineering skeletal muscle organoids in vitro", *In Vitro Cellular & Developmental Biology - Animal*, vol. 33, no. 9, pp. 659-661, 1997.
[26] C. Powell, B. Smiley, J. Mills and H. Vandenburgh, "Mechanical stimulation improves tissue-engineered human skeletal muscle", *AJP: Cell Physiology*, vol. 283, no. 5, pp. C1557-C1565, 2002.

[27] H. Vandenburgh, J. Shansky, F. Benesch-Lee, V. Barbata, J. Reid, L. Thorrez, R. Valentini and G. Crawford, "Drug-screening platform based on the contractility of tissue-engineered muscle", *Muscle & Nerve*, vol. 37, no. 4, pp. 438-447, 2008.

[28] H. Vandenburgh, "High-Content Drug Screening with Engineered Musculoskeletal Tissues", *Tissue Engineering Part B: Reviews*, vol. 16, no. 1, pp. 55-64, 2010.

[29] R. Strohman, E. Bayne, D. Spector, T. Obinata, J. Micou-Eastwood and A. Maniotis, "Myogenesis and histogenesis of skeletal muscle on flexible membranes in vitro", *In Vitro Cellular & Developmental Biology*, vol. 26, no. 2, pp. 201-208, 1990.

[30] R. Dennis And P. Kosnik, Ii, "Excitability And Isometric Contractile Properties Of Mammalian Skeletal Muscle Constructs Engineered In Vitro", *In Vitro Cellular & Developmental Biology - Animal*, vol. 36, no. 5, p. 327, 2000.

[31] M. Li, C. Dickinson, E. Finkelstein, C. Neville and C. Sundback, "The Role of Fibroblasts in Self-Assembled Skeletal Muscle", *Tissue Engineering Part A*, vol. 17, no. 21-22, pp. 2641-2650, 2011.

[32] Personal Correspondence with Jason Forte, WPI, Page Lab. 2016.

[33] N. Martin, S. Passey, D. Player, A. Khodabukus, R. Ferguson, A. Sharples, V. Mudera, K. Baar and M. Lewis, "Factors affecting the structure and maturation of human tissue engineered skeletal muscle", Biomaterials, vol. 34, no. 23, pp. 5759-5765, 2013.

[34] A. Brevet, E. Pinto, J. Peacock and F. Stockdale, "Myosin synthesis increased by electrical stimulation of skeletal muscle cell cultures", *Science*, vol. 193, no. 4258, pp. 1152-1154, 1976.

[35] S. Lund, G. Holman, O. Schmitz and O. Pedersen, "Contraction stimulates translocation of glucose transporter GLUT4 in skeletal muscle through a mechanism distinct from that of insulin.", *Proceedings of the National Academy of Sciences*, vol. 92, no. 13, pp. 5817-5821, 1995.

[36] S. Düsterhöft and D. Pette, "Effects of electrically induced contractile activity on cultured embryonic chick breast muscle cells", *Differentiation*, vol. 44, no. 3, pp. 178-184, 1990.

[37] K. Donnelly, A. Khodabukus, A. Philp, L. Deldicque, R. Dennis and K. Baar, "A Novel Bioreactor for Stimulating Skeletal Muscle In Vitro", *Tissue Engineering Part C: Methods*, vol. 16, no. 4, pp. 711-718, 2010.

[38] "IonOptix Culture Pacer Brochure", 2017. [Online]. Available: http://www.ionoptix.com/wp-content/uploads/2014/07/Culture-Pacer-Brochure_digital.pdf. [Accessed: 05- Jan- 2017].

[39] H. Fujita, T. Nedachi and M. Kanzaki, "Accelerated de novo sarcomere assembly by electric pulse stimulation in C2C12 myotubes", *Experimental Cell Research*, vol. 313, no. 9, pp. 1853-1865, 2007.

[40] T. Nedachi, H. Fujita and M. Kanzaki, "Contractile C2C12 myotube model for studying exercise-inducible responses in skeletal muscle", *AJP: Endocrinology and Metabolism*, vol. 295, no. 5, pp. E1191-E1204, 2008.

[41] "High Content Screening for Muscular Dystrophy | SBIR.gov", *Sbir.gov*, 2017. [Online]. Available: https://www.sbir.gov/sbirsearch/detail/242111. [Accessed: 12- Jan- 2017].

[42] A. Cunha, A. Howard, and S. Jones, *4D Maturation Bioartificial Muscle for High Content Drug Screening.* Worcester, MA: Worcester Polytechnic Institute, 2016.

[43] JT. Biliouris, G. Scuderi, C. Teed , Maturation of an In Vitro Skeletal Muscle Tissue Model By Mechanical Stimulation. Worcester, MA: Worcester Polytechnic Institute, 2016.

[44] D. G. Moon, G. Christ, J. D. Stitzel, A. Atala, and J. J. Yoo, "Cyclic mechanical preconditioning improves engineered muscle contraction," *Tissue Engineering Part A,* vol. 14, pp. 473-482, 2008.

[45] P. Heher, B. Maleiner, J. Prüller, A. H. Teuschl, J. Kollmitzer, X. Monforte*, et al.*, "A novel bioreactor for the generation of highly aligned 3D skeletal muscle-like constructs through orientation of fibrin via application of static strain," *Acta Biomaterialia,* vol. 24, pp. 251-265, 9/15/ 2015.

[46] K. Ikeda, A. Ito, M. Sato, Y. Kawabe and M. Kamihira, "Improved contractile force generation of tissue-engineered skeletal muscle constructs by IGF-I and Bcl-2 gene transfer with electrical pulse stimulation", *Regenerative Therapy*, vol. 3, pp. 38-44, 2016.

[47] W. Herzog, *Skeletal muscle mechanics : from mechanisms to function*, 1st ed. Chichester [etc.]: John Wiley & Sons, 2000.

[48] M. Li, C. Dickinson, E. Finkelstein, C. Neville and C. Sundback, "The Role of Fibroblasts in Self-Assembled Skeletal Muscle", *Tissue Engineering Part A*, vol. 17, no. 21-22, pp. 2641-2650, 2011.

[49] J. I. Andersen, M. Juhl, T. Nielsen, J. Emmersen, T. Fink, V. Zachar*, et al.*, "Uniaxial cyclic strain enhances adipose-derived stem cell fusion with skeletal myocytes," *Biochemical and Biophysical Research Communications,* vol. 450, pp. 1083-1088, 7/25/ 2014.

Table 12. Authorship and Contributions

Section	Author(s)	Editor(s)
Chapter 1	All	All
Chapter 2	All	All
Section 2.1	Mina	Ben
Section 2.2	Mina	Ben
Section 2.3	Mina	Ben
Section 2.4	Annabella	Mina
Section 2.5	Annabella	Mina
Section 2.6	Ben	Alex
Section 2.7	Ben and Mina	Alex and Annabella
Chapter 3	All	All
Section 3.1	All	All
Section 3.2	Mina	Ben
Section 3.3	Ben	All
Section 3.4	Ben	All

Section 3.5	All	All
Chapter 4	All	All
Section 4.1	Ben	Mina
Section 4.2	Ben	Mina
Section 4.3	Mina and Alex	Ben
Chapter 5	Ben and Mina	Mina and Ben
Section 5.1	Ben	Mina
Section 5.2	Mina and Ben	Mina and Ben
Section 5.3	Mina	Ben
Section 5.4	Ben	Mina
Chapter 6	All	All
Section 6.1	Mina	Ben
Section 6.2	Annabella and Alex	Mina and Ben
Chapter 7	Mina and Ben	Mina and Ben
Section 7.1	Ben	Mina
Section 7.2	Mina	Ben

Section 7.3	Ben	Mina
Chapter 8	Ben, Alex, Mina	All
Section 8.1	Mina	Ben
Section 8.2	Ben and Alex	All

Table 13: Budget Analysis.

Item	Date of Purchase	Price Estimates	Total Budget Left as of Today: ($600)
Horse Serum	11/07/16	$10.00	$590.00
NIPAAM	12/02/16	$102.00	$488.00
3D Printed Mold	12/04	$1.00	$487.00
3D Printed Lid	2/20	$217.00	$274.00
Fixation Frame	2/28	$40.00	$234.00

APPENDIX A: Schematics of Design

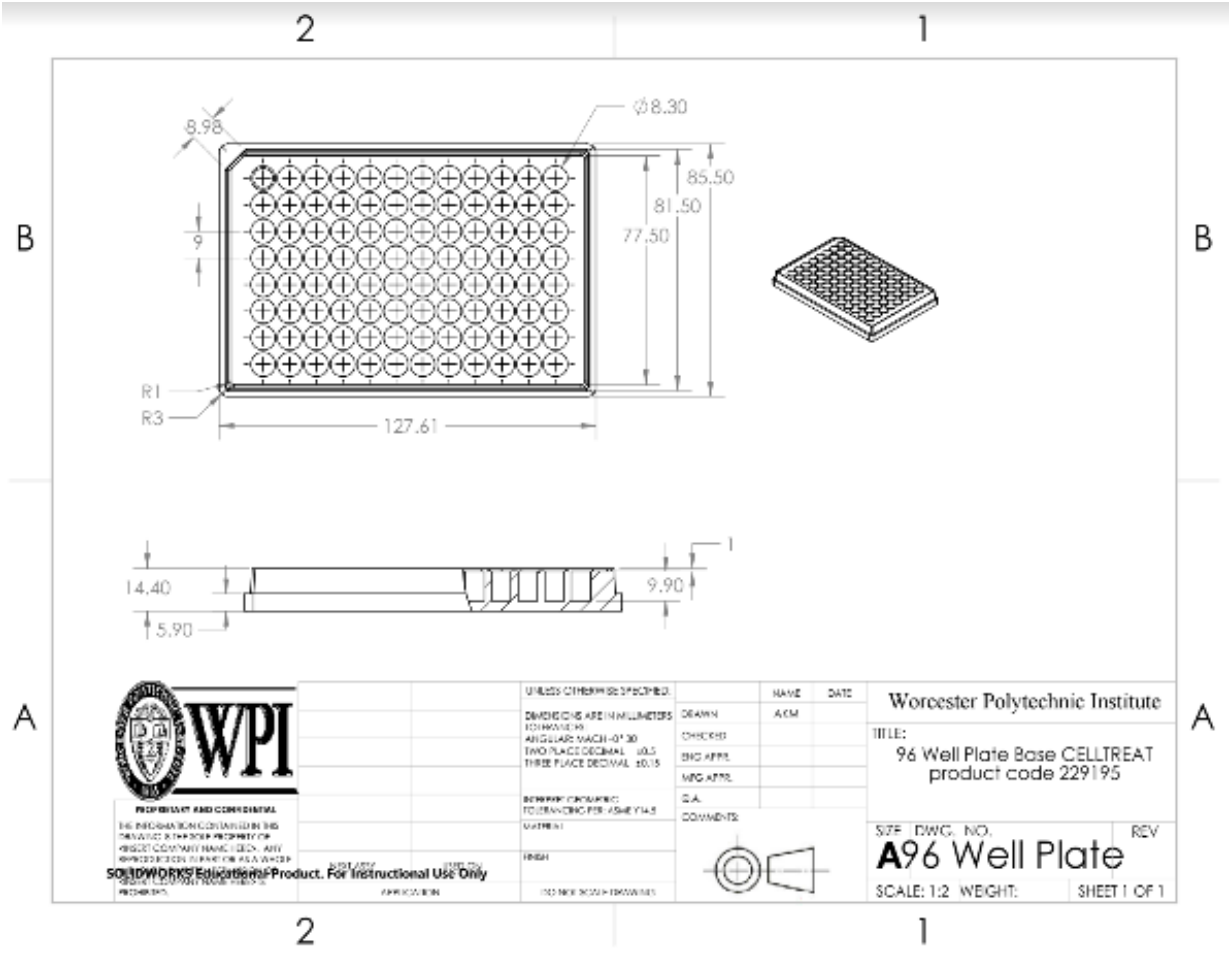

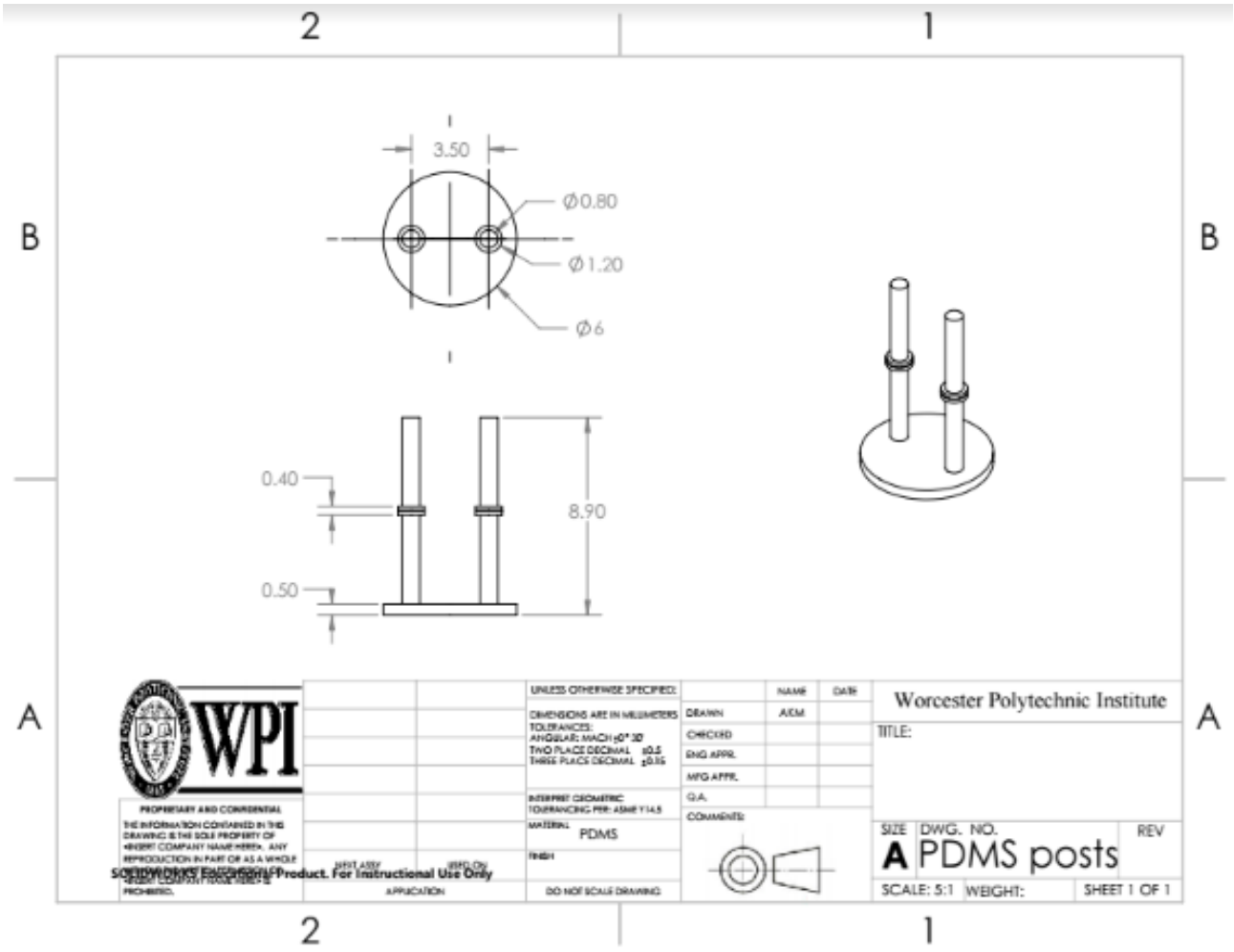

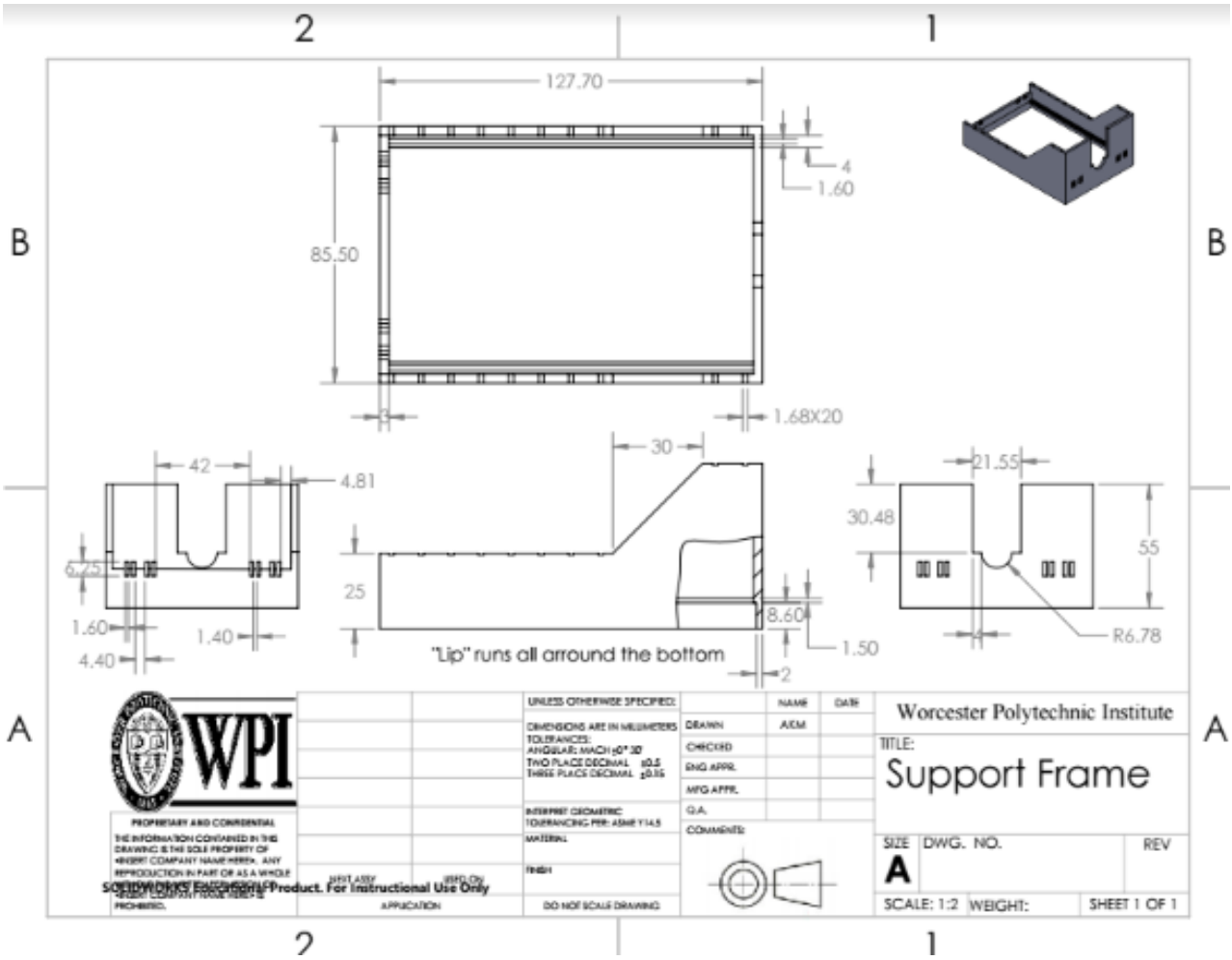

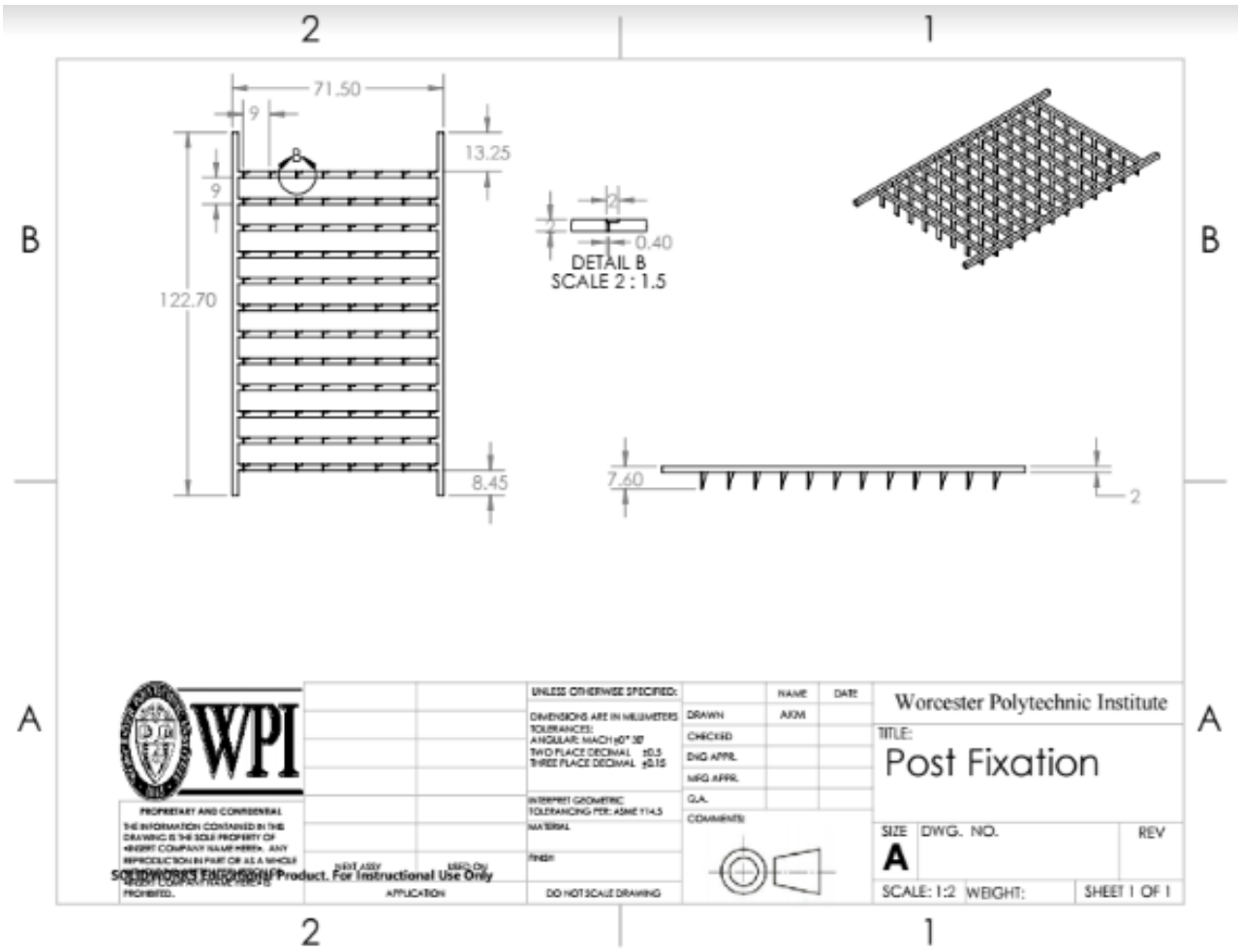

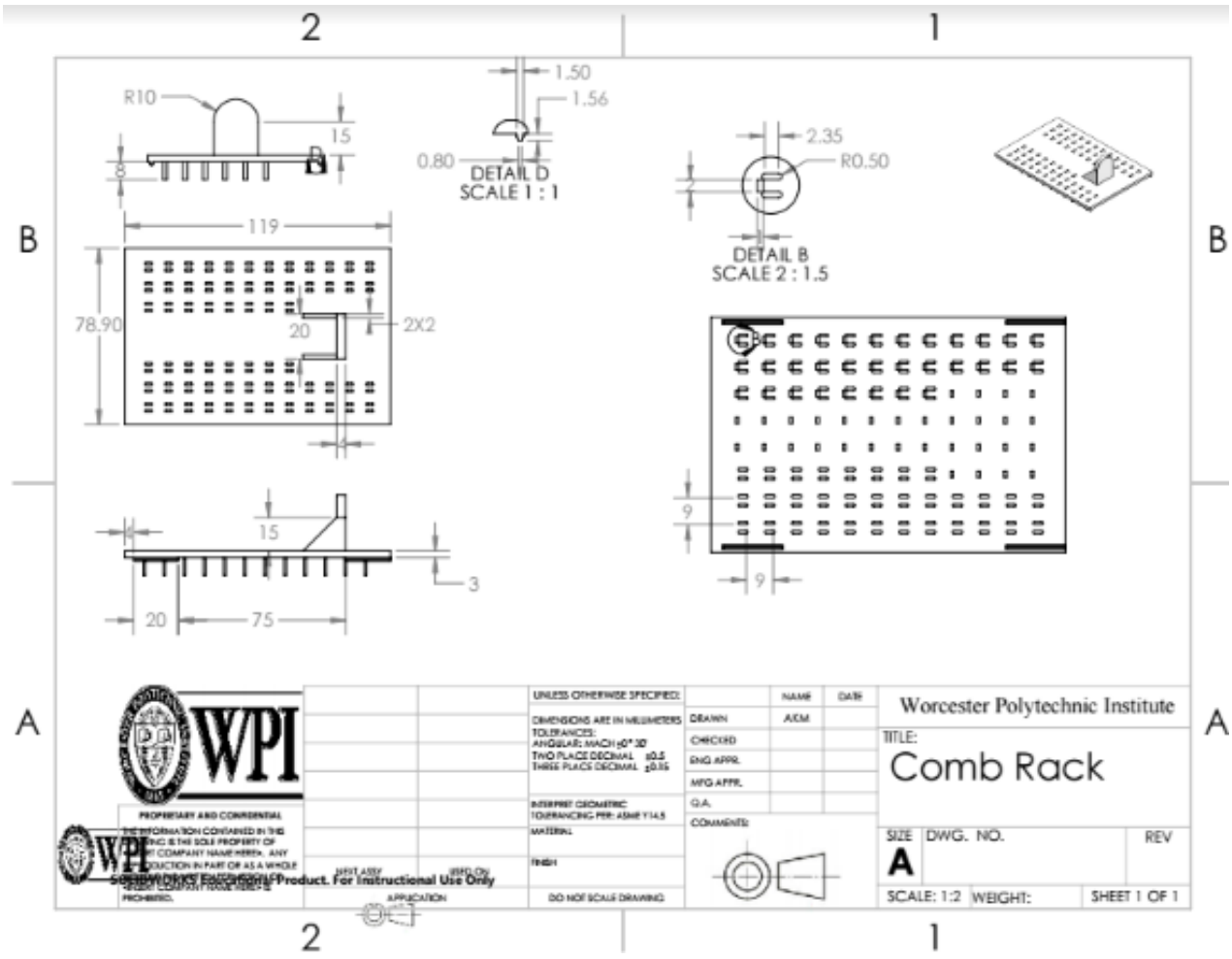
2
1
B
A
R10
15
8
119
78.90
20
2X2
15
3
20
75
1.50
1.56
0.80
DETAIL D
SCALE 1 : 1
2.35
R0.50
DETAIL B
SCALE 2 : 1.5
9
9
UNLESS OTHERWISE SPECIFIED:
DIMENSIONS ARE IN MILLIMETERS
TOLERANCES:
ANGULAR: MACH ±0° 30'
TWO PLACE DECIMAL ±0.5
THREE PLACE DECIMAL ±0.05
INTERPRET GEOMETRIC TOLERANCING PER: ASME Y14.5
MATERIAL
FINISH
DO NOT SCALE DRAWING
NEXT ASSY
USED ON
APPLICATION
NAME
DATE
DRAWN
A.K.M.
CHECKED
ENG APPR.
MFG APPR.
Q.A.
COMMENTS:
Worcester Polytechnic Institute
TITLE:
Comb Rack
SIZE
A
DWG. NO.
REV
SCALE: 1:2
WEIGHT:
SHEET 1 OF 1
PROPRIETARY AND CONFIDENTIAL
Solidworks Educational Product. For Instructional Use Only